PNL--8356-Vol.2

DE93 002946

ESTIMATION OF THE RELEASE AND MIGRATION OF LEAD THROUGH SOILS AND GROUNDWATER AT THE HANFORD SITE 218-E-12B BURIAL GROUND

VOLUME 2: APPENDICES

K. Rhoads
B. N. Bjornstad
R. E. Lewis
S. S. Teel
K. J. Cantrell
R. J. Serne
J. L. Smoot
C. T. Kincaid
S. K. Wurstner

October 1992

Prepared for
the U.S. Department of Energy
under Contract DE-AC06-76RLO 1830

Pacific Northwest Laboratory
Richland, Washington 99352

MASTER

DISTRIBUTION OF THIS DOCUMENT IS UNLIMITED

CONTENTS

<u>FIGURES</u>

TABLES

GLOSSARY

Modified from Gary et al. (1974).

Aggradation: The building of the Earth's surface by deposition.

Air-fall tuff: A compacted deposit of volcanic ash that settled from the air.

Alluvial fan: A low, outspread, relatively flat to gently sloping mass of loose rock material, shaped like an open fan or a segment of a cone, deposited by a stream at the place where it issues from a narrow mountain valley upon a plain or broad valley.

Anastomosing: Braided stream channel geometry.

Anticline: Folded rock that convexes upward.

Bar: A ridge-like accumulation of sand or gravel formed in a channel, along the banks, or at the mouth, of a stream where a decrease in velocity induces deposition.

Basalt: Dark volcanic rock erupted upon the surface of the Earth.

Clay: A rock fragment or particle smaller than 1/256 mm.

Conglomerate: A coarse-grained sedimentary rock composed of larger fragments (>2 mm) set in a fine-grained matrix of sand and silt.

Cross-bed: A single, thin-bedded, often lenticular layer of homogeneous or gradational lithology, deposited at an angle to the original surface of deposition.

Diagenetic: Pertaining to the chemical, physical, and biologic changes undergone by a sediment after its initial deposition and during and after its transformation into a rock.

Dip: The maximum angle that a surface makes with a horizontal plane.

En echelon: Geologic features that are in a staggered arrangement.

Epiclastic: Pertaining to sedimentary rock whose fragments are derived by weathering or erosion.

Facies: The sum of all primary rock characteristics exhibited by a sedimentary rock and from which its origin and environment of deposition my be inferred.

Fanglomerate: Sedimentary rock deposited by an alluvial fan.

Foreset bed:	A gently inclined layer of material deposited upon an advancing and relatively steep frontal slope of a sand wave.
Fluvial:	Pertaining to, produced by, or formed in a river.
Glaciofluvial:	Pertaining to the meltwater streams flowing from a glacier.
Grading:	The gradual reduction, in a progressively upward direction within an individual stratification unit, of the upper particle-size limit.
Interbed:	A thin bed on one kind of rock occurring between beds of another kind.
Isopach:	A line drawn on the map connecting points of equal thickness.
Lacustrine:	Pertaining to, produced by, or formed in a lake.
Lamination:	Sedimentary layer less than 1 cm thick.
Mud:	A mixture of silt- and clay-size particles.
Overbank:	Fine-grained sediment deposited from suspension on a flood plain by floodwaters that can not be contained within the stream channel.
Overturned:	Pertaining to the limb of a fold that has tilted beyond perpendicular.
Paleocurrent:	An ancient current whose direction is inferred from sedimentary structures.
Plunge:	The inclination of the axis of a fold.
Shale:	A fissile, laminated rock formed by consolidation of clay, mud, and silt.
Silt:	A rock fragment having a diameter between 1/256 and 1/16 mm.
Suprabasalt:	Sedimentary strata that overlie the Columbia River Basalt Group.
Syncline:	Folded rock that concaves upward.
Tectonic:	Pertaining to the forces involved in deforming the earth.
Tholeiitic:	Silica-rich basalt.
Tuffite:	A compacted deposit of volcanic ash and detrital material.

APPENDIX A

TECHNICAL BASIS FOR A GROUNDWATER TRANSPORT ANALYSIS AT THE HANFORD SITE 218-E-12B BURIAL GROUND

A.1 INTRODUCTION

This appendix describes the technical basis for a groundwater transport analysis that was conducted to evaluate migration of potentially hazardous materials from the Hanford Site 218-E-12B burial ground. The analysis characterized the geologic, chemical, and hydrologic properties of the disposal site, and used that information to perform a screening analysis for transport of materials from the burial ground to downgradient groundwater locations and to the Columbia River. Subsequent sections of the appendix describe the geologic setting, geochemistry, and hydrology of the disposal site and their relationship to the transport analysis.

A.2 GEOLOGIC STRUCTURE AND PHYSICAL-HYDRAULIC PROPERTIES OF SEDIMENTS BENEATH THE HANFORD SITE 218-E-12B BURIAL GROUND

This section of the appendix presents the results of a geologic and hydrologic study of the 218-E-12B Burial Ground, located within the 200-East Area of the Hanford Site in south-central Washington State (Figure A.1). It includes a description of the burial ground, discussions of the local geologic and hydrologic settings, and the geohydrology of the saturated and unsaturated zones beneath the site. A key task in this project was the collection of outcrop and borehole samples for physical analysis. These data are presented in Appendix B, along with as-built diagrams and well history sheets for the two groundwater monitoring wells adjacent to the 218-E-12B Burial Ground. The geohydrology in the vicinity of the 218-E-12B Burial Ground is influenced primarily by unsaturated flow within the vadose zone; generally only a few feet of unconfined aquifer is present above the top of basalt.

A.2.1 STRATIGRAPHY

Four principal stratigraphic units are represented near the 218-E-12B Burial Ground (from oldest to youngest): 1) the Miocene Columbia River Basalt Group (Saddle Mountains Basalt), interbedded with 2) sedimentary deposits of the Ellensburg Formation; 3) the Mio-Pliocene fluvial-lacustrine Ringold Formation; and 4) the glacio-fluvial Hanford formation (Figure A.2). This stratigraphy is based on hundreds of boreholes drilled in the area. Stratigraphic information for this report was compiled from regional studies (Tallman et al. 1979; Last et al. 1989; DOE 1988; Lindsey et al. 1992), as well as ongoing local studies used to characterize and monitor several site-specific Resource Conservation and Recovery Act (RCRA) projects that are close to the burial ground (within 1 to 2 mi). These latter sources of data include the Low-Level Burial Grounds (Last et al. 1989; Barton 1990), 216-B-Pond, the Liquid Effluent Retention Facility (Doremus and Pearson 1990), and 216-B-63 Trench (Bjornstad and Dudziak 1989). Stratigraphic sections used in this report were gathered from the previous reports. Their interpretations were updated, where necessary, based on a combination of drillers' and geologists' logs, gross gamma geophysical logs, and particle-size/ $CaCO_3$ data

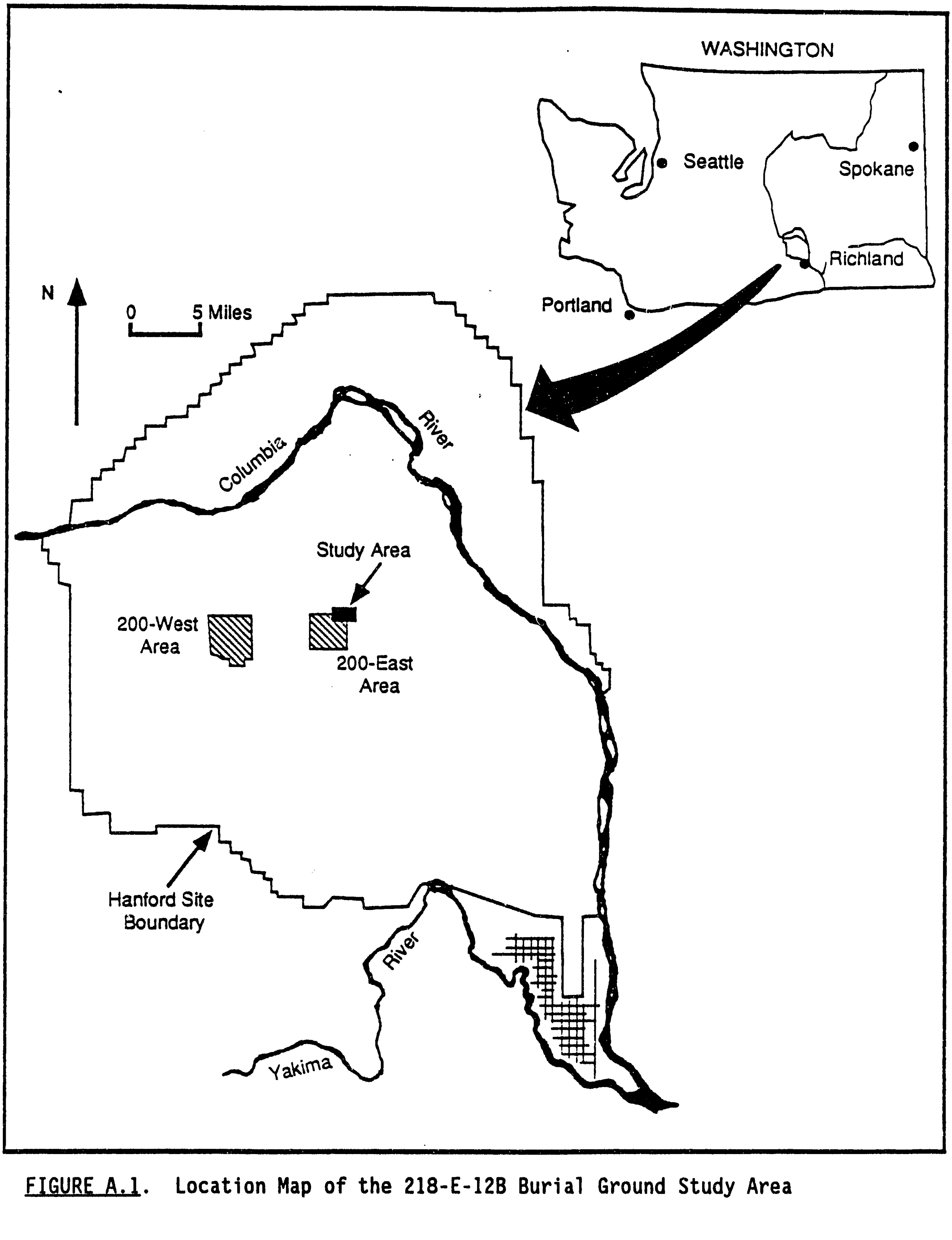

FIGURE A.1. Location Map of the 218-E-12B Burial Ground Study Area

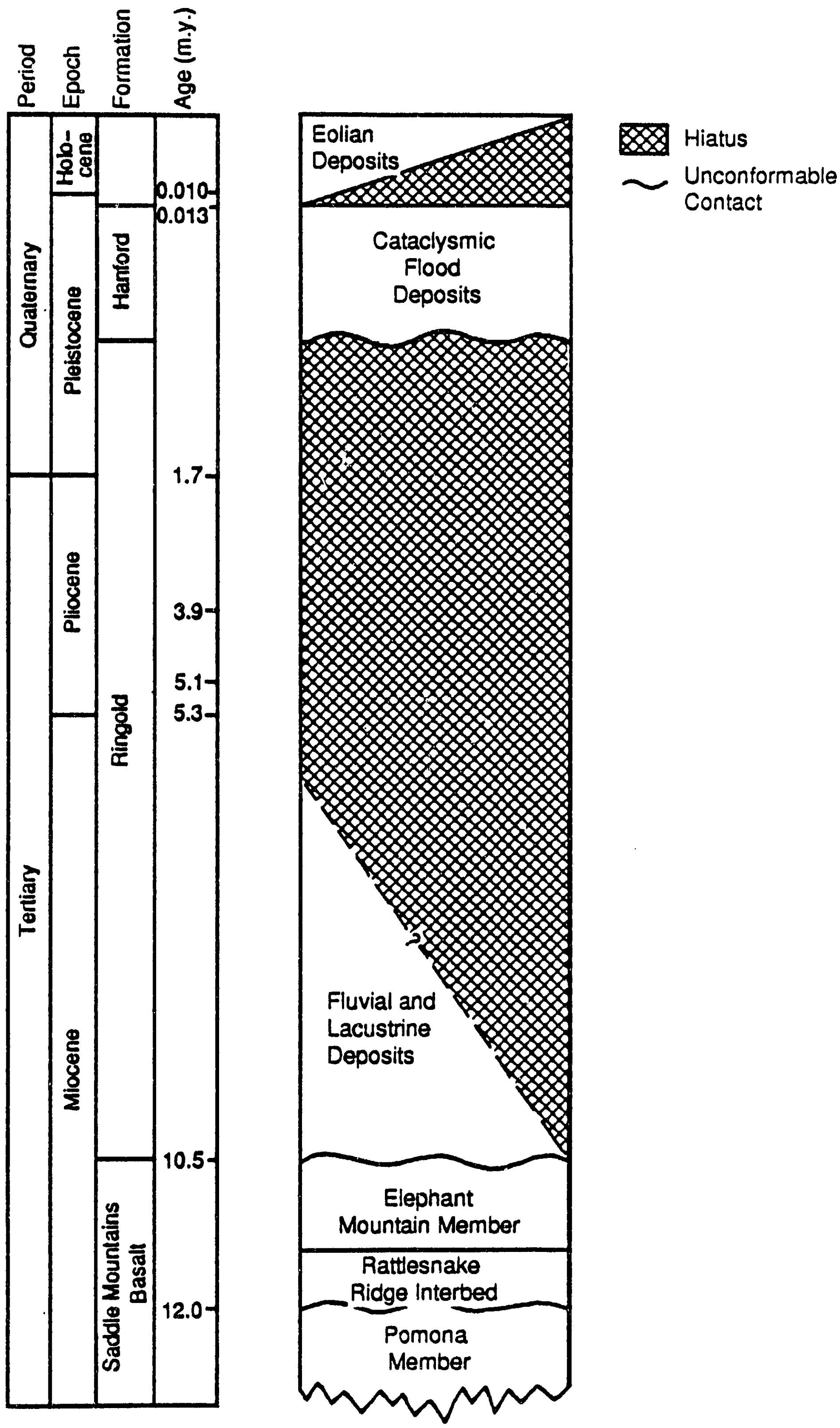

FIGURE A.2. Generalized Stratigraphic Column for the 200-East Area from the ROCSAN database (WHC 1991). The wells used and the characterization data associated with each well are listed in Table A.1. Figure A.3 is a location map of the boreholes in the vicinity of the burial ground. Cross sections, located in Figure A.3, that show the interpreted subsurface stratigraphy based on the data from these wells are presented in Figures A.4 and A.5.

In addition to borehole studies, detailed observations were made and samples were collected from the excavated exposures of the 218-E-12B Burial Ground itself. A geologic map (Plate A.1) of the exposed burial ground wall was prepared and samples of the different lithologic types present were collected for a variety of laboratory analyses. These analyses include grain-size distribution, moisture content, porosity, permeability, bulk density, clay mineralogy, and bulk geochemistry. The analyzed samples are listed in Tables A.2 and A.3 and were collected from locations shown in Plate A.1 and Figures A.6 and A.7. Data from the completed analyses are provided in Appendix B (Parts 1-5). For comparison with outcrop samples, similar analyses were performed on selected samples of borehole cuttings obtained from two wells immediately adjacent to the 218-E-12B Burial Ground (299-E35-1 and 299-E34-7, Figure A.4). Completed analyses are reported in Appendix B (Parts 4-6).

A.2.1.1 Columbia River Basalt Group

The Columbia River Basalt Group is an assemblage of tholeiitic, continental flood basalt flows of Miocene age. These flows cover much of the Columbia Plateau, which includes an area greater than 163,700 km^2 (63,000 mi^2) in Washington, Oregon, and Idaho, and have an estimated volume of about 174,000 km^3 (40,800 mi^3) (Tolan et al. 1989). Isotopic age determinations indicate that basalt flows were erupted from approximately 17 to 6 million years before present (Ma). More than 98% of this volume was erupted in a 2.5-million-year period between 17 and 14.5 Ma (Reidel et al. 1989). The youngest basalt flows in the vicinity of the 218-E-12B Burial Ground belong to the Elephant Mountain Member of the Saddle Mountains Basalt, which is about 8.5 Ma (McKee et al. 1977).

TABLE A.1. Boreholes in the Vicinity of the 218-E-12B Burial Ground

GEOGRAPHIC INFORMATION							HYDROLOGIC INFORMATION			
Borehole	Plant Coordinates Northing	Plant Coordinates Westing	Date Completed	Total Depth	Casing Elevation	Brass Cap Elevation	Open Interval	Elevation Water Table (June 1991)	Saturated Thickness	MEASURED AQUIFER
2-E26-01	44774	48025	5/48	248	617.25	NAV	217-227	404.05	12	Hanford Formation
2-E26-09	44779	46960	9/90	203	602.90	599.89	190-201	404.03	5	Hanford Formation
2-E26-10	44420	46919	8/90	207	601.49	598.49	190-201	404.01	10	Hanford Formation
2-E26-11	44779	44979	9/90	206	599.70	596.72	200-206	405.81	7	Ringold Fm?
2-E27-08	44496	49742	9/87	257	637.83	634.64	226-246	403.25	22	Hanford Formation
2-E27-09	44484	49122	8/87	245	629.21	627.31	219-239	403.49	19	Hanford Formation
2-E27-10	44520	48522	8/87	240	624.47	622.42	213-233	403.73	20	Hanford Formation
2-E27-11	44558	49990	10/89	265	643.29	640.34	230-251	403.16	22	Hanford Formation
2-E34-01	45129	50023	6/61	245	629.42	626.79	215-230	403.66	10	Hanford Formation
2-E34-02	45076	50048	9/87	242	630.80	629.03	220-240	403.44	13	Hanford Formation
2-E34-03	45337	48488	8/87	214	611.52	609.48	193-213	403.96	5	Hanford Formation
2-E34-04	46791	49419	8/87	177	587.56	585.17	157-177	NA	NR	NR
2-E34-05	46791	50014	8/87	192	590.79	589.01	171-191	404.26	2	Hanford Formation
2-E34-06	46784	50609	8/87	196	597.83	596.56	175-195	403.29	1	Hanford Formation
2-E34-07	45520	47949	10/89	206	604.25	601.14	194-205	403.47	7	Hanford Formation
2-E35-01	45870	47339	12/89	194	598.30	595.25	181-192	403.92	1	Hanford Formation
2-E35-02	45180	46959	8/90	202	602.12	599.15	191-201	404.03	5	Hanford Formation
6-47-46A	47039	45994	8/61	207	580.14	NAV	168-181	404.52	1	Hanford Formation
6-47-50	47266	49508	6/80	295	583.87	581.6	260-295	405.51	39	Rattlesnake Ridge Interbed
6-47-51	47481	50969	10/59	167	583.45	NAV	NA	NA	0	NP
6-48-48A (DC-1)	48000	48200	12/72	5661	572.10	NAV	NA	NA	NA	NA
6-48-48B (DC-2)	47968	48255	9/77	3300	572.14	NAV	NA	NA	NA	NA

All data in feet

NR=not reached; NP=not present, NA=not applicable, NAV=not available

Y=yes, N=no

TABLE A.1. Boreholes in the Vicinity of the 218-E-12B Burial Ground (cont.)

Borehole	STRUCTURAL INFORMATION				DATA SOURCES			
	Depth TOB	Elevation TOB	Depth Slackwater Bed	Elevation Slackwater Bed	ROCSAN	Gross Gamma	Drillers Log	Geologists Log
2-E26-01	225	392	40	577.25	Y	Y	Y	Y
2-E26-09	201	399	40	562.90	N	Y	Y	Y
2-E26-10	204	394	27	574.49	N	Y	Y	Y
2-E26-11	198	399	53	546.70	v. few	Y	Y	Y
2-E27-08	257	381	50	587.83	Y	Y	Y	Y
2-E27-09	245	384	50	579.21	Y	Y	Y	Y
2-E27-10	240	384	40	584.47	Y	Y	Y	Y
2-E27-11	262	381	58	585.29	N	Y	Y	Y
2-E34-01	235	394	49	580.21	Y	Y	Y	N
2-E34-02	241	390	NP	NP	Y	Y	Y	Y
2-E34-03	213	399	NP	NP	Y	Y	Y	Y
2-E34-04	176	412	NP	NP	Y	Y	Y	Y
2-E34-05	189	402	34	556.79	Y	Y	Y	Y
2-E34-06	194	403	568 or 562	568 OR 562	Y	Y	Y	Y
2-E34-07	205	396	45	559.27	N	Y	Y	Y
2-E35-01	192	403	NP	NP	0-80	Y	Y	Y
2-E35-02	200	399	39	563.12	v. few	Y	Y	Y
6-47-46A	174	404	35	545.14	Y	Y	Y	N
6-47-50	215	367	50	533.87	265-295	Y	Y	N
6-47-51	159	424	NP	NP	N	Y	Y	N
6-48-48A (DC-1)	205	365	NP	NP	N	N	N	N
6-48-48B (DC-2)	205	365	NP	NP	N	Y	Y	N

All data in feet

NR=not reached; NP=not present, NA=not applicable, NAV=not available

Y=yes, N=no

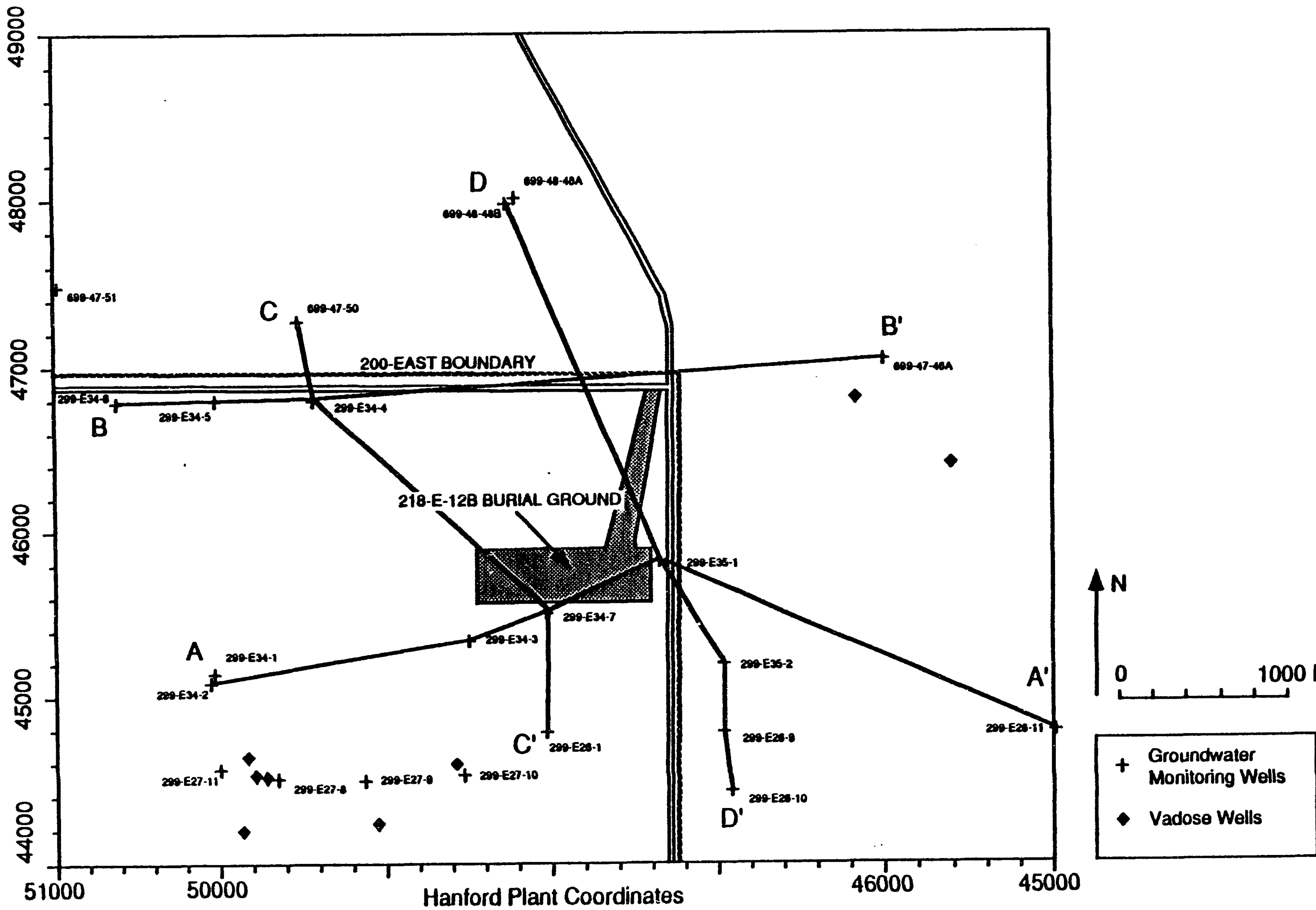

FIGURE A.3. Borehole and Cross Section Location Map

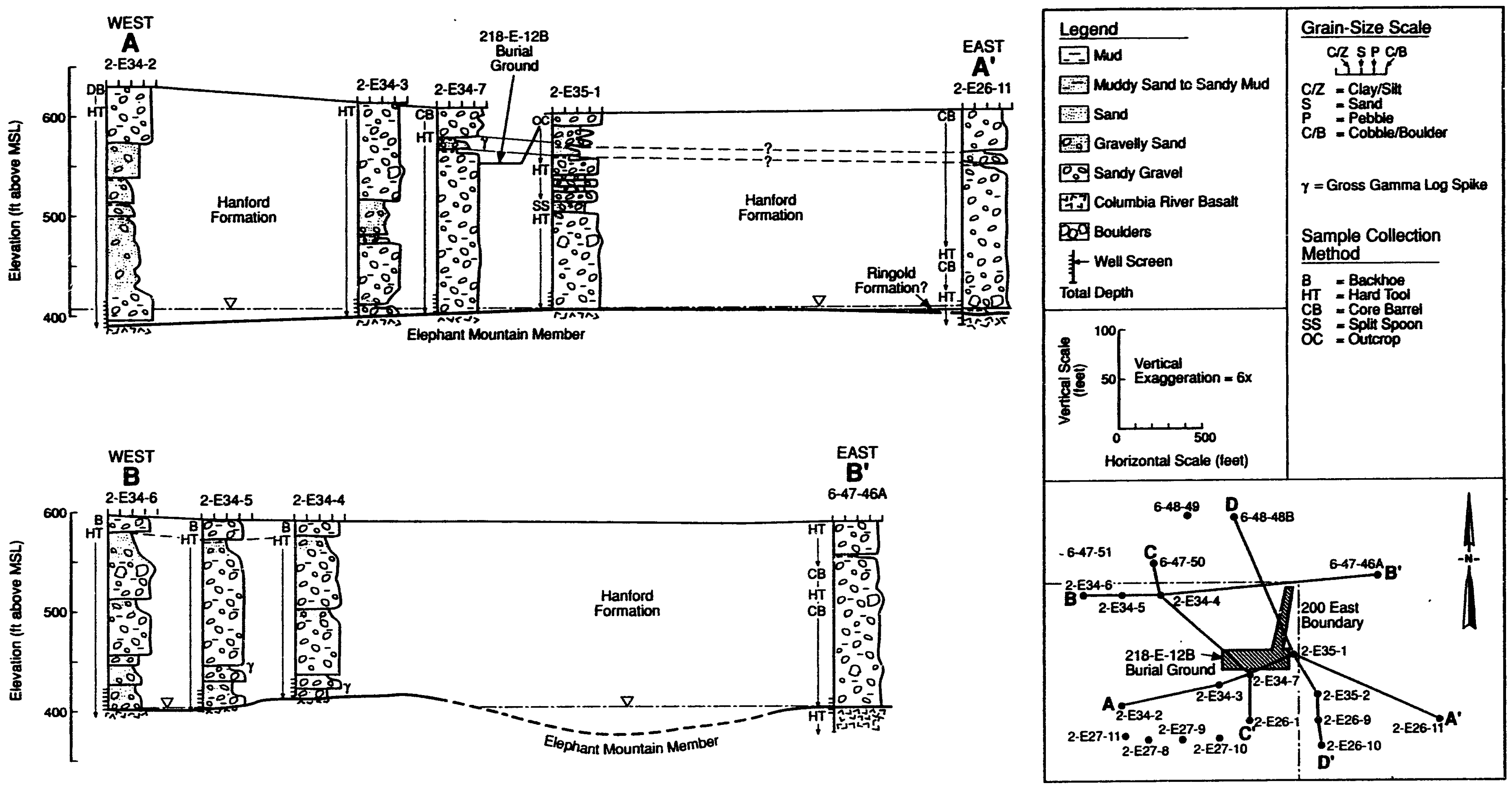

FIGURE A.4. East-West Geohydrologic Cross Sections Near the 218-E-12B Burial Ground

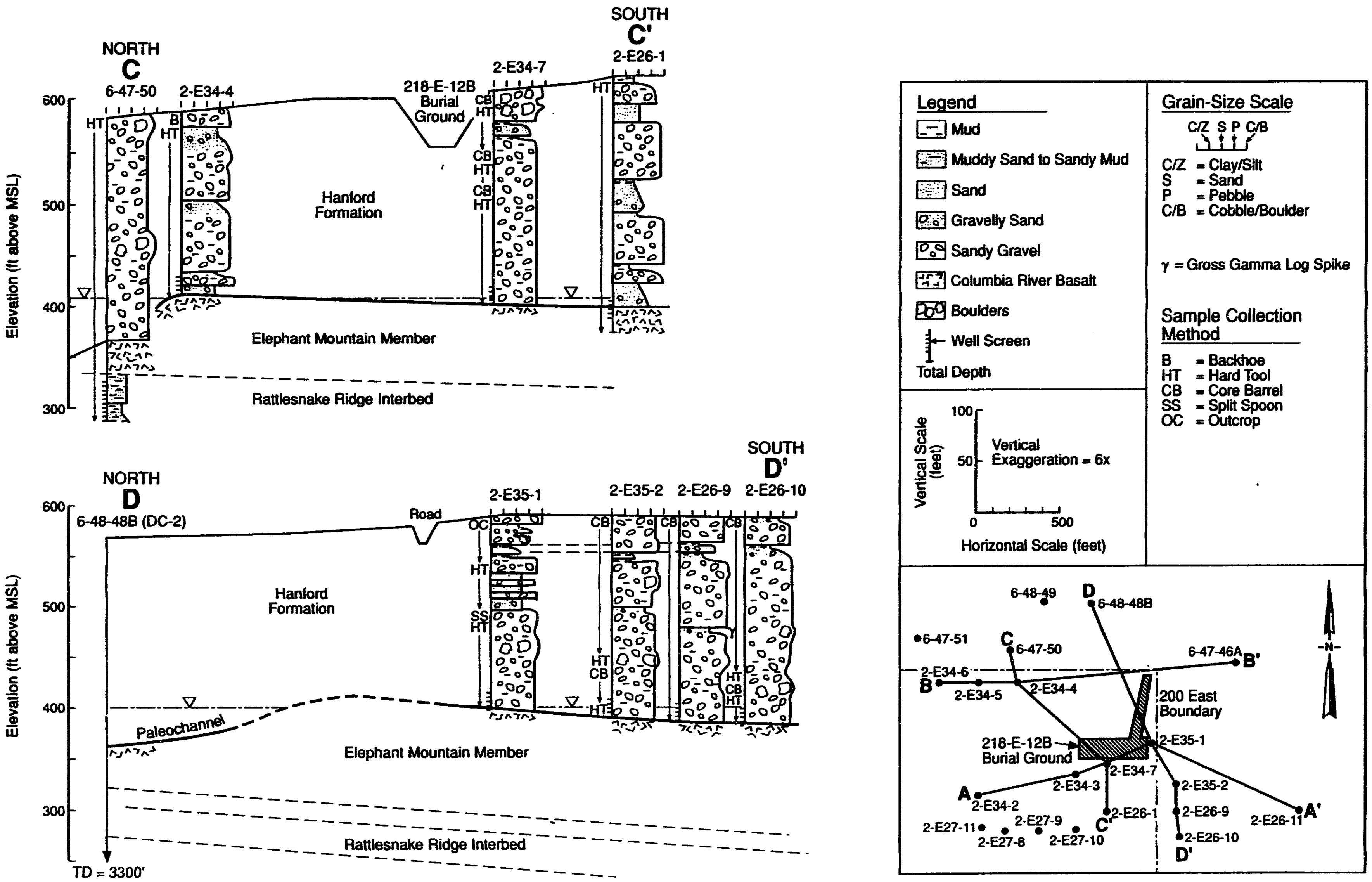

FIGURE A.5. North-South Geohydrologic Cross Sections Near the 218-E-12B Burial Ground

TABLE A.2. Samples from the 218-E-12B Burial Ground Taken for Laboratory Analysis (The location of samples and map units are shown in Plate 1 and Figures A.6 and A.7)

SAMPLE #	DESCRIPTION	MAPPED UNIT	PARTICLE SIZE	PERMEAMETER	BULK DENSITY	POROSITY	BULK GEOCHEMISTRY	CLAY MINERALOGY
1	Sandy Gravel	Qhc						
2	Sandy Foreset	Qhb		X	X	X		
3	Sand	Qha	X	X	X	X		
4	Gravelly Sand Foreset	Qha						
5	Upper Silt	Qha						
6	Upper Silt	Qha		X	X	X		
7	Sandy Gravel	Qhb	X					
8	Gravelly Sand	Qhc						
9	Slightly Muddy Gravelly Sand	Qhb	X					
10	Sandy Gravel	Qhb	X					
11	Fine Sand	Qha	X					
12	Very Fine Sand to Silt	Qha	X					
13	Clay	Qha					X	X
14	Lower Sandy Mud	Qha	X	X	X	X	X	X
15	Plane Laminated Sand	Qha	X	X	X	X	X	
16	Clay	Qha					X	
17	Clay	Qha					X	X
18	Fine Gravelly Sand	Qhb		X	X	X	X	
19	Coarse Gravelly Sand	Qhb		X	X	X	X	
20	Coarse Sandy Gravel	Qha		X	X	X	X	
21	Sandy Mud from 299-E27-11	Qha (?)		X	X	X	X	

TABLE A.3. Samples from Borehole 299-E35-1 Taken for Laboratory Analysis (Map Units refer to Plate 1 and are described in Figures A.6 and A.7.)

DEPTH (FT)	PARTICLE SIZE	BULK GEOCHEMISTRY	CLAY MINERALOGY	MAP UNIT	DRILL METHOD
10		X		Qhb	HT
20		X	X	Qhb	HT
30		X		Qhb	HT
35	X	X	X	Qha	DB
45		X		Qha	DB
49	X	X	X	Qha	DB
60	X				HT
65	X				HT
75	X	X	X		HT
90	X	X			HT
115		X	X		HT
180	X	X	X		HT

HT-Hard Tool
DB-Drive Barrel

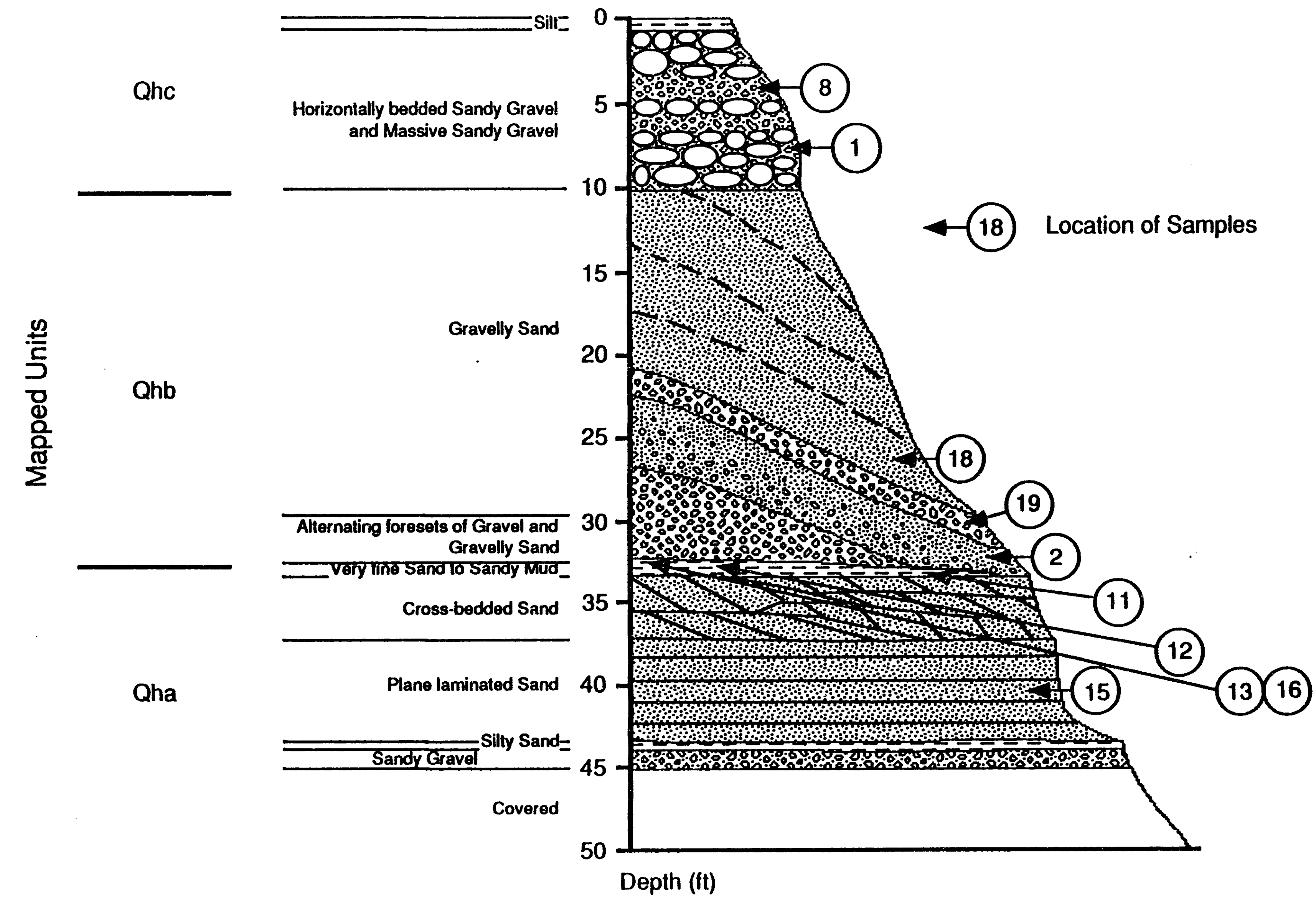

FIGURE A.6. Stratigraphic Section 1 from 218-E-12B Burial Ground Showing Sample Locations and Mapped Units (Refer to Tables A.2 and A.3.)

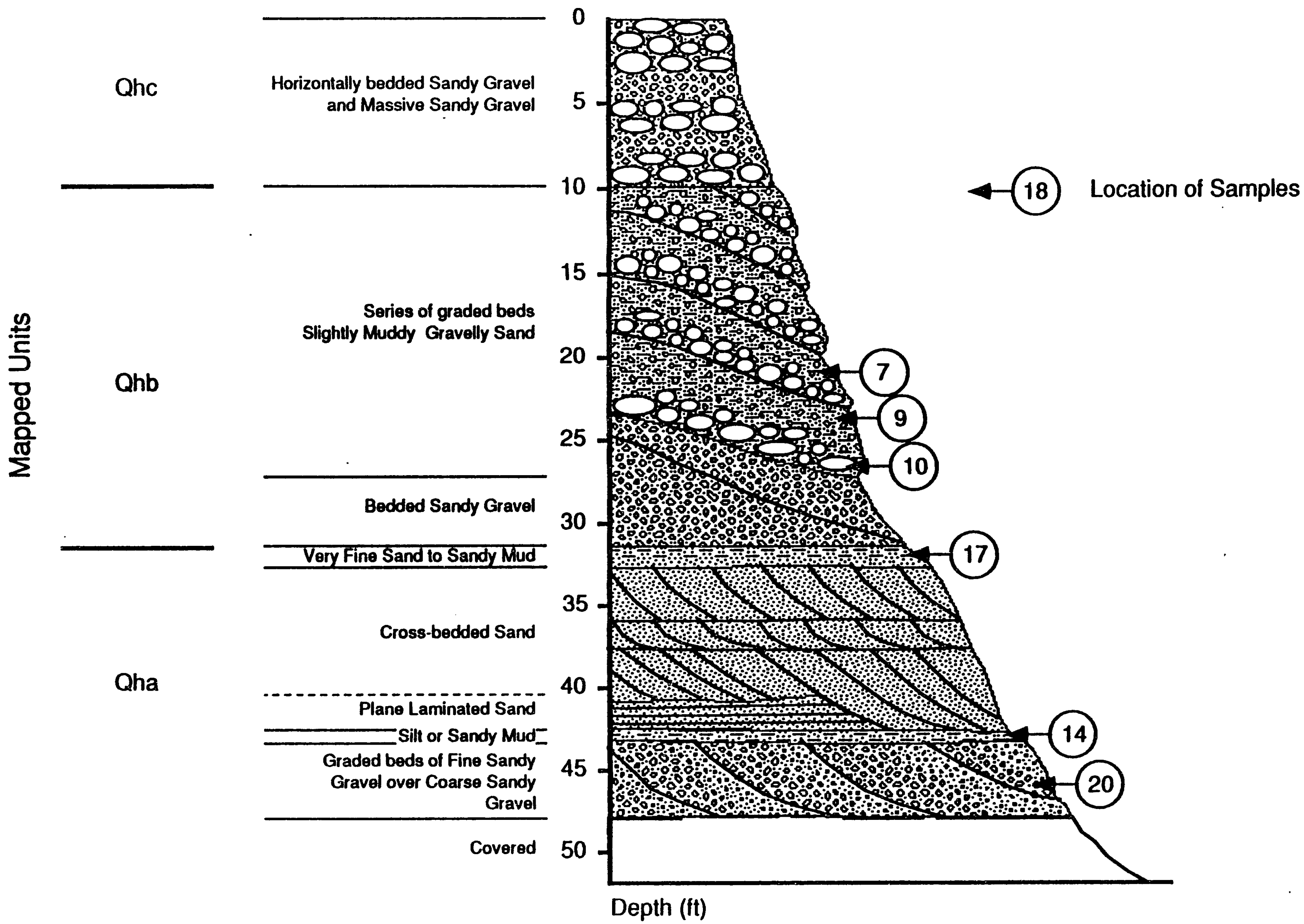

FIGURE A.7. Stratigraphic Section 2 from 218-E-12B Burial Ground Showing Sample Locations and Mapped Units (Refer to Tables A.2 and A.3.)

A.2.1.2 Ellensburg Formation

The Ellensburg Formation consists of all sedimentary interbeds that separate the basalt flows of the Columbia River Basalt Group in the central Columbia Basin (DOE 1988). The frequency and thickness of these interbeds increase stratigraphically upward within the basalt sequence, reflecting an increasing time span separating the younger flows. Interbeds in the vicinity of the 218-E-12B Burial Ground generally consist of fine-grained fluvial and overbank deposits. The uppermost interbed beneath the burial ground is the Rattlesnake Ridge Interbed (see Figure A.2). Regionally it has been divided into four facies (in ascending order): 1) a clayey basalt conglomerate, 2) an epiclastic fluvial-floodplain unit, 3) an air-fall tuff, and 4) a tuffite composed of reworked tuff and epiclastic detritus (Graham et al. 1984).

A.2.1.3 Ringold Formation

The Ringold Formation consists of interbedded clays, silts, sands, and gravels deposited by the ancestral Columbia and Salmon-Clearwater Rivers subsequent to basaltic volcanism (DOE 1988). The Ringold Formation is restricted to topographic and structural basins of south-central Washington. Within the Pasco Basin, it is subdivided into a number of facies associations, including fluvial gravel; fluvial sand; and overbank, lacustrine, and alluvial fan facies associations (Lindsey 1991).

The Ringold Formation is present to the south and east of the study area but is not present within the study area or to the northwest (Figure A.8). During the late Pliocene, several hundred feet or more of Ringold Formation filled this portion of the Pasco Basin. At the end of Ringold time, however, a period of downcutting ensued, first by the Columbia River and later by a series of cataclysmic floods. These erosional episodes removed much of the Ringold Formation from the center of the basin and locally stripped away the entire Ringold Formation, as well as the underlying Elephant Mountain Member.

A.2.1.4 Hanford Formation

The Hanford formation (informal name) is the principal suprabasalt unit in the study area, averaging about 61 m (200 ft) in thickness (Figure A.9). The Hanford formation was deposited intermittently during periods of cataclysmic floods, unmatched by any others on Earth, that inundated the Pasco

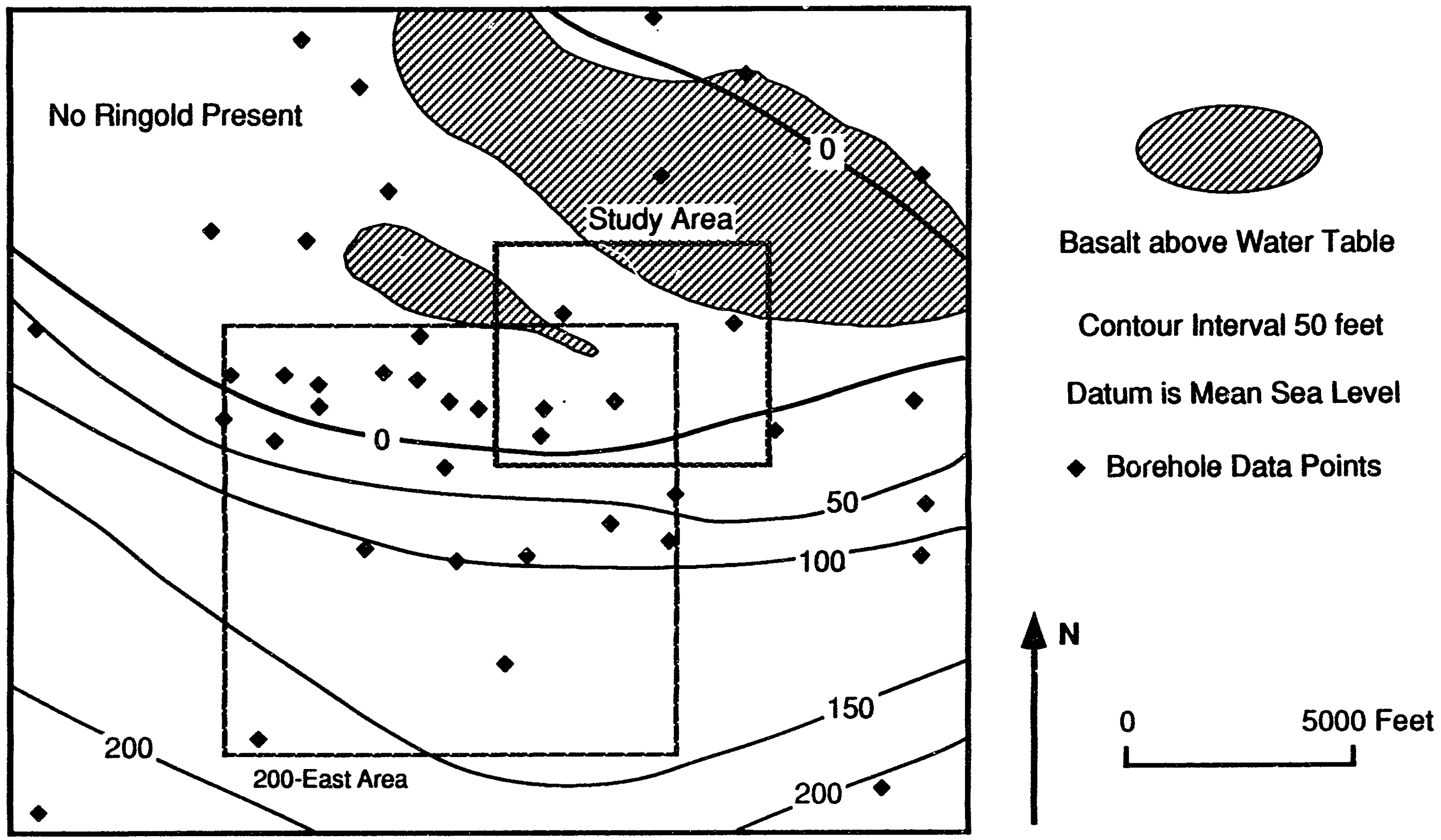

FIGURE A.8. Isopach Map of the Ringold Formation, 200-East Area (modified from Lindsey 1991)

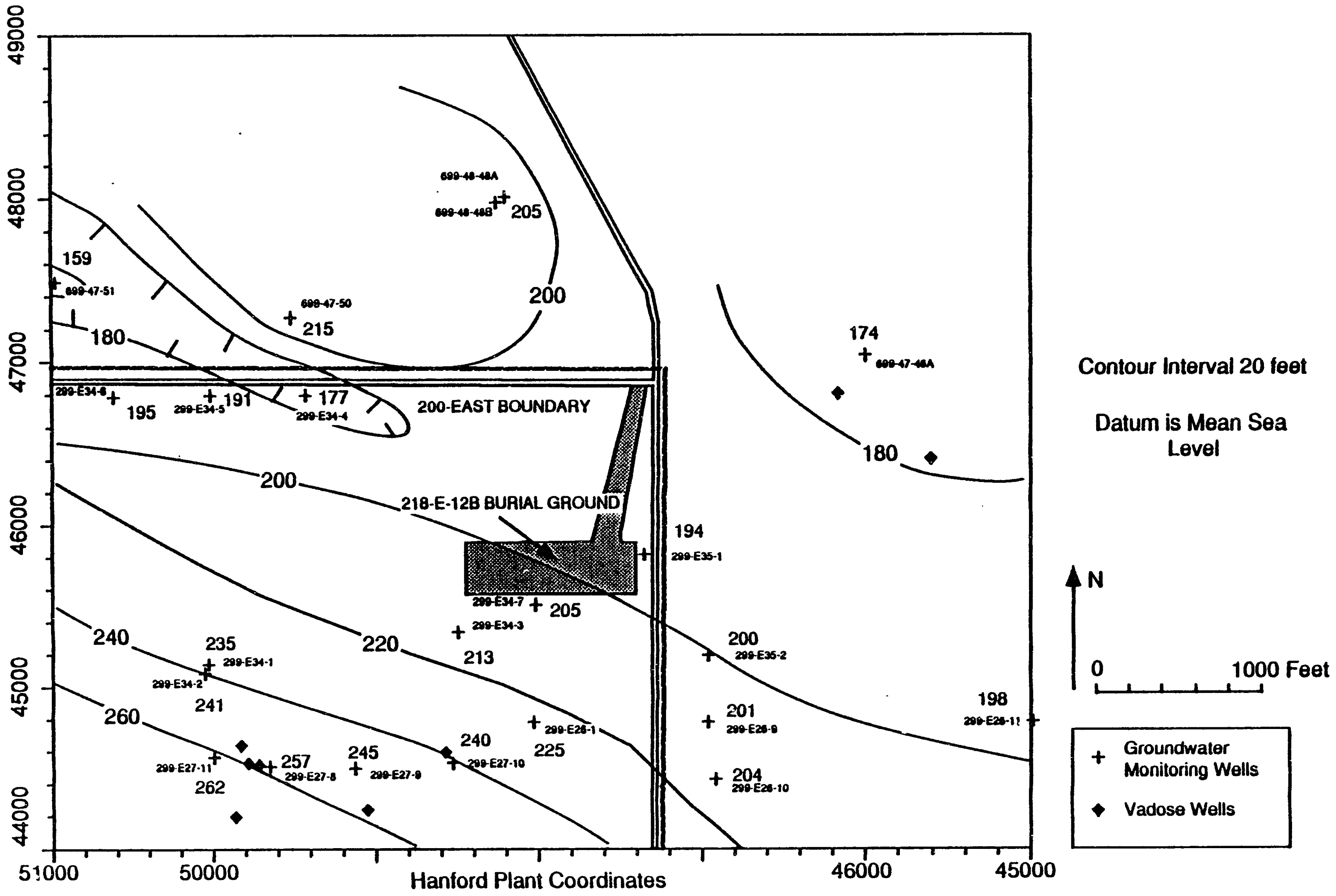

FIGURE A.9. Isopach Map of the Hanford Formation

Basin dozens or more times during the Pleistocene epoch. The earliest floods occurred prior to 800,000 years ago (Bjornstad and Fecht 1989), and the last flood took place approximately 13,000 years ago (Mullineaux et al. 1978). The floodwaters were derived from huge ice-dammed lakes situated along the northern and eastern boundaries of the Columbia Plateau (Baker and Nummedal 1978; Waitt 1980). These lakes discharged at intervals ranging from tens to hundreds of thousands of years and coursed through the Pasco Basin forming a series of anastomosing flood channels. The 200-East Area and the 218-E-12B Burial Ground lie along the margin of one of the principal flood channels. Adjacent to this channel, within the study area, huge levee-type bar deposits (Cold Creek Bar, Figure A.10) composed of mostly coarse-grained sand and gravel were deposited.

Facies Distribution and Sedimentary Structures

The Hanford formation is divided into three facies associations principally on the basis of texture: 1) gravel dominated, 2) sand dominated, and 3) slackwater. While all three facies are present within the study area, the gravel-dominated facies is predominant. Characteristics of the gravel-dominated facies, in contrast to the other facies, include a generally higher basalt content, poorer sorting, and characteristic large-scale foreset bedding (Figure A.11). Less commonly, the flood gravels show horizontal bedding. The beds are usually discernible by minor gradations in particle size, of which maximum sizes range from pebbles to boulders greater than 1 m in diameter. Sediments in the subsurface generally are finer grained to the south and west of the 218-E-12B Burial Ground, as a result of the decrease in current energy away from the flood channel axis. This gradation is apparent in the regional geologic cross section (Figure A.12), where the proportion of sand-dominated facies increases to the south of the burial ground. A similar gradation occurs with increasing distance to the west toward the interior of Cold Creek Bar, as shown in cross sections A-A′ and B-B′ (see Figure A.4).

Although sand-dominated facies are not common in the study area, a well exposed sand-dominated sequence is preserved in the northeast wall of the 218-E-12B Burial Ground (Figure A.13). Sand-dominated facies are better sorted than the gravel-dominated facies and have a "salt and pepper" appearance resulting from a relatively high percentage (30 to 50%) of dark

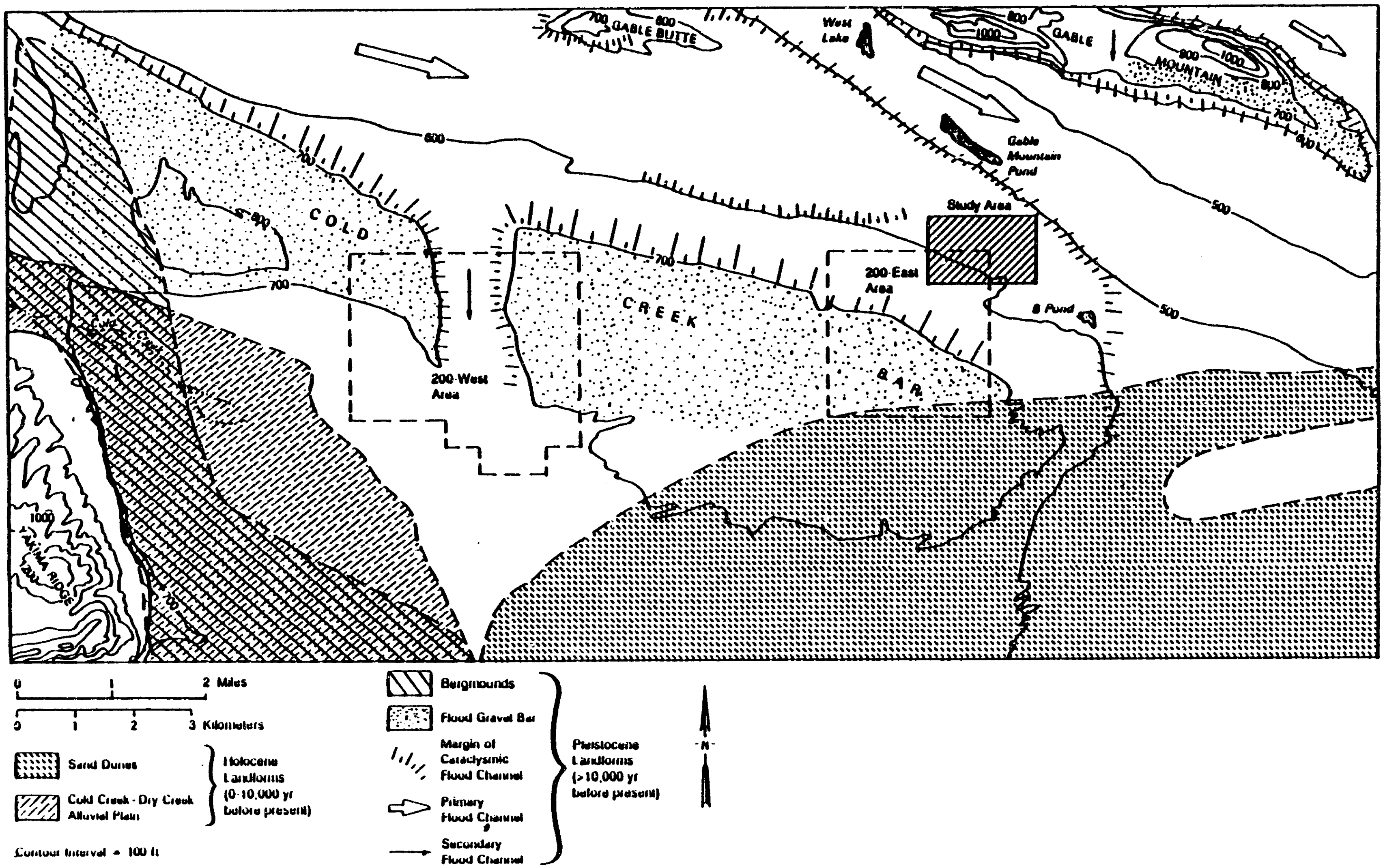

FIGURE A.10. Geomorphic Features Within the Central Pasco Basin (modified from Last et al. 1989)

(A)

(B)

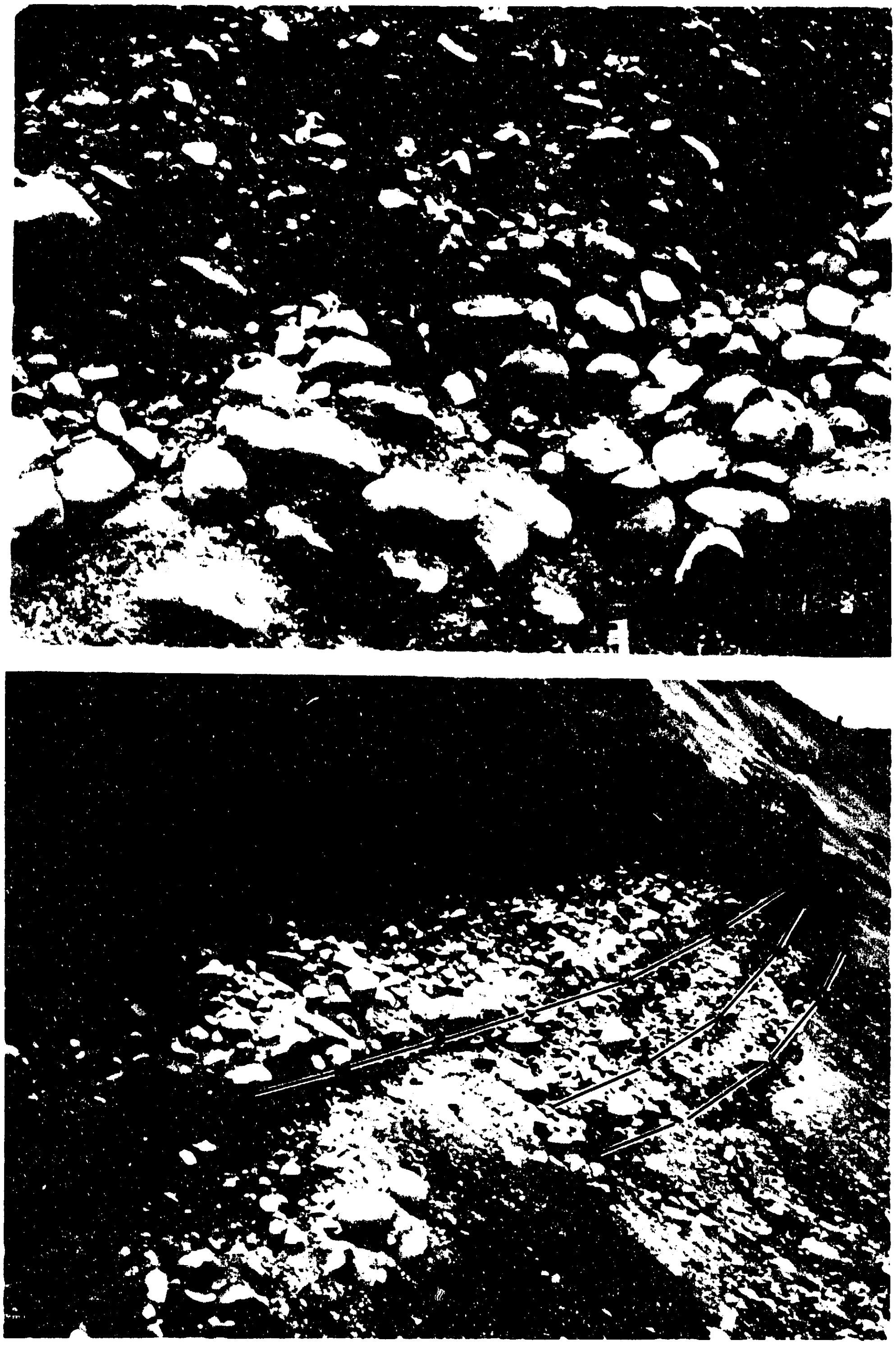

FIGURE A.11. Gravel-Dominated Facies of the Hanford Formation -- Close-up photo (A) shows the coarse-grained, poorly sorted nature of this sedimentary type. Large-scale foreset bedding [indicated by dashed lines in (B)], is common in the gravel-dominated facies.

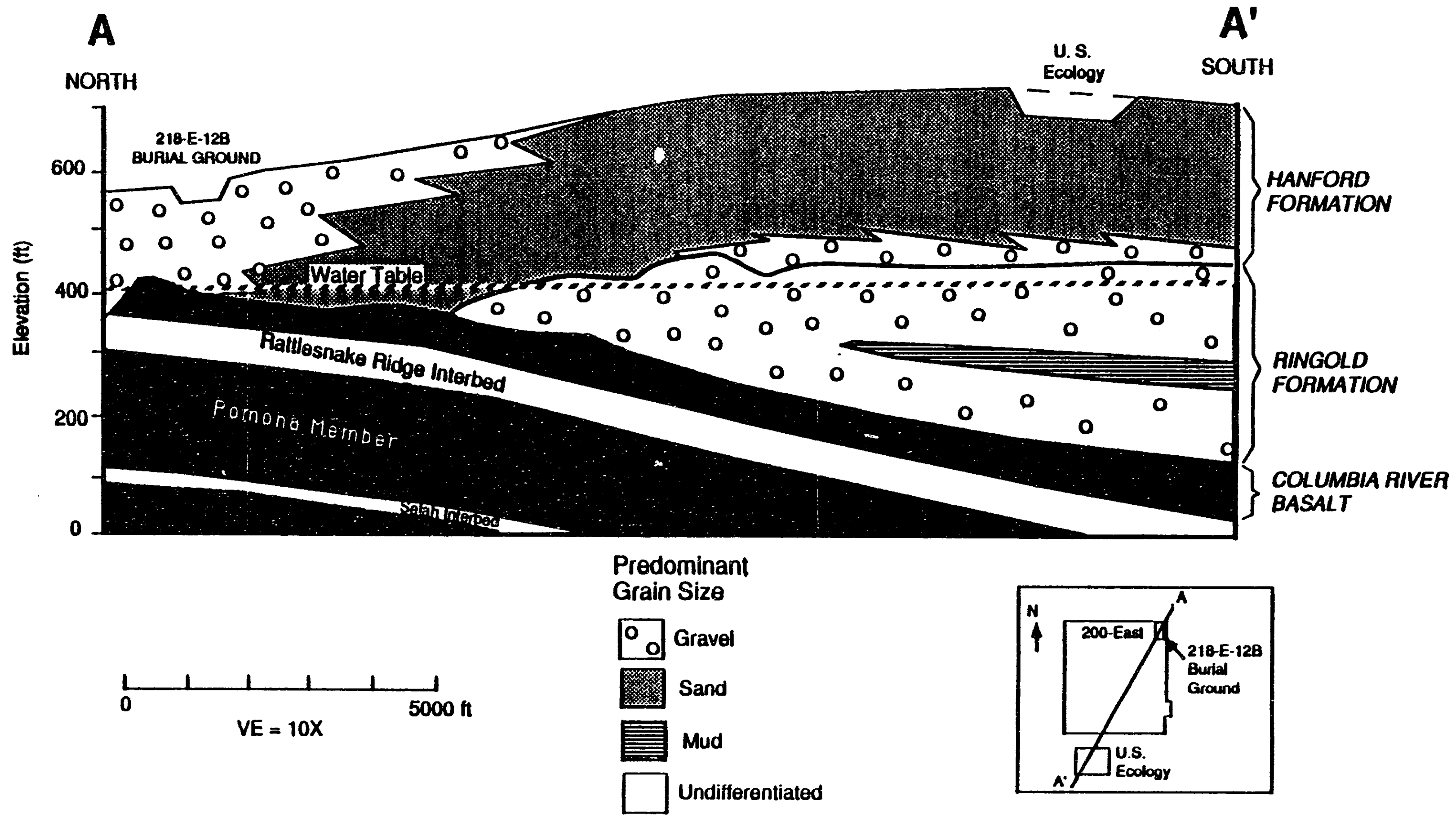

FIGURE A.12. North-South Geologic Cross Section in the Vicinity of the 200 East Area

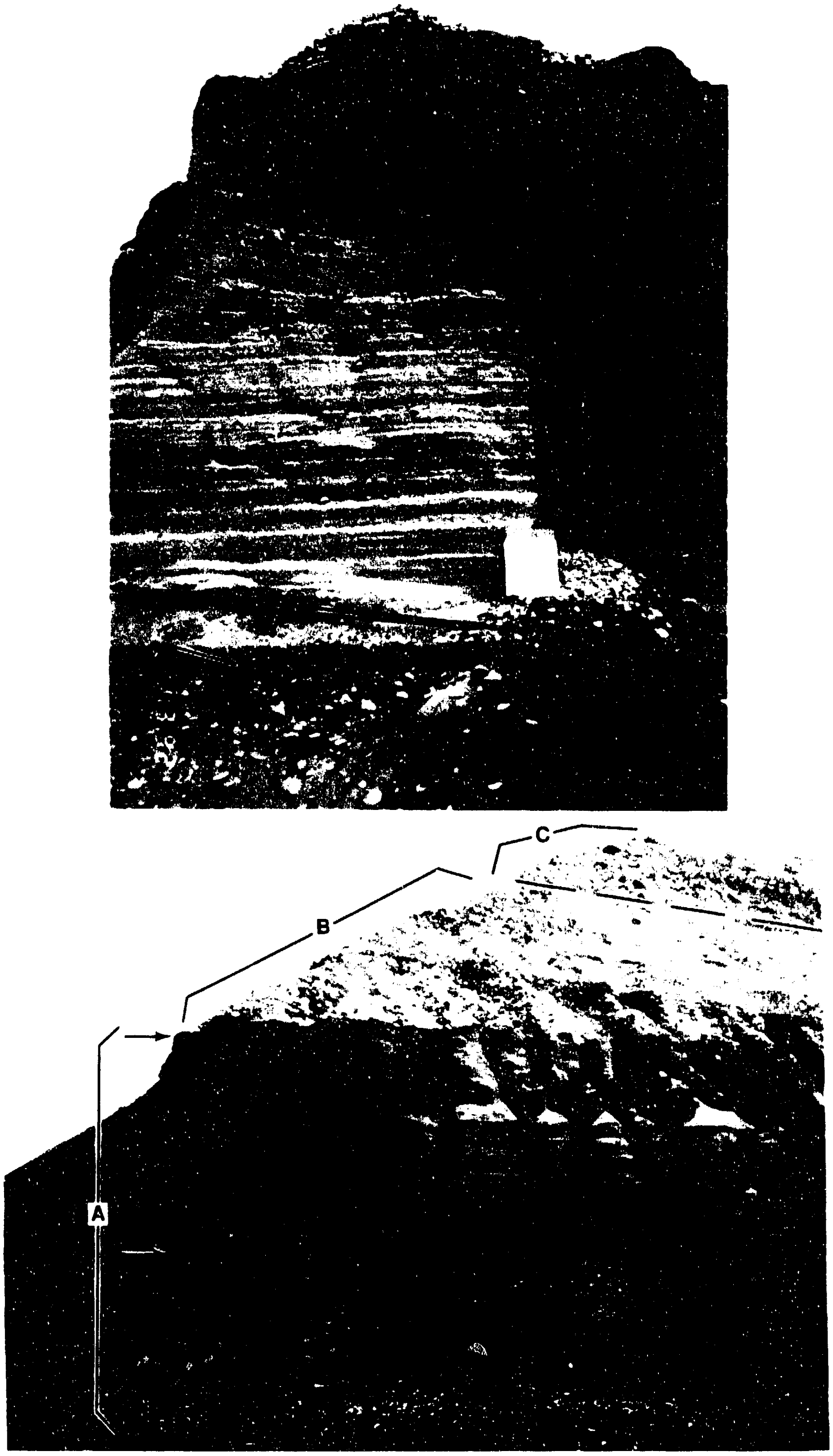

FIGURE A.13. Sand-Dominated Facies of the Hanford Formation -- Slackwater beds above and below the sand-dominated facies are indicated by arrows. Mappable units (Qha, Qhb, and Qhc) within the pit are indicated in the lower photograph.

basaltic grains. Structurally, the sand-dominated facies generally display planar subhorizontal laminations; less commonly, these facies have large-scale tangential cross bedding. Both types of sedimentary structures, planar lamination and tangential cross bedding, are represented in Figure A.13.

Slackwater facies (predominantly silt- to fine sand-sized particles) compose a relatively small proportion of the Hanford formation in the study area. Slackwater deposits, however, are no less significant because they tend to concentrate and control vadose-zone transport of moisture as a result of their higher moisture-retention capacity. In the study area, slackwater deposits represent late-flood sedimentation during the final, waning stages of flooding as currents lost energy. Elsewhere (south of the 200-East Area, for example), slackwater flood deposits are the predominant facies because of less vigorous currents throughout flood duration.

Two thin (a few feet or less) beds of slackwater sand and mud (undifferentiated silt- and clay-sized particles) occur in the exposed upper 15 m (50 ft) of the 218-E-12B Burial Ground and are traceable around most of the excavation (see Plate A.1). Characteristics of these slackwater beds, besides their fine-grained texture, are small-scale climbing ripples or horizontal laminations, grading, and a relatively low percentage of basaltic particles (<10%). These deposits generally contain more moisture than do adjacent coarser-grained deposits of sand and gravel. The lower slackwater bed is shown in Figure A.14, the upper bed in Figure A.15.

Several interesting structural features are displayed in the exposed north wall of the 218-E-12B Burial Ground (see Figure A.15). Of particular interest is a set of three giant current waves composed of coarser-grained (i.e., higher-energy) sand and gravel. Wave crests are approximately 45 m apart and preserved approximately 10 m below the undisturbed surface. Draped over the tops of these waves are slackwater deposits whose thicknesses vary significantly over relatively short distances. The deposits are thinner toward the crest of the wave and thicker in the troughs, especially on the lee sides of the waves. The measured axis of one of the waves strikes N20E, a direction consistent with other paleoflow indicators that suggest deposition by floodwaters moving from northwest to southeast. Waveforms of similar scale

FIGURE A.14. Slackwater Facies of the Hanford Formation. An approximately 1-ft-thick bed of slackwater sand and silt (arrow) lies between foreset-bedded gravels (below) and cross-bedded sand (above). Slackwater deposit formed during the waning stages of flooding associated with the underlying gravels.

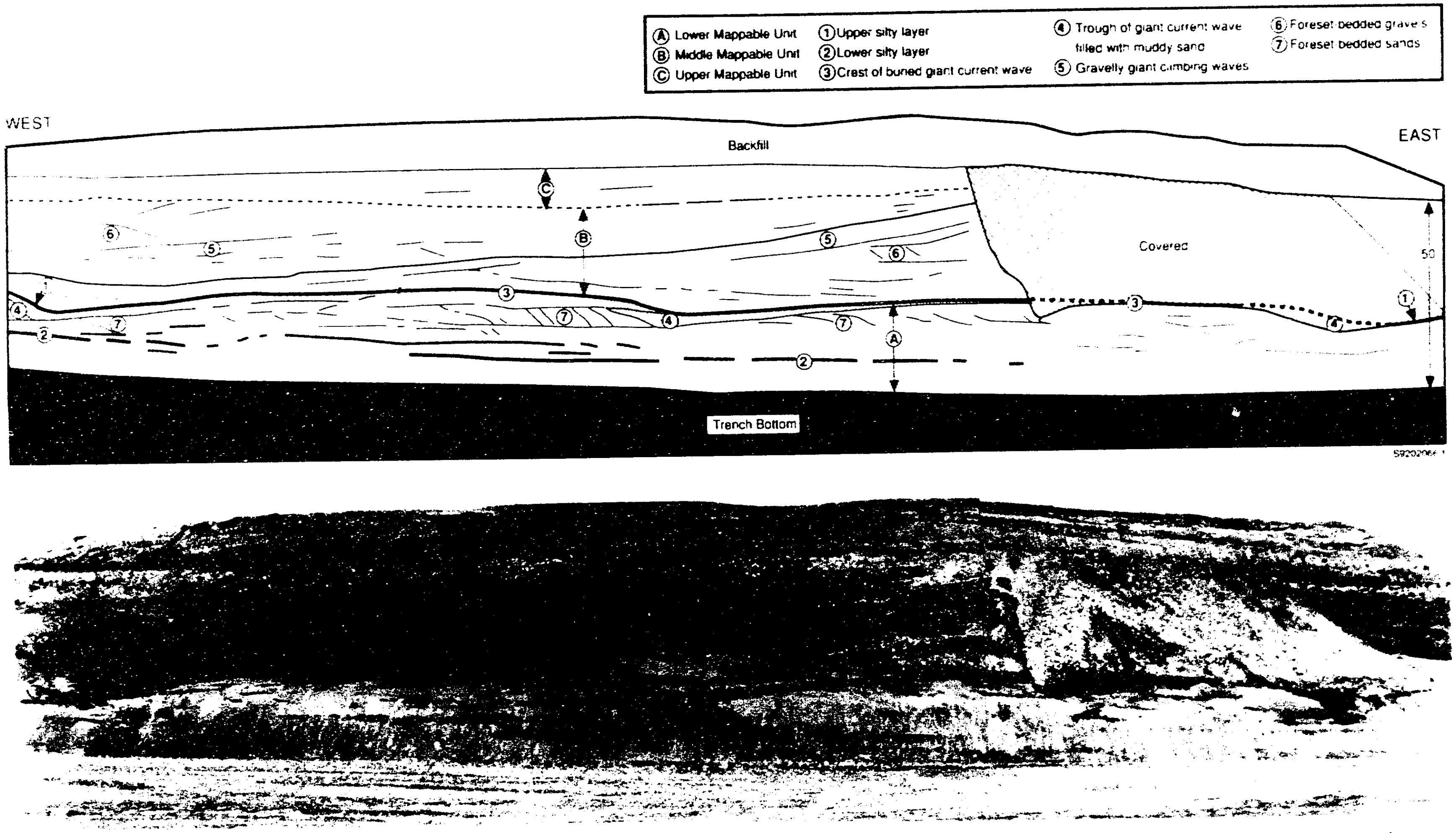

FIGURE A.15. Photomosaic (A) and Trace (B) of the North Wall of the 218-E-12B Burial Ground. Trench wall roughly parallels flood paleocurrent. The cross section of several buried giant waves is apparent by a draping slackwater bed, designated by the #3 on B. Other structural features include climbing waves of gravel (#5), as well as ubiquitous foreset-bedded gravels (#6) and sands (#7).

and origin, left behind by the most recent flood (approximately 13,000 years ago), are well documented at the surface within the Pasco Basin and Channeled Scabland (Baker 1978).

Heterogeneity

Unlike conditions within the Ringold Formation, lateral continuity and correlation of individual strata within the Hanford formation are more difficult. Correlations within the Hanford formation are uncertain because 1) multiple floods occurred that inundated the Pasco Basin from different directions, 2) sedimentation occurred rapidly under an extremely complex and constantly changing system of flood channels and bars, and 3) samples collected during drilling may be unrepresentative. Interpretations based on borehole cuttings and geophysical logs of varying relevance and quality are open to question because drilling with a hard-tool bit tends to homogenize samples, thus obscuring heterogeneities.

Heterogeneity within the Hanford formation occurs at such a scale that strata identified in one borehole often cannot be correlated to adjacent boreholes, partially as a result of the complex history of flooding. Dozens of floods, or more, probably have occurred during the last million years (Waitt 1980) with the floodwaters coming from many directions. The last flood(s) appear to have inundated the Pasco Basin from the northwest, but good evidence suggests that other floods also entered the Pasco Basin from the north (Baker and Nummedal 1978; Waitt 1980) and the east (Malde 1968; Scott et al. 1983). Successive floods tended to destroy or cloud the evidence from previous floods, particularly near high-energy flood channels. This is true for boreholes near the 218-E-12B Burial Ground, with the possible exception of a slackwater bed located 10 to 15 m below the surface. (This bed will be discussed further in the structure section of this report.) Another complicating factor is the extremely rapid rate of sedimentation and lack of reworking of the sedimentary deposits. Often, the end result of erosion and backfilling in proximity to the flood channels is a single sequence of undifferentiated gravels (i.e., gravel-dominated facies) with occasional lenses of sand or gravelly sand (i.e., sand-dominated facies).

Limitations and Uncertainties Related to Using Some Data

As indicated previously, hard-tool samples may not be representative of the formation. Unlike samples collected via the drive-barrel tool,which provide relatively representative samples, those collected with a hard tool may be significantly altered during drilling; commonly they are pulverized. The degree of pulverization varies inconsistently, depending on the driller and formation characteristics. Thus, physical properties such as grain-size distribution, sorting, and structure are altered or destroyed in the process of hard-tool drilling. Another limiting factor is that hard-tool samples represent a homogenization of several or more feet of formation so that thinner strata often go unnoticed. Therefore, more credence should be applied to those interpretations based on core-barrel samples versus those from hard-tool samples. The sampling methods are identified on the geologic cross sections (see Figures A.4 and A.5).

Gross gamma geophysical logs are sometimes useful for differentiating slackwater facies from coarser-grained facies. However, their utility is limited by the lack of contrast in natural radioactivity between the slackwater beds and the coarser facies. Under these conditions, the slackwater beds must be several feet thick to be detected, a criterion which is not often satisfied.

As a test to determine how borehole cuttings compare to in situ samples from outcrop exposures, characterization samples were collected from two boreholes immediately adjacent (within a few tens of feet) to the 218-E-12B Burial Ground and from the burial ground walls themselves. Results, based on available data, indicate significantly more variability and heterogeneity in the outcrop than can be deciphered from borehole cuttings, or from the present generation of gross gamma geophysical logs collected at Hanford (Figures A.16 and A.17).

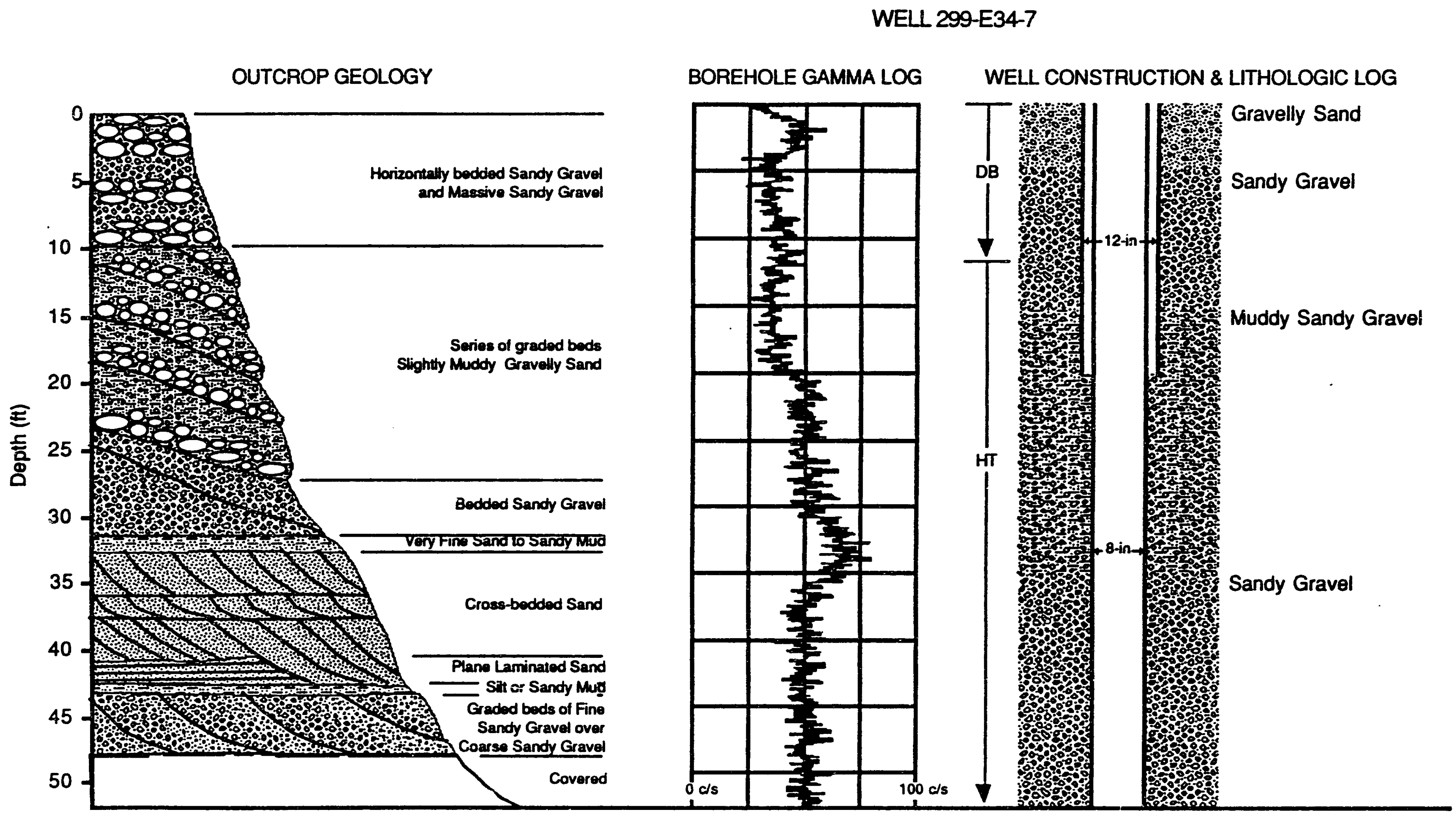

FIGURE A.16. Comparison of Outcrop Exposed Along Southern Wall of 218-E-12B Burial Ground with Borehole 299-E34-7

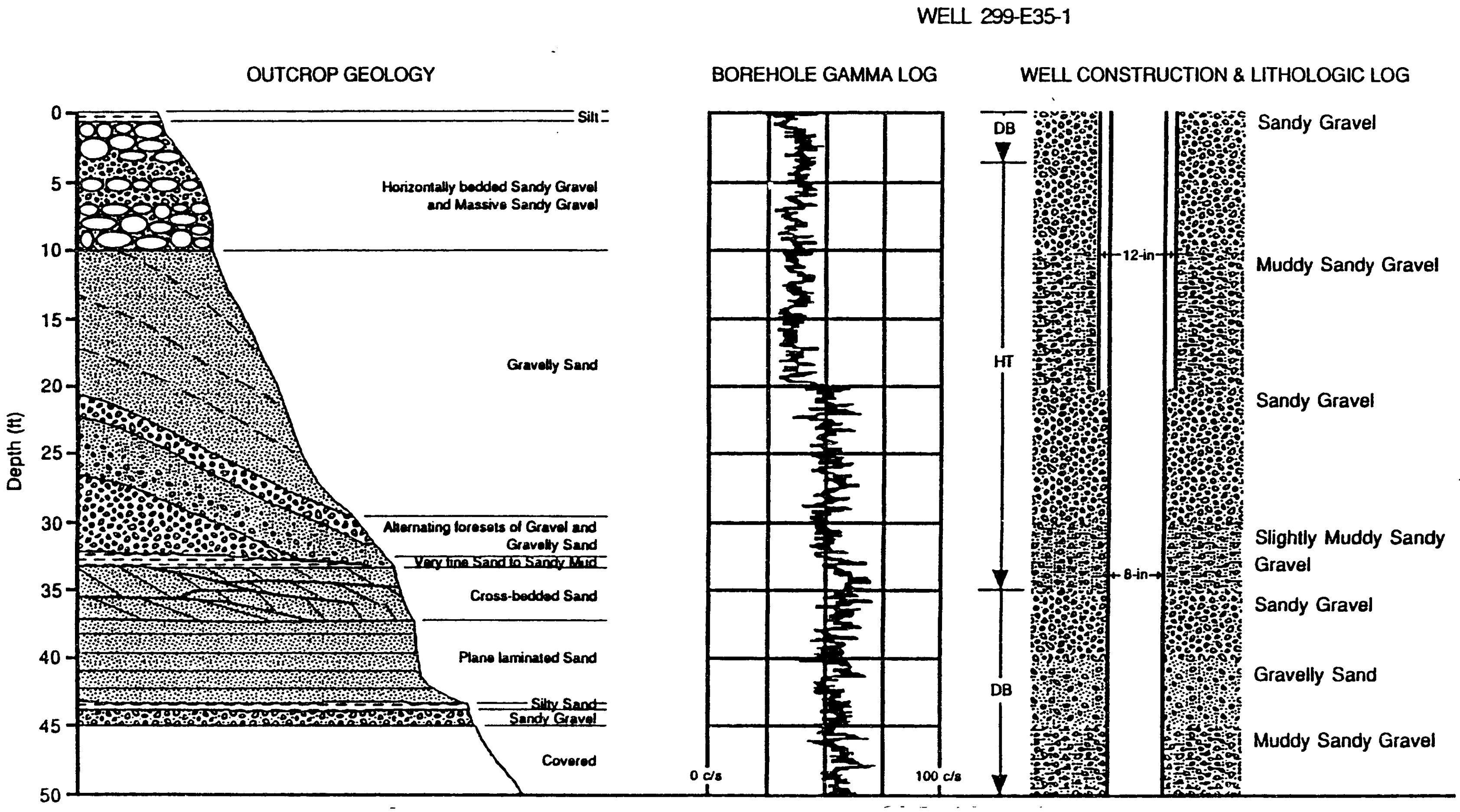

FIGURE A.17. Comparison of Outcrop Exposed Along Eastern Wall of 218-E-12B Burial Ground with Borehole 299-E35-1

A.2.2 STRUCTURE

A.2.2.1 Regional Structure

The Hanford Site lies along the eastern margin of the Yakima Fold Belt (DOE 1988). The fold belt is characterized by long narrow anticlines, generally capped by basalt, separated by broad synclines filled with fluvial and lacustrine sediments. The anticlines trend west or northwest. They are typically asymmetric with one steep, commonly overturned limb; the opposing limb is gently deformed. The Umtanum Ridge structure is one of these anticlines. Its eastern terminus is marked by a series of doubly plunging, en echelon anticlines. Gable Mountain, north of the study area (Figure A.18), lies along the easternmost end of this structure. The southern limb of the Gable Mountain Anticline dips gently (average 2 degrees), to the south (Fecht 1978) toward the axis of the Cold Creek Syncline. The 218-E-12B Burial Ground lies on this southern limb.

A.2.2.2 Local Structure

In the study area, the tectonic structure at the top of the Columbia River Basalt Group is dominated by a plunging anticline and a pothole. Tectonic structures within the Hanford formation, if any are present, are difficult to discern because of its relatively young age with respect to folding and the lack of correlatable units.

A probable anticline at the top of the basalt occurs within the northwestern part of the study area (Figure A.19). It strikes northwest and plunges to the southeast, directly toward the 218-E-12B Burial Ground. Up to 20 m of the basalt flow has been removed locally by erosion during the cataclysmic Hanford flooding (Graham et al. 1984). Nevertheless, this anticline and another larger one to the northeast (Figure A.20) both persist after restoration to a pre-erosion thickness of 30 m. Within the study area, the smaller fold has an amplitude, measured on eroded basalt, of around 6 m.

Several small plunging anticlines occur adjacent to the Gable Mountain and Gable Butte structures (see Figure A.18). Fecht (1978) considered these structures to be parasitic to the eastern extension of the Umtanum Ridge

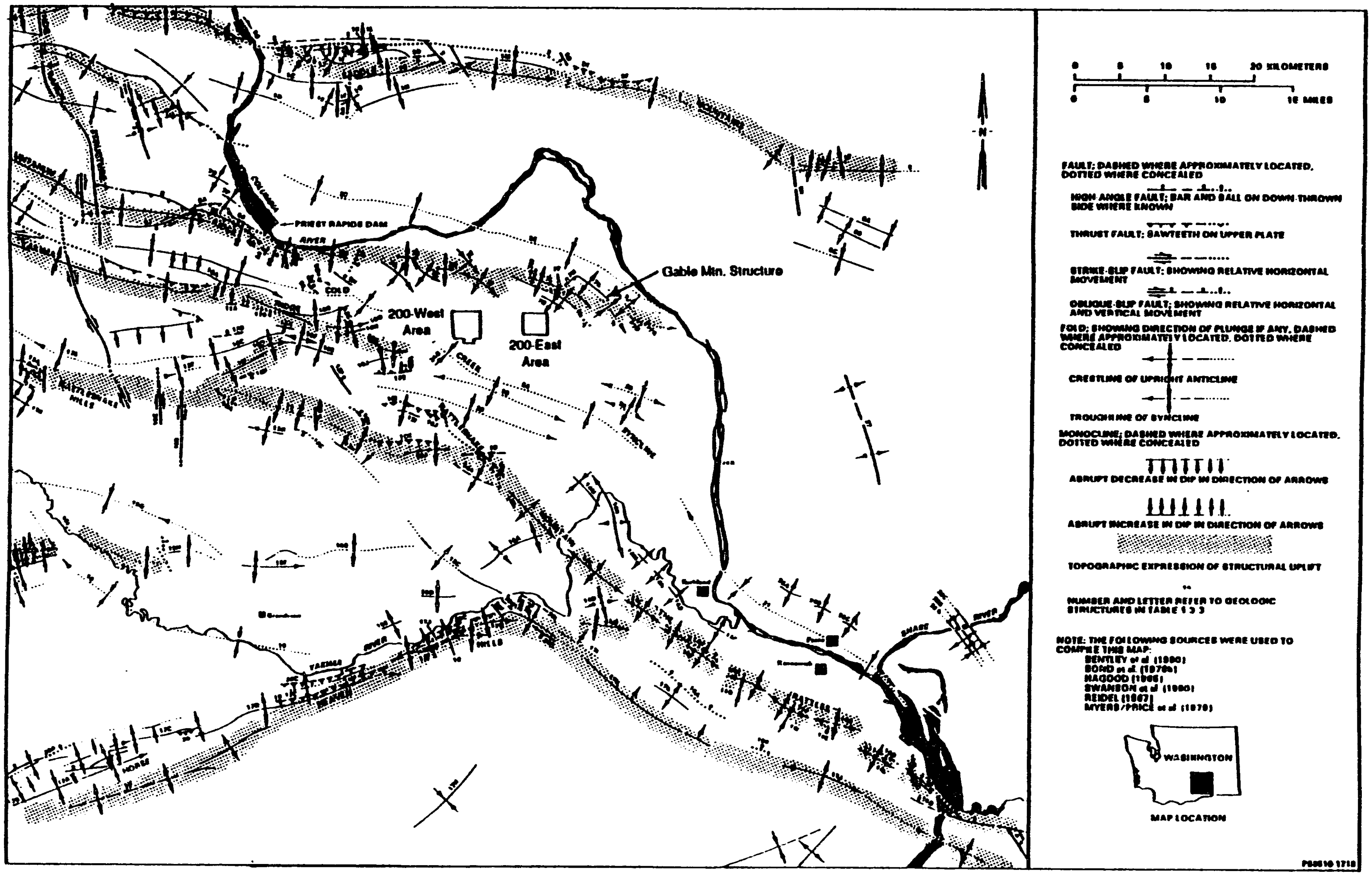

FIGURE A.18. Structural Elements of the Yakima Fold Belt (from BWIP 1982)

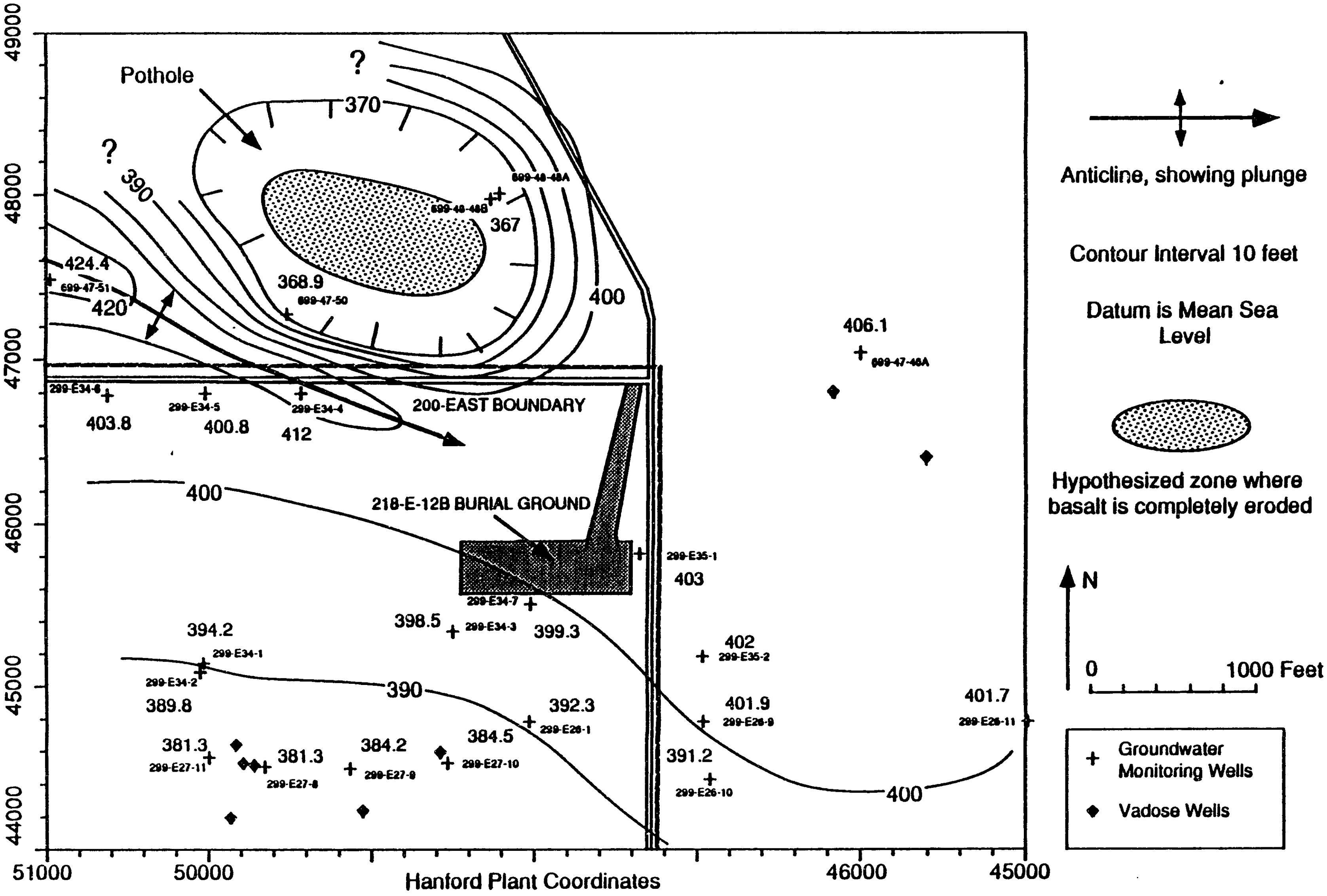

FIGURE A.19. Structure Map of Top of Columbia River Basalt Group

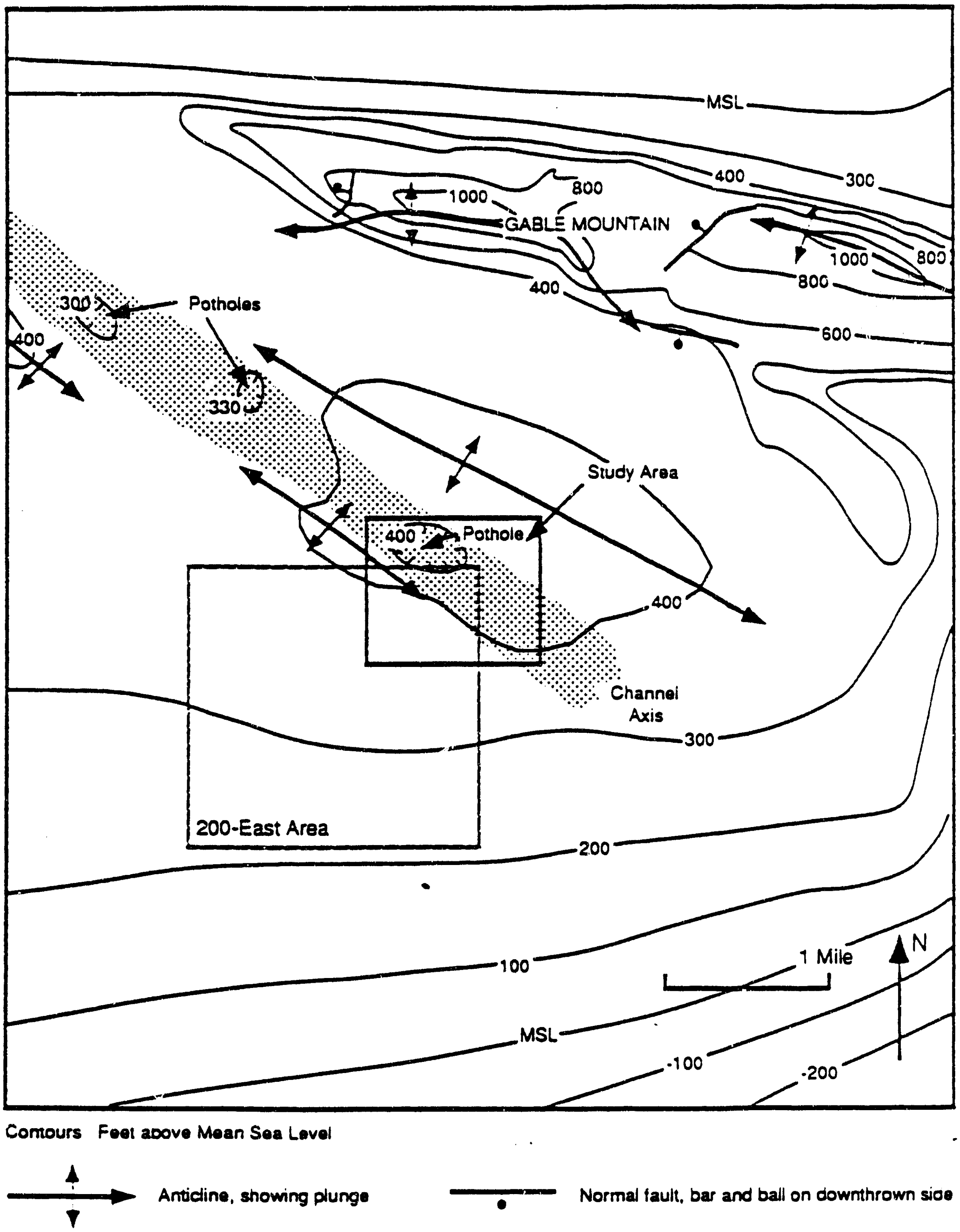

FIGURE A.20. Structure Map of Top of Columbia River Basalt Group, Central Hanford Site (modified from Graham et al. 1984) structure. The presence of Ringold fanglomerates along the southern flank of Gable Mountain suggests that these structures were present during Ringold time. It is not possible to determine whether the Hanford formation has been folded by these structures. However, such a situation is unlikely because the Hanford formation near the channels is probably late Pleistocene (<30,000 years ago).

A distinctive depression forms the northeastern boundary of the anticline within the study area (see Figure A.19). Well control for the shape of the depression is weak toward its northwest; however, it appears to be circular and steep sided, with a maximum diameter of 490 m and a minimum depth of 10 m. The maximum depth is around 30 m. The shape and size are similar to those of potholes, geomorphic features formed during the cataclysmic floods.

The mechanics of pothole formation within the Channeled Scabland are not well understood. Potholes probably developed from macroturbulent flow -- very large-scale turbulent flow typified by the development of secondary circulation, flow separation, and birth and decay of vorticity around obstacles and along irregular boundaries (Baker 1978). The most important form of erosion in macroturbulence is the "kolk" (Matthes 1947), an intense energy dissipation by upward vortex action that can produce phenomenal hydraulic lift forces. These forces would be capable of plucking out large pieces of basalt from irregular surfaces to form potholes.

Potholes would be expected in zones of very high fluid flow and relatively low sediment content (Baker 1978). The flow of the floodwaters within the study area was probably initially confined to the pre-existing main channel of the ancestral Columbia River (see Figure A.20). As the floodwaters eroded downward, the top of the basalt was encountered and erosion continued. In the region near the study area, the channel was localized by small anticlines, and this initial confinement of the floodwaters probably promoted the local development of potholes (see Figure A.20).

A single slackwater sand and mud bed similar to the two exposed within the 218-E-12B Burial Ground was traced from the burial ground to many of the wells within the study area (Figure A.21). This bed was recognized from a combination of geologists' logs, drillers' logs, moisture content data, and

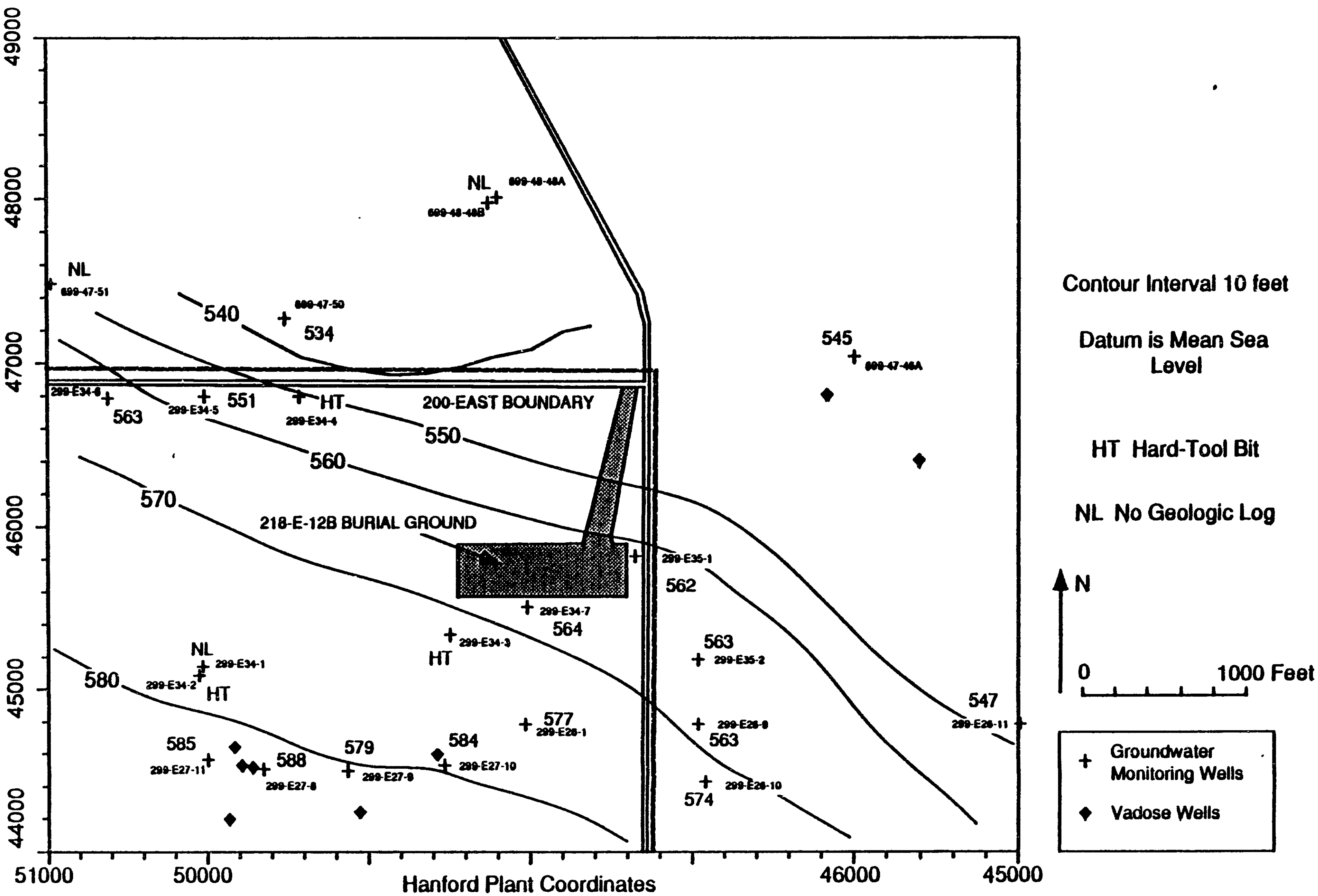

FIGURE A.21. Structure Map of Shallow Slackwater Deposit of Hanford Formation drill-penetration data. The bed was not recognized in some wells drilled with a hard tool; either the bed was not present at these locations or the drilling process obliterated any evidence.

The variability of thickness of the slackwater beds within the 218-E-12B Burial Ground suggests it is highly unlikely that a single bed occurs continuously throughout this region. However, the well evidence suggests that bed continuity cannot be dismissed. The aggradational nature of the overlying sands and gravels, in concert with the cohesiveness of the shale within the slackwater bed, may have protected it from erosion.

The structure at the top of the slackwater bed dips gently to the northeast and mimics the local topography (Figure A.22). This is consistent with the aggradational nature of the Hanford formation expressed along Cold Creek Bar, and the lack of erosion at its surface subsequent to deposition of the Hanford formation.

A.2.3 HYDROLOGY

Regional hydrology will be discussed in a separate section of this appendix. Several published reports also cover this subject (Newcombe et al. 1972; LaSala and Doty 1975; Gephart et al. 1979; Graham et al. 1981). The present discussion will be limited to hydrology of the study site.

Groundwater in the vicinity of the study area exists under both unconfined and confined conditions. The unconfined aquifer is generally contained within the Hanford formation, the lower confining layer being the Elephant Mountain Member of the Saddle Mountains Basalt (see Figures A.4, A.5, and A.12). A generalized stratigraphic column of these units was shown in Figure A.2. Although the Elephant Mountain flow generally acts as a confining layer between the unconfined and uppermost confined aquifers, there are areas where these aquifers are hydrologically or physically connected (see the section on aquifer intercommunication). Saturated hydraulic conductivities for the Hanford formation, based on aquifer tests, range from 25 to 27,500 m/day (80 to 90,000 ft/day) (Graham et al. 1981; Last et al. 1989, Borghese et al. 1990). The highest hydraulic conductivities are associated with matrix-depleted bouldery gravels, which are generally not present beneath the

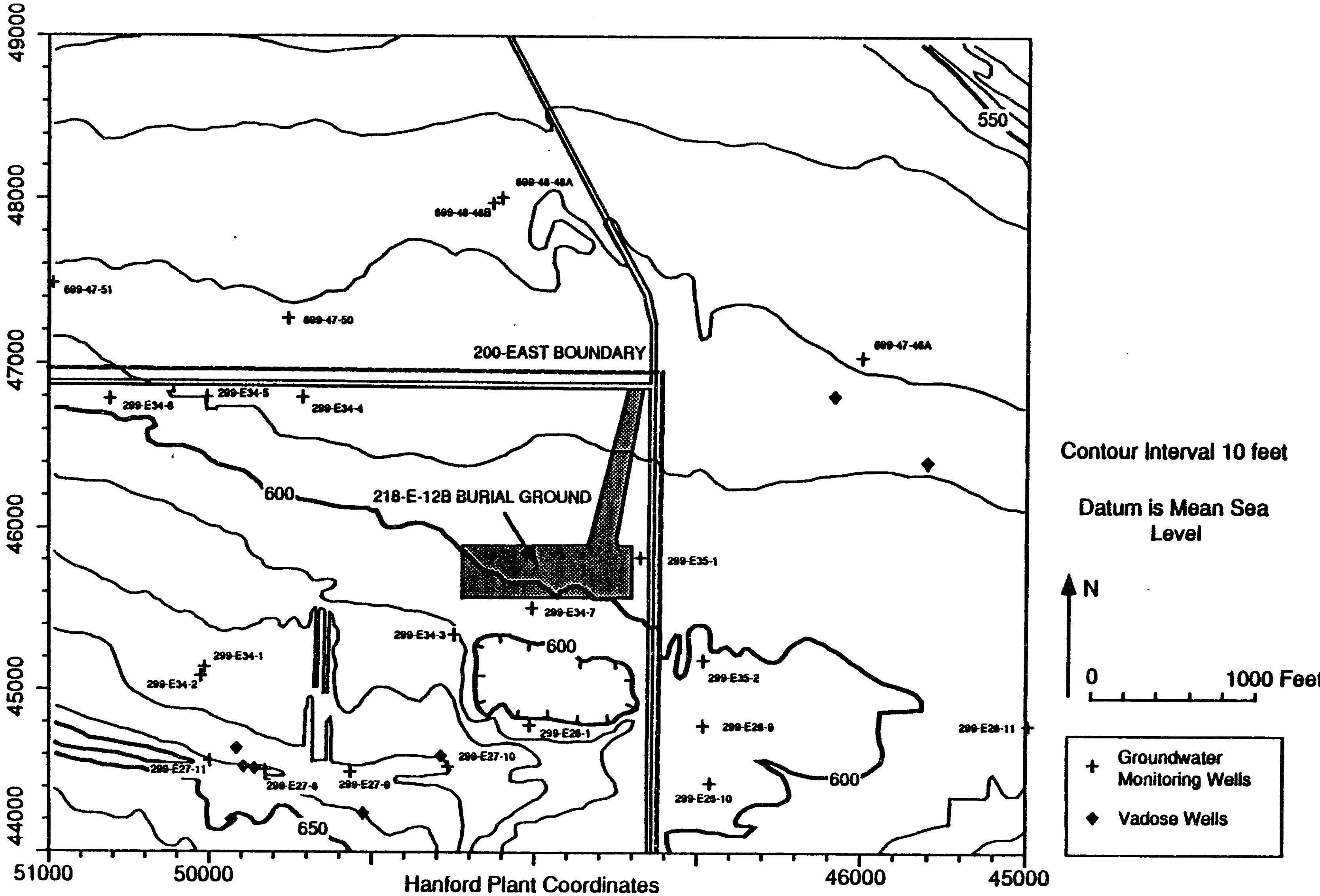

FIGURE A.22. Topographic Map of Study Area

218-E-12B Burial Ground. In contrast, the saturated hydraulic conductivity of basalt underlying the unconfined aquifer is less than 1 m/day in the horizontal direction and 3 x 10^{-5} m/day in the vertical direction (Lum et al. 1990).

Confined aquifers exist beneath the study area within sedimentary interbeds and/or interflow zones between basalt flows of the Columbia River Basalt Group. The uppermost confined aquifer is the Rattlesnake Ridge Interbed. It is bounded by the Elephant Mountain flow interior and the Pomona Member of the Saddle Mountains Basalt. Saturated hydraulic conductivities for the Rattlesnake Ridge Interbed range from 0.01 to 10 m/day (0.03 to 30 ft/day) (BWIP 1982; Graham et al. 1984).

A.2.3.1 Groundwater Flow Direction

Figure A.23 is a regional water-table map with presumed flow directions for the area surrounding the 200 Areas. A mound in the water table beneath 216-B-Pond (B Pond) causes the predominant westward direction of groundwater flow within the study area. B Pond is a series of unlined, interconnected waste water disposal ponds that receive effluent from the 200-East Area. In the northern part of the study area, groundwater appears to flow south to southeast through the divide between the two basalt highs south of Gable Mountain. Figure A.24 presents a more detailed water-table map for the 218-E-12B Burial Ground.

The saturated thickness of the unconfined aquifer is shown in Figure A.25. Beneath the 218-E-12B Burial Ground, this thickness ranges from 0.6 to 1.3 m (2 to 4.2 ft). Adjacent to the northern boundary of the 200-East Area, the saturated thickness of the unconfined aquifer increases sharply, to a maximum of at least 15 m. This circular area corresponds to an erosional "hole" in the underlying Elephant Mountain Member (Figure A.26) that was filled with flood deposits of the Hanford formation.

Maps of the elevation of the potentiometric surface of the Rattlesnake Ridge Interbed in Graham et al. (1984), Jensen (1987), Poston et al. (1991), and Kasza et al. (1991) show a dominantly westward direction of groundwater flow. Also, comparison of potentiometric surfaces with the corresponding water-table maps of the unconfined aquifer in these four reports indicates a

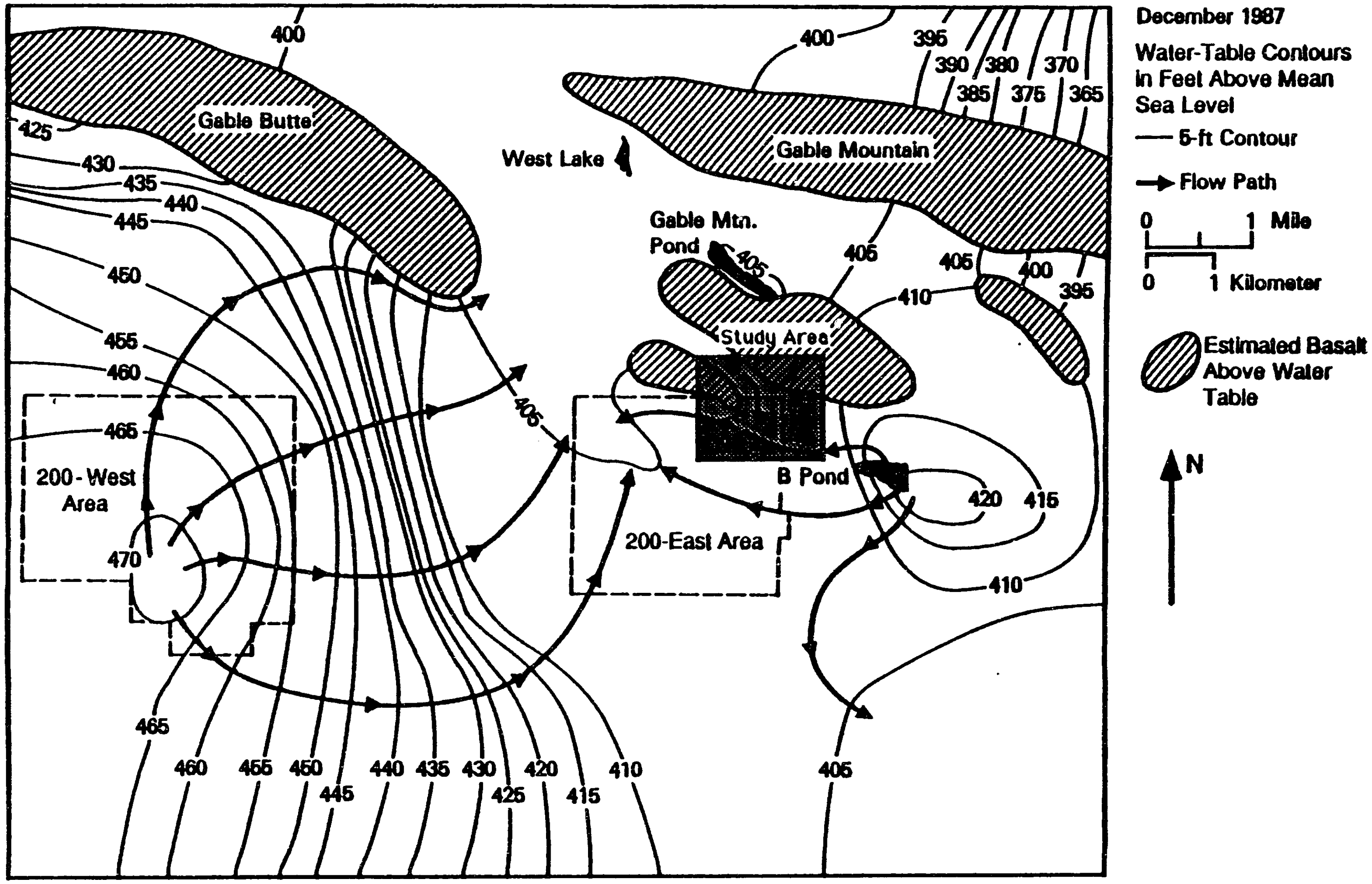

FIGURE A.23. Presumed Ground-Water Gradients and Flow Directions in 200 Areas (modified from Schatz and Ammerman 1988)

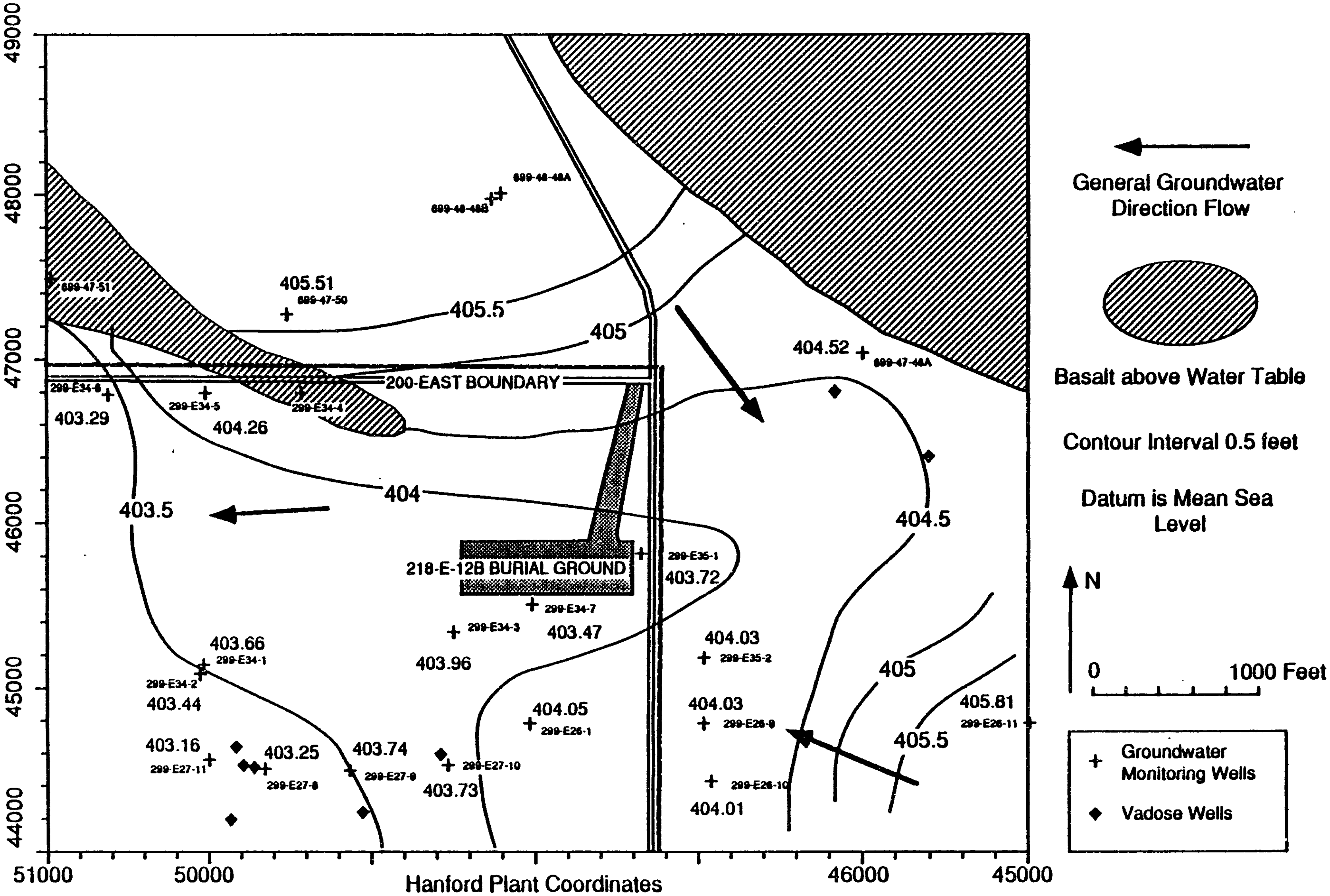

FIGURE A.24. Top of Water Table, June 1991 (modified from Kasza et al. 1991)

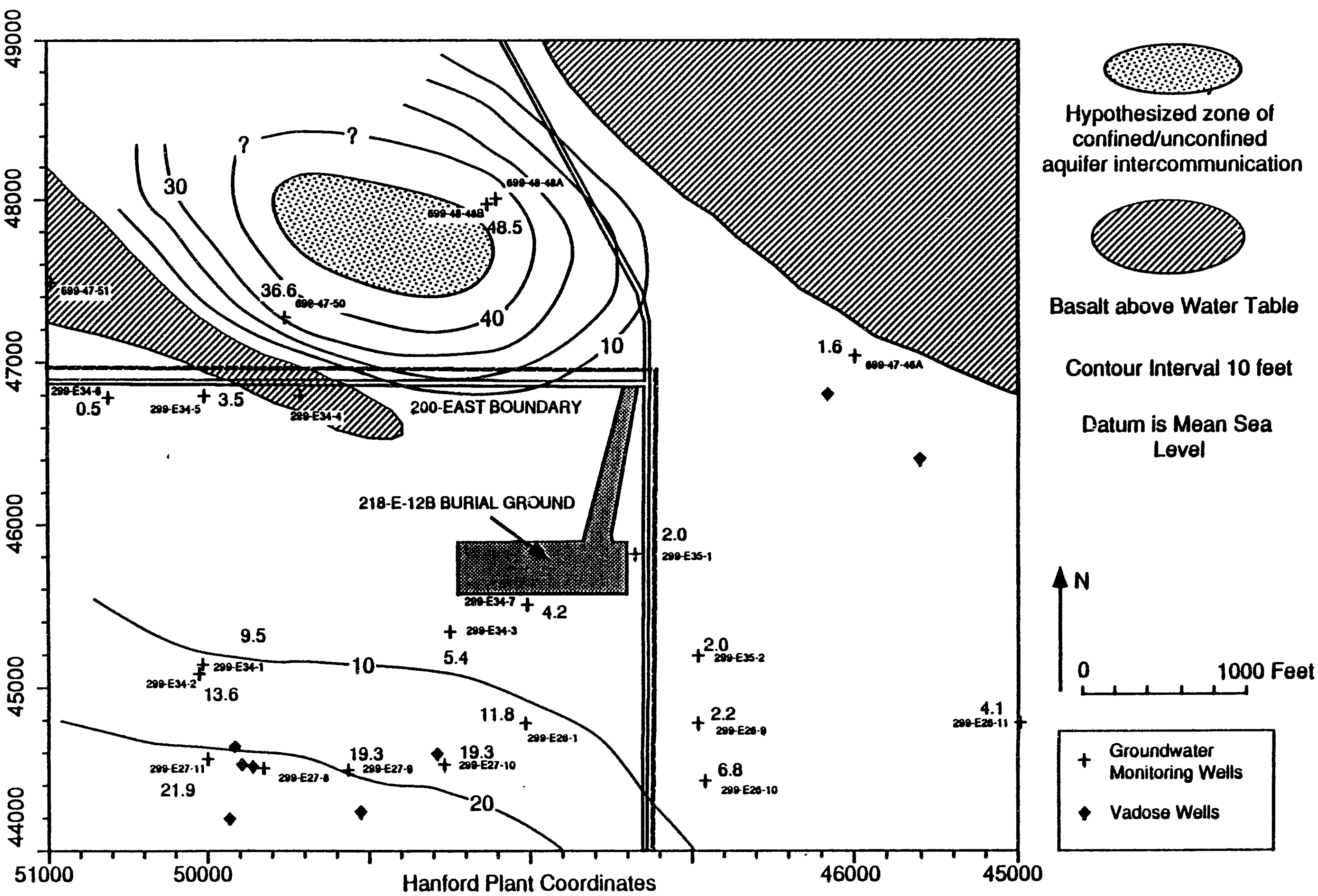

FIGURE A.25. Saturated Thickness of Unconfined Aquifer

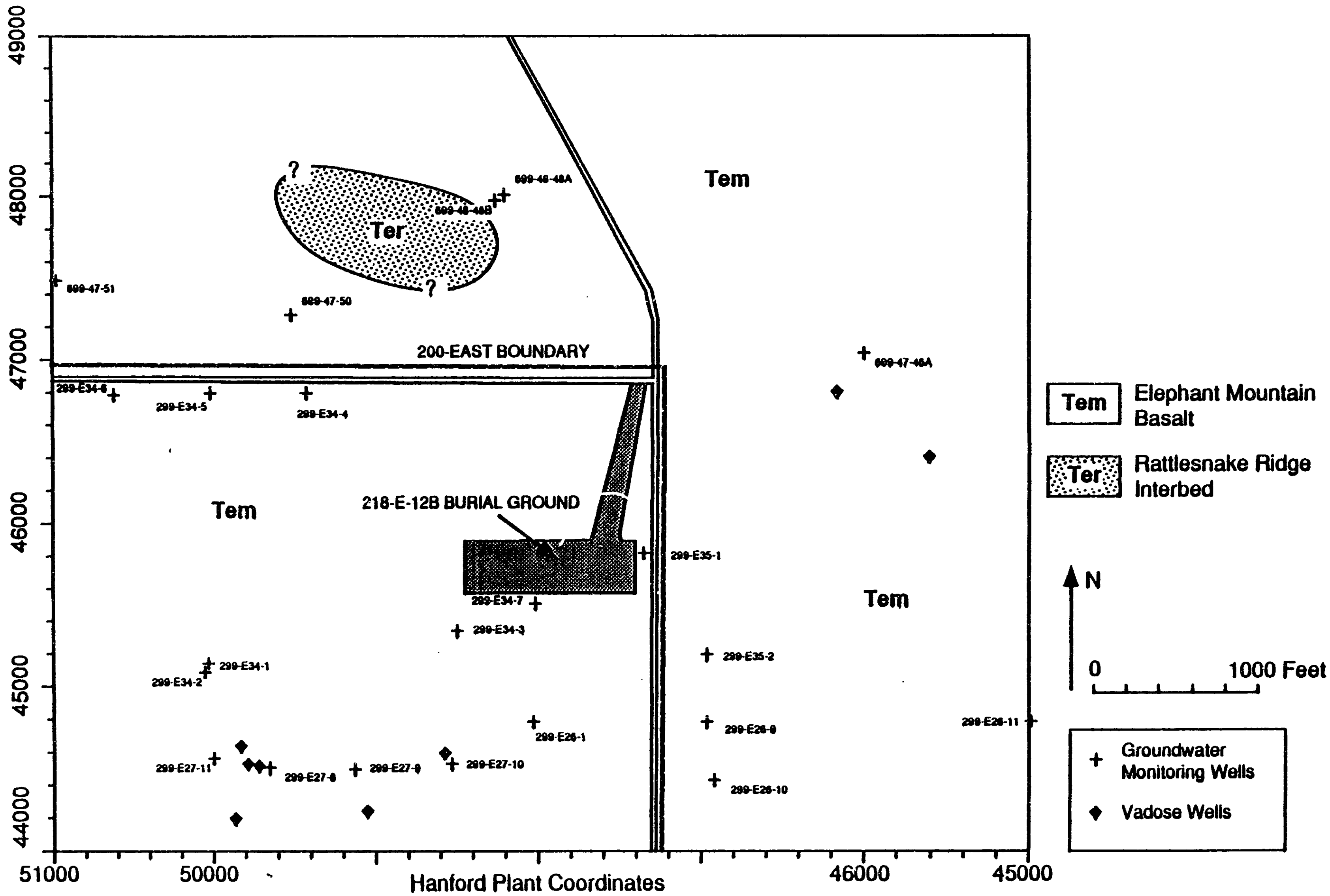

FIGURE A.26. Geologic Map of Bedrock Surface (modified from Graham et al. 1984) slight upward potential from the uppermost confined aquifer to the unconfined aquifer in the study area.

A.2.3.2 Aquifer Intercommunication

Strait and Moore (1982) and Graham et al. (1984) have investigated aquifer intercommunication at the Hanford Site near the study area and identified an area of possible downward flow from the unconfined aquifer to the confined aquifer. They also mapped areas where the Elephant Mountain Member has been completely eroded, including three erosional holes aligned along the axis of a probable paleochannel (see Figure A.20) and an area west of Gable Mountain that includes West Lake.

One of these holes between the confined and unconfined aquifers is believed to occur just north of the 218-E-12B Burial Ground (see Figure A.26). Low barometric efficiencies calculated by Graham et al. (1984) for well 699-47-50 suggest local intercommunication between the two aquifers. A potentiometric map by the same authors calculates an upward potentiometric gradient, indicating that the confined aquifer should flow upward into the unconfined aquifer. Furthermore, the water table atop the pothole is higher than for any other region on the local water-table map (see Figure A.24) and directs groundwater flow to the south, toward the burial ground.

A.2.3.3 Groundwater Chemistry

The two groundwater-monitoring wells nearest to the 218-E-12B Burial Ground are designated 299-E34-7 and 299-E35-1. These wells are part of the RCRA monitoring network for the 200-East Area Low-Level Burial Grounds. Analytical results from groundwater samples collected from these two wells and several other nearby wells are available in RCRA quarterly reports (DOE 1990a, 1990b). Other sources of groundwater analyses include annual reports of the Hanford Sitewide Monitoring Project (Bryce and Gorst 1990; Evans et al. 1990). Reports containing information on the hydrochemistry of the uppermost confined aquifer in the study area include Strait and Moore (1982), Graham et al. (1984), and Jensen (1987).

A.2.4 SUMMARY OF GEOLOGICAL FEATURES

Within the 218-E-12B Burial Ground the vadose zone is comprised exclusively of the Hanford formation. It consists predominantly of transmissive sands and gravels. There are some slackwater deposits, composed of fine-grained sands, silts, and clays, that are barriers to the downward movement of moisture. They typically have higher moisture contents and lower hydraulic conductivities (see Appendix B). Within the study area, these deposits may be laterally continuous (Figure A.21), and they could provide a pathway for migration of contaminants. Excavation of the trench removed the slackwater deposits, thus removing this barrier to transport of materials buried in the trench.

Groundwater transport in the 218-E-12B Burial Ground area is dominated by discharge to B Pond and the inferred intercommunication between the confined and unconfined aquifers within the pothole (Figures A.23, A.24, and A.26). Presently, there are no groundwater wells that can discriminate between contamination introduced into the pathway between the two aquifers and that introduced by the 218-E-12B Burial Ground.

A.3 CONCEPTUAL MODELS OF CONTAMINANT ADSORPTION

Solute (including contaminant) transport in the subsurface is controlled by advection, hydrodynamic dispersion, molecular diffusion, and geochemical interaction. Advection and hydrodynamic dispersion refer to movement of solute at a rate dependent on the various water pathways and velocities. Molecular diffusion refers to the gradual mixing of molecules of two or more substances as a result of random motion and/or a chemical concentration gradient. Diffusion disperses solute via the concentration gradient (i.e., Fick's law). Diffusion is generally only important in the absence of advection, and is usually a negligible transport mechanism when water is being advected in response to various forces. Variability in the advection process gives rise to the transport process called hydrodynamic dispersion. Hydrodynamic dispersion is a result of variability in travel paths, or velocities, taken by the advected solute. Geochemical interactions cover all reactions that are driven by chemical and biochemical forces.

Once contaminants are leached from the buried wastes, they may chemically interact with the soils and sediments. The major processes affecting transport include the following: dissolution/precipitation, adsorption/desorption, filtration of colloids and small suspended particles, and diffusion into micropores within mineral grains. The former two processes are considered more important. Furthermore, for Hanford Site low-level waste (LLW) disposal applications, precipitation is likely to be important only for cases where significant pH and/or redox changes occur when leachates migrate away from the wastes. In most Hanford Site LLW situations, it is assumed that adsorption processes are the key to contaminant migration, especially outside areas where the waste has dramatically altered the sediment's natural chemical environment.

Adsorption reactions have been identified as the most important contaminant retardation process in far-field transport analyses for hazardous waste disposal options. Adsorption processes are known to increase the travel times for some contaminants by 10^3 to 10^6 times relative to the groundwater. Sufficiently long travel times allow many radionuclides to decay before reaching the accessible environment (i.e., the biosphere).

A.3.1 DISTRIBUTION COEFFICIENT

To predict the effects of retardation using safety-assessment computer codes, adsorption processes must be described in quantitative terms. An empirical parameter, the distribution coefficient (often called R_d or K_d), is readily measured by laboratory experimentation and allows a quantitative estimate of nuclide migration. Knowledge of the R_d and of media bulk density and porosity (for porous flow), or of media fracture surface area, aperture width, and matrix diffusion attributes (for fracture flow), allows calculation of the retardation factor, R_f. The retardation factor is defined as

$$R_f = \frac{V_w}{V_n} \qquad (A.3.1)$$

where V_w is the velocity of water through a control volume and V_n is the velocity of the contaminant.

For one-dimensional advection-dispersion flow with chemical reaction, the transport equation can be written as:

$$\frac{\partial C_i}{\partial t} = \frac{\left[D_x \dfrac{\partial^2 C_i}{\partial x^2} - v_x \dfrac{\partial C_i}{\partial x} \right]}{R_{fi}} \qquad (A.3.2)$$

where C_i = concentration of a particular radioactive species (i) in solution (mass/unit volume)

D_x = dispersion coefficient of species (i) (length^2/time)

v_x = pore velocity of groundwater (distance/time)

R_{fi} = retardation factor for species (i).

(For simplicity, radioactive decay has not been included in this formula.)

The retardation factor is a function of all contaminant retardation mechanisms: 1) chemical precipitation/dissolution of bulk solid phases, 2) chemical substitution of one element for another in a solid phase, 3) exchange of a stable nuclide of an element with a radioactive nuclide in solution, 4) physical filtration of colloids, 5) cation and anion exchange, and 6) adsorption (Muller et al. 1983). Typically, all these mechanisms are folded into a single empirical distribution coefficient that implicitly assumes that the reactions go to equilibrium and are reversible, and that the chemical environment along a solute flow path does not vary in either space or time. The limitations associated with this assumption are well known to investigators, but the paucity of site-specific geochemical data at most disposal sites usually precludes a more rigorous conceptual model, especially for bounding or preliminary performance assessment calculations such as presented in the final report. Geochemical processes may also be irreversible or at least directionally dependent (e.g., adsorption and desorption may be represented by different model parameters), and yet the assumption of reversibility and single values for model parameters are generally employed, with the justification that the approach builds conservatism into the analysis.

In the constant R_d model, the distribution of the contaminant of interest between solution and the solid adsorbent is assumed to be a constant value. There is no explicit accommodation of dependence on characteristics of the sediments, groundwater, or contaminant concentration. Typically, an R_d value for a given contaminant is determined in the laboratory using sediment from the study area and actual or simulated groundwater to which a radioactive tracer is added at low concentration. Then,

$$R_d = \frac{\text{amount of radionuclide adsorbed on solid per gram}}{\text{amount of radionuclide in solution per milliliter}} \qquad \text{(A.3.3)}$$

The term "tracer" typically denotes that a low mass is added; however, the final activity in soil and solution must be sufficient to facilitate good counting statistics. The experiments are often equilibrated by contacting the solid with several aliquots of water before adding the radiotracer, in an attempt to approach the condition expected in the field. Several standardized laboratory techniques (ASTM 1984; Serne and Relyea 1983) are commonly used to determine this ratio. In experiments where a radioactive tracer is not used, the R_d value can be calculated using chemical analysis of the influent and effluent solutions in the following equation:

$$R_d = \frac{(C_{inf} - C_{eff})}{C_{eff}} \frac{V}{W} \simeq \frac{C_{Soil}}{C_{Solution}} \frac{V}{W} \quad \text{(A.3.4)}$$

where C_{inf} = contaminant concentration or tracer activity in influent solution (g/mL or counts/mL)

C_{eff} = contaminant concentration or tracer activity in effluent solution (g/mL or counts/mL)

C_{soil} = contaminant concentration or tracer activity in soil (g contaminant/g soil or counts tracer/g soil)

$C_{solution}$ = contaminant concentration or tracer activity in solution (g/mL or counts/mL)

V = volume of solution used (mL)

W = weight of soil used (g).

Because it is an empirical measurement, the R_d value does not necessarily denote an equilibrium value or imply some of the other assumptions inherent in the more rigorous use of the term "K_d." The term "R_d" will be used to represent the observed distribution ratio of nuclide between the solid and solution. The term "K_d" is reserved for true equilibrium reactions that show reversibility. Furthermore, it is customary with the constant R_d model to measure the total concentration or radioactivity of the tracer and thus to treat the tracer as being one chemical species. This assumption is not an inherent requirement, but it is generally applied for convenience. If one knows that the tracer distributes among several species and one can measure or predict the distribution, separate R_d values can be, and should be, calculated for each species.

The constant R_d model is mathematically very simple and readily incorporated into transport models and codes via the retardation factor term. That is, for porous flow

$$R = 1 + \frac{\rho_b}{\phi_\epsilon} R_d \quad \text{(A.3.5)}$$

or

$$R = 1 + \frac{1-\phi_\epsilon}{\phi_\epsilon} \rho_p R_d \quad \text{(A.3.6)}$$

where R = the retardation factor v_w/v_n (velocity of water ÷ velocity of solute)

ρ_b = porous media bulk density (mass/unit volume)

ϕ_ϵ = effective porosity at saturation of media or volumetric moisture content for unsaturated media (dimensionless)

R_d = distribution coefficient (mL/g)

ρ_p = particle density (mass/unit volume).

A large R_d value leads to a large retardation factor, which signifies that the contaminant is not very mobile compared with water percolating through the soil. An R_d value of zero means there is no adsorption and the equivalent retardation factor equals 1. That is, no adsorption leads to no retardation, R = 1, and the contaminant travels at the same velocity as the pore water through the sediment (see Bouwer 1991 for more discussion).

For the constant R_d model, the retardation factor (R_f) is a constant for each layer of geologic media; each layer is assumed to have a constant bulk density and saturated effective porosity or volumetric moisture content for unsaturated sediments. Thus, this transport equation does not require knowledge of any other parameters such as pH or surface area, and it is easily solved to determine the solution concentration as a function of time and at any given point.

A.3.2 ISOTHERM ADSORPTION MODELS

The results of a suite of experiments evaluating the effect of nuclide concentration on adsorption while other parameters are held constant are called an "adsorption isotherm." Two adsorption isotherm models used frequently are the Langmuir and Freundlich models.

The Langmuir model has been used to describe adsorption of gas molecules onto homogeneous solid surfaces (crystalline materials) that exhibit one type of adsorption site (Langmuir 1918). Many investigators have tacitly extended the Langmuir adsorption model to describe adsorption from solution onto solid adsorbates including heterogeneous solids. The Langmuir model for adsorption is

$$X = \frac{bX_mC}{1 + bC} \qquad \text{(A.3.7)}$$

where X = amount of solute adsorbed per unit weight of solid
b = a constant related to the energy of adsorption
X_m = maximum adsorption concentration of the adsorbate
C = equilibrium solution concentration of the adsorbate.

Substituting $1/B$ for b, we obtain

$$X = \frac{X_m C}{B + C} \tag{A.3.8}$$

A plot of values of X (y-axis) versus values of C (x-axis) passes through the origin and is nearly linear at low values of C. As C increases, X should approach X_m. One can rearrange Equation (A.3.8) by taking its reciprocal and multiplying both sides by $X \cdot X_m$, to yield $X = -B(X/C) + X_m$. Then by plotting X on the y-axis and (X/C) on the x-axis, we can determine the value for $-B$ from the slope of the best-fit line and the value of X_m from the intercept. For radionuclide adsorption onto heterogeneous soils and sediments, the Langmuir model is typically a weak predictor of actual adsorption events, although Salter et al. (1981a) cite several instances where the Langmuir isotherm has successfully fit adsorption of trace solutes on natural substrates. Furthermore, Salter et al. (1981b) discuss recent modifications of the Langmuir model to accommodate two distinct sites and competition of two adsorbates (the nuclide and the ion it replaces on the adsorbent), which should further extend this conceptual model's usefulness on natural substrates.

The Freundlich isotherm model (Freundlich 1926) is defined as

$$X = KC^N \tag{A.3.9}$$

where X = amount of solute adsorbed per unit weight of solid
C = equilibrium solute solution concentration
and K, N = constants.

The Freundlich model does not account for finite adsorption capacity at high concentrations of solute, but when considering trace constituent adsorption, ignoring such physical constraints is usually not critical. The

Freundlich isotherm can be transformed to a linear equation by taking the logarithms of both sides of Equation (A.3.9):

$$\log X = \log K + N \log C. \qquad (A.3.10)$$

When log X is plotted on the y-axis and log C on the x-axis, the best-fit straight line has a slope of N, and log K is its intercept. When N = 1, the Freundlich isotherm represented by Equation (A.3.9) reduces to a linear relationship, and because X/C is the ratio of the amount of solute adsorbed to the equilibrium solution concentration (the definition of R_d), the Freundlich K is equivalent to the value of R_d.

Because adsorption isotherms at very low solute concentrations are often linear, either the Freundlich isotherm or the Langmuir isotherm (when the product bC is much smaller than 1) can be used to fit data at low solute concentrations. The value of N for the adsorption of many radionuclides is often significantly different from 1. In this case, K_d values are not constants, but are functions of the solute concentrations.

Both isotherm models can be compared to data from experiments that systematically vary the mass of trace constituent or radionuclide while holding all other parameters as constant as possible. It is important to consider the total mass of the element present, including all stable and other radioactive nuclides, when evaluating isotherms. It is incorrect to calculate isotherms based on only one nuclide if the system includes several nuclides (both stable and radioactive) for a particular element. For convenience, isotherm experiments generally consider only the total concentration or radioactivity for a given contaminant, combining all species present in the system.

The isotherm concept is a step up in sophistication over the constant distribution coefficient (R_d) model. It must be stressed that isotherm models as expressed by Equations (A.3.8), (A.3.9), and (A.3.10) explicitly consider dependency of the distribution coefficient only on the concentration of the contaminant of interest in a solution. Isotherm models do not consider other solid and solution parameters that can influence adsorption. Serne and Muller

(1987) describe additional detailed adsorption conceptual models that are rarely used in scoping performance assessment activities.

A.4 ADAPTATION OF THE GROUNDWATER FLOW MODEL

The Coupled Fluid, Energy, and Solute Transport (CFEST) code (Gupta et al. 1982, 1987) was applied to model groundwater flow in the unconfined aquifer at the Hanford Site under post-closure conditions for dry- and wet-climate scenarios. Results from the model for this study are described in Sections 2.3 and 4.3 of the main report and consist of groundwater streamlines and travel times from the 218-E-12B Burial Ground to a 100-m well, a 5000-m well, and finally to the Columbia River. This information is used as input to the transport model. Evans et al. (1988) and Jacobson and Freshley (1990) developed a model of the unconfined aquifer at the Hanford Site using CFEST and described construction and calibration of the model in detail. They selected CFEST because the code allows simulation of groundwater flow and contaminant transport in two or three dimensions, including steady-state or transient conditions, recharge and discharge from the aquifer, and radioactive decay of transported species. The present study of lead migration is based on this earlier model. The following sections describe modifications to the finite-element grid, boundary conditions, and aquifer transmissivity that were required to simulate dry- and wet-climate scenarios for Hanford Site performance assessments.

A.4.1 CFEST MODIFICATIONS TO GRID AND BOUNDARY CONDITIONS

The CFEST finite-element grid of Jacobson and Freshley (1990) for the unconfined aquifer is shown in Figure A.27. They based their calibration on water levels for the year 1979. The finite-element model grid was designed with high resolution in areas of high waste-water discharge and areas of rapid changes in hydraulic conductivity and hydraulic gradient. The finite-element grid design was based on the distribution of transmissivity and other hydraulic property data from a previous model of the unconfined aquifer (referred to as the Variable Thickness Transient or VTT model, Kipp et al. 1972; Reisenauer 1979a, 1979b, 1979c; DOE 1987). The VTT model utilized a finite-difference approach with a constant grid spacing of 2000 ft (610 m). The VTT-model grid was designed to ensure that the distribution of hydraulic conductivity was adequately represented (i.e., values were not averaged over

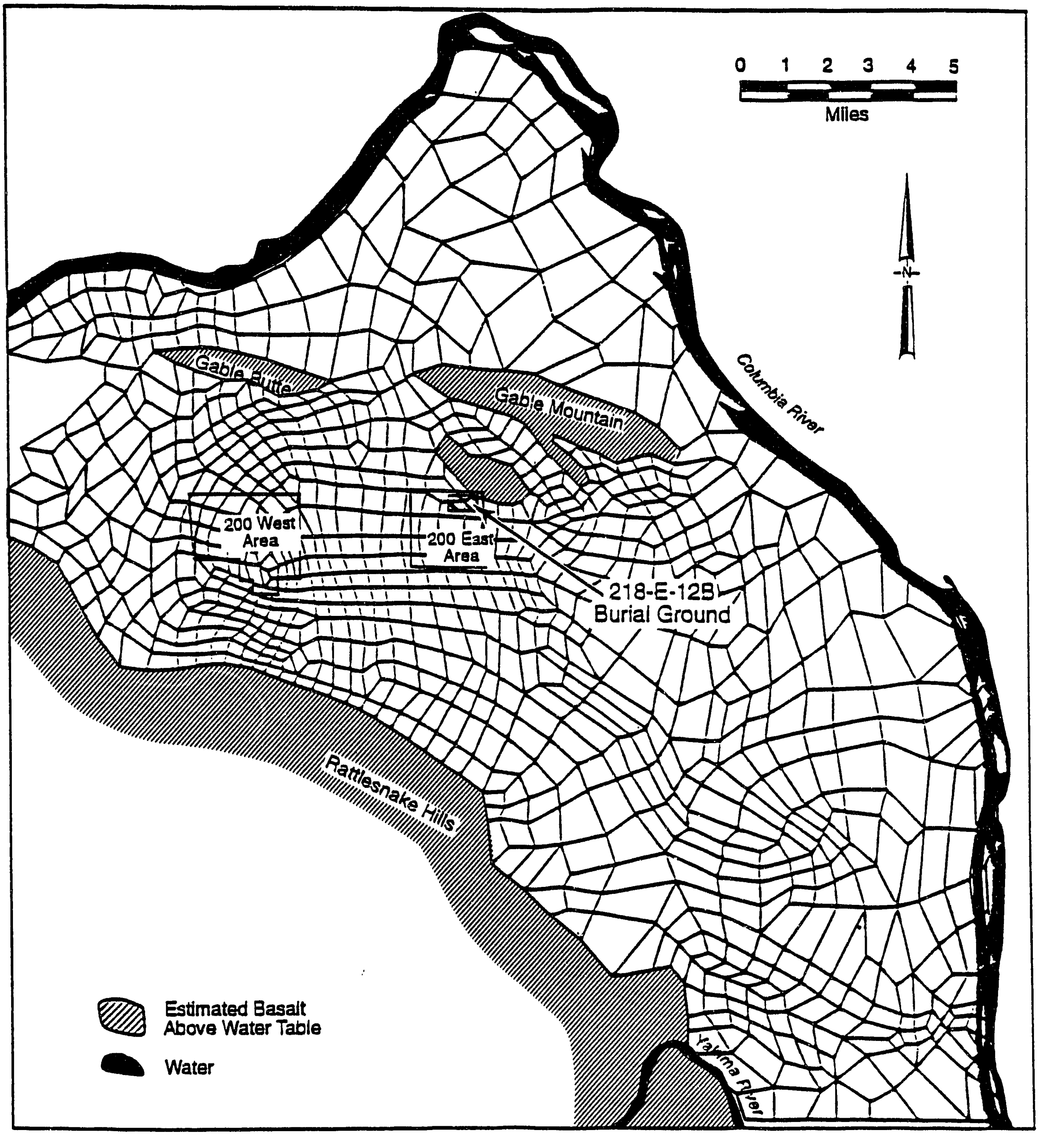

FIGURE A.27. Finite-Element Grid for the CFEST Model of the Unconfined Aquifer large elements in areas of rapid change). Although the spatial resolution provided by the CFEST grid in some locations is much coarser than 2000 ft, all known variations in hydraulic conductivity are well represented. Larger elements were used where spatial resolution was not required.

Boundary conditions were specified for two specific postclosure cases used in analysis of the 218-E-12B Burial Ground: a drier climate case (0.5-cm/yr recharge rate) and a wetter climate case (5.0-cm/yr recharge rate). Present-day boundary conditions are the same as those applied to the VTT model; they are described here because some of the boundary conditions are common to the two postclosure cases.

Boundary conditions for the postclosure cases were developed iteratively. Because operational discharges to the ground were not included, and overall recharge was reduced for the 0.5 cm/yr recharge case, lower water levels reduced the volume and area occupied by the aquifer. Areas in the model with zero aquifer thickness do not contribute to groundwater flow. Prescribed head conditions are specified along the Columbia River and Yakima River boundaries of the model. The prescribed heads are equal to the yearly average river level at each boundary node during 1979, generally ranging from about 400 ft to 350 ft above mean sea level through the Hanford Reach.

Prescribed flux distributions were different for the two postclosure cases and will be described in detail. Prescribed fluxes were specified along the Cold Creek and Dry Creek valleys to incorporate inflow of groundwater from these valleys to the study area. The contribution from spring discharges along the northeast side of Rattlesnake Mountain was also accounted for by specified flow rates. No-flow conditions were assumed in areas where the aquifer is bordered by basalt outcrops and subcrops (where the basalt surface intersects the water table) near Gable Mountain and Gable Butte. The locations of the no-flow boundary conditions varied between the two post-closure cases.

The finite-element grid used for the simulations of postclosure conditions with 5.0-cm/yr recharge is similar to the present-day grid (Figure A.27), with the exception of two additional elements located near Gable Mountain. The addition of these two elements was necessary because of the higher water table elevations in this area. The flux values used for Cold Creek were generated based on the volume of water entering the aquifer from a watershed with an area of 140 km^2 with 5.0 cm/yr recharge. A flux of 19,200 m^3/d (677,000 ft^3/d) was distributed across three nodes. The flux for Dry Creek was calculated in a similar manner. The watershed area for Dry Creek is 260 km^2, providing a flux of 35,600 m^3/d (1.26 million ft^3/d), also distributed across three nodes.

Figure A.28 shows the finite-element grid used for the simulations of postclosure conditions with 0.5-cm/yr recharge. Because of the small volume of recharge, the water table drops considerably, leaving a larger portion of the basalt exposed in the area of Gable Mountain and Gable Butte, including the vicinity of the 218-E-12B Burial Ground. The additional area of exposed basalt is assumed to be removed from the aquifer system and is not modeled as part of the aquifer. The fluxes for Cold Creek and Dry Creek were calculated in the same manner as for the 5-cm/yr recharge case. Because the finite-element grid for the low recharge scenario was different from that in the 5.0 cm/yr case, the flux from Cold Creek (1920 m^3/d or 67,700 ft^3/d) was distributed across four nodes and that from Dry Creek (3560 m^3/d or 126,000 ft^3/d) was distributed across three nodes.

A.4.2 AQUIFER TRANSMISSIVITY DISTRIBUTION

An early model of groundwater flow in the unconfined aquifer was developed during the 1970s. The model was calibrated with an iterative routine developed by Cearlock et al. (1975). Calibration generally consists of adjustments in transmissivity and other hydraulic properties in order to best reproduce measured hydraulic heads (water-level elevations) in the aquifer. The iterative technique was based on numerical integration of the unconfined groundwater flow equation along streamlines in the unconfined aquifer drawn on a hand-contoured water-table map for 1973. A transmissivity value obtained from aquifer field-test data was required in each stream tube, defined by bounding streamlines. For streamtubes where no aquifer test data were available, transmissivity values were estimated by interpolation.

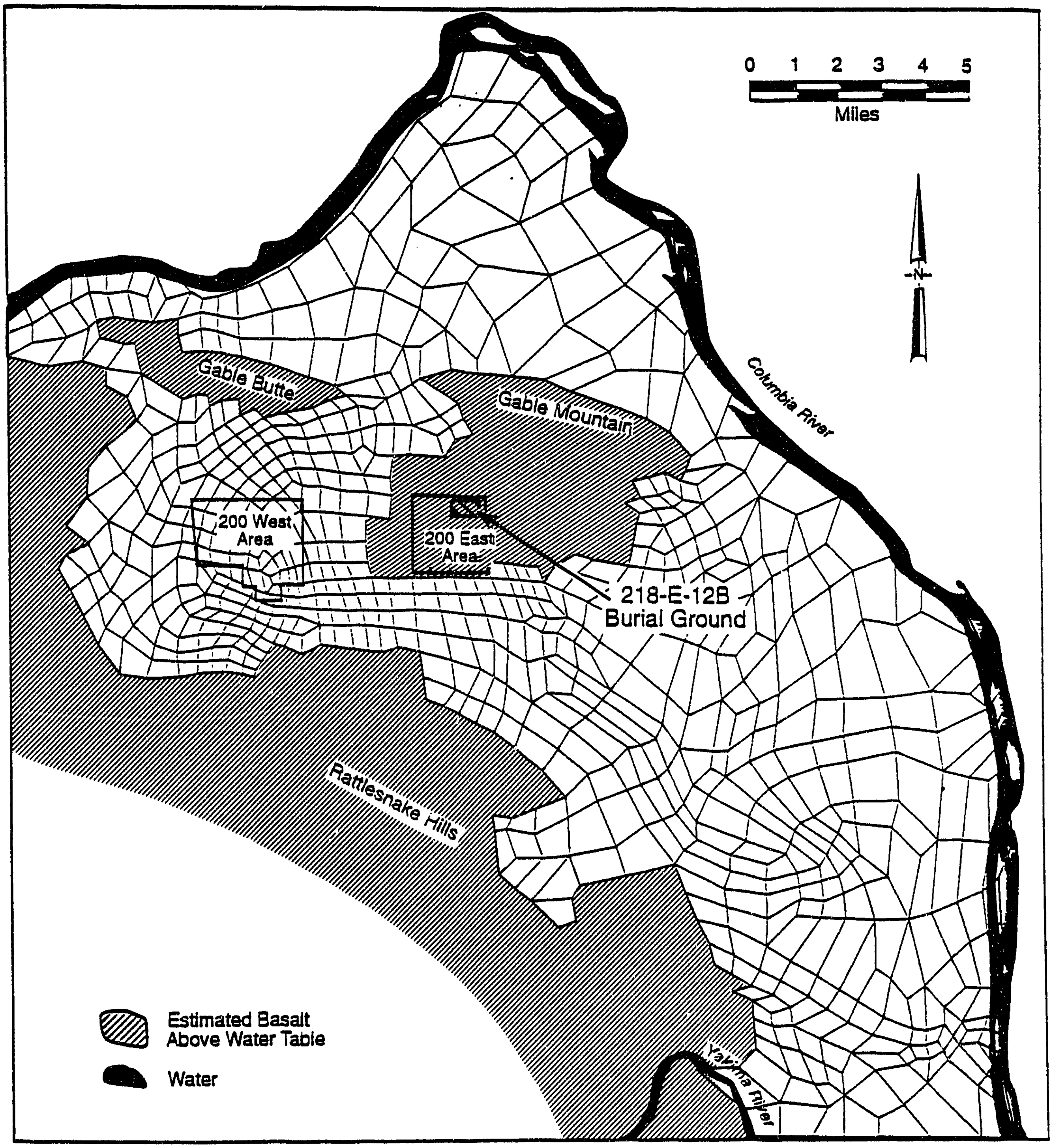

FIGURE A.28. Finite-Element Grid for the Postclosure 0.5 cm/yr Recharge Case

The transmissivity distribution from the VTT model was transferred directly into the CFEST model. However, an attempt to improve the calibration was made by application of an inverse method developed by Neuman (1980) and modified by Jacobson (1985). This method requires use of steady-state information about the aquifer being modeled. Review of waste-water discharge information at the major disposal facilities within the 200-East and 200-West Areas suggested that, compared with other time periods, the discharges remained relatively constant from 1976 through 1979 (Jacobson and Freshley 1990). Application of the inverse method required both hydraulic-head measurements and previous estimates of transmissivity. The water levels for the unconfined aquifer measured during December 1979 were used for the calibration. The transmissivity distribution from the VTT model calibration was used to provide prior estimates of the transmissivities. Application of the inverse method with prescribed head conditions in the Cold Creek Valley (Case 3 in Jacobson and Freshley 1990) yielded a reasonable calibration. The transmissivity distribution from the inverse calibration is shown in Figure A.29.

The calibrated transmissivity distribution was used as the basis for investigation of the dry- and wet-climate scenarios for analysis of groundwater flow from the 218-E-12B Burial Ground. Application of the CFEST model required that the transmissivities in the model be separated into aquifer thicknesses and hydraulic conductivities. The separation was made in order to adjust aquifer thicknesses for the two different recharge rates that were simulated for the dry- and wet-climate conditions. As the hydraulic heads in the unconfined aquifer increased or decreased in response to variations in recharge, the simulated aquifer thicknesses changed with corresponding changes in the areas of the saturated and unsaturated regions.

The hydraulic head distributions for both the 0.5-cm case and the 5.0-cm case and the resulting streamlines are described in detail in Sections 2.3 and 4.3 of the final report. The detailed breakdown of groundwater travel time through the vadose zone (Section 4.2) and then in the aquifer to a 100-m well, a 5000-m well, and to the Columbia River are also described.

FIGURE A.29. Distribution of Transmissivities from Case 3 of the Inverse Application (from Jacobson and Freshley 1990)

A.5 SOFTWARE VERIFICATION AND VALIDATION

The following section addresses quality assurance activities conducted to verify or validate software used for the analysis described in this report. The current version of each computer code is briefly described, including the quality assurance requirements applied during the development of each package (if any) and efforts to verify and validate the models implemented in the software.

A.5.1 MINTEQ

Estimates of lead and nickel solubility, and the chemical forms of these elements that are expected to be stable in Hanford groundwater, were obtained by application of the computer code MINTEQA2 version 3.0 (Allison et al. 1991). This code is a U.S. Environmental Protection Agency adaptation of the original MINTEQ computer code (Felmy et al. 1984a). Two test cases, a seawater test case and a river-water test case, were run to verify the original version of the code as described in Felmy et al. (1984b). The MINTEQ output was benchmarked against the published results from several other geochemical models (Nordstrom et al. 1979). A discussion of the comparison, including an explanation of any differences between the MINTEQ results and those from other codes, appears in Felmy et al. (1984b).

A.5.2 CFEST

The CFEST code (Coupled Fluid, Energy, and Solute Transport code, Gupta et al. 1987) was developed to analyze coupled hydrologic, thermal, and solute transport processes. It treats single-phase Darcy ground-water flow in a horizontal or vertical plane, or in fully three-dimensional space under nonisothermal conditions. The code has the capability to model discontinuous and continuous layering, time-dependent and constant sources/sinks, and transient as well as steady-state ground-water flow. The version of the code used to develop the Hanford Site hydrologic model for this application was

CFEST Version SC-01, an adaptation of the original code for use on supercomputers.[1]

The CFEST code was developed in accordance with NUREG-0856 (Silling 1983) for development, improvement, verification, validation, and documentation of performance-assessment computer codes. Verification tests have been conducted for the major processes modeled by the CFEST code. The code has a proven track record; ten applications to national and international problems are discussed in Gupta et al. (1987). In addition, the CFEST code was benchmarked, verified, and partially validated using test cases identified by HYDROCOIN (Hydrologic Code Intercomparison), an international project organized by the Swedish Nuclear Inspectorate. The objectives of HYDROCOIN were 1) to verify the numerical accuracy of codes by code intercomparison and by comparison with analytical solutions, 2) to compare model predictions with experimental results, and 3) to investigate the importance of different phenomena and uncertainties inherent in the modeling and site-characterization process through sensitivity and uncertainty studies.

A.5.3 TRANSS

The TRANSS code (Simmons et al. 1986) was designed as a simplified ground-water transport model to estimate the migration rate of radionuclides and other inorganic contaminants that are subject to sorption governed by a linear isotherm. Transport is modeled as a contaminant mass transmitted along a collection of streamlines constituting a streamtube, which connects a source release zone with an environmental arrival zone. The probability-weighted contaminant arrival distribution along each streamline is represented by an analytical solution of the one-dimensional advection dispersion equation with constant velocity and dispersion coefficient. The appropriate effective constant velocity for each streamline is based on the exact travel time required to traverse a streamline with a known length. An assumption used in

[1]Cole, C. R., S. B. Yabusaki, and C. T. Kincaid. 1988. CFEST-SC, Coupled Fluid, Energy, and Solute Transport Code, SuperComputer Version: Documentation and User's Manual. Battelle, Pacific Northwest Laboratories, Richland, Washington.

the model to facilitate the mathematical simplification is that transverse dispersion within a streamtube is negligible.

Release of contaminant from a source is described in terms of a fraction-remaining curve provided as input information. However, an option included in the code is the calculation of a fraction-remaining curve based on four specialized release models: 1) constant release rate, 2) solubility-controlled release rate, 3) adsorption-controlled release, and 4) diffusion-controlled release from beneath an infiltration barrier. To apply the code, a user supplies a minimal number of parameters: a probability-weighted list of travel times for streamlines, a local-scale dispersion coefficient, a sorption distribution coefficient, total initial radionuclide inventory, radioactive half-life, a release model choice, and the size dimensions of the source. The code is intended to provide scoping estimates of contaminant transport and does not predict the evolution of a concentration distribution in a groundwater flow field. Moreover, the required travel times along streamlines must be obtained from a separate groundwater flow simulation code.

The TRANSS code contains a wide variety of options and models. The model has been tested against a variety of problems and has been used in a wide variety of performance-assessment evaluations at Hanford. Because the code contains a wide variety of release options, results of specific applications are generally checked by hand calculation to ensure correct conceptualization of the problem and correct application of the code. Hand calculations for applications in the 281-E-12B Burial Ground evaluation were consistent with the TRANSS results.

A.6 REFERENCES

Allison, J. D., D. S. Brown and K. J. Novo-Gradac. 1991. MINTEQA2/PRODEFA2, A Geochemical Assessment Model for Environmental Systems: Version 3.0 User's Manual. EPA/600/3-91/021, Environmental Research Laboratory, Office of Research and Development, U. S. Environmental Protection Agency, Athens, Georgia.

American Society for Testing Materials (ASTM). 1984. "Standard Test Method for Distribution Ratios by the Short-Term Batch Method." D4319-83. In Annual Book of ASTM Standards, Vol. 04.08, pp. 766-773. American Society for Testing Materials, Philadelphia, Pennsylvania.

Baker, V. R. 1978. "Paleohydraulics and Hydrodynamics of Scabland Floods." In The Channeled Scabland, eds. V. R. Baker and D. Nummedal, pp. 59-79. National Aeronautics and Space Administration, Washington, D.C.

Baker, V. R., and D. Nummedal. 1978. The Channeled Scabland. National Aeronautics and Space Administration, Washington, D.C.

Barton, K. R. O. 1990. Borehole Completion Data Package for the Low-Level Burial Grounds - 1990. WHC-MR-0205, Westinghouse Hanford Company, Richland, Washington.

Basalt Waste Isolation Project (BWIP) Staff. 1982. Site Characterization Report for the Basalt Waste Isolation Project. DOE/RL 82-3, U. S. Department of Energy, Richland, Washington.

Bjornstad, B. N., and K. R. Fecht. 1989. Pre-Wisconsin Glacial-Outburst Floods: Pedogenic and Paleomagnetic Evidence from the Pasco Basin and Adjacent Channeled Scabland. Cordilleran/Rocky Mountain Sections, Spokane, Washington.

Bjornstad, B. N., and S. Dudziak. 1989. 40 CFR 265 Interim Status Indicator-Evaluation Ground-Water Monitoring Plan for the 216-B-63 Trench. PNL-6862, Pacific Northwest Laboratory, Richland, Washington.

Borghese, J. V., D. R. Newcomer, W. E. Cronin, and S. M. Goodwin. 1990. Hydrologic Testing at the Low-Level Burial Grounds, 1989. PNL-7333, Pacific Northwest Laboratory, Richland, Washington.

Bouwer, H. 1991. "Simple Derivation of the Retardation Equation and Application to Preferential Flow and Macrodispersion," Ground Water 29:41-46.

Bryce, R. W., and W. R. Gorst. 1990. Hanford Site Environmental Data for Calendar Year 1989 - Ground Water. PNL-7390, Pacific Northwest Laboratory, Richland, Washington.

Cearlock, D. B., K. L. Kipp, and D. R. Friedrichs. 1975. The Transmissivity Iterative Calculation Routine - Theory and Numerical Implementation. BNWL-1706, Pacific Northwest Laboratory, Richland, Washington.

Doremus, L. A., and A. W. Pearson. 1990. Borehole Completion Data Package for the Liquid Effluent Retention Facility. WHC-MR-0235, Westinghouse Hanford Company, Richland, Washington.

Evans, J. C., D. I. Dennison, R. W. Bryce, P. J. Mitchell, D. R. Sherwood, K. M. Krupka, N. W. Hinman, E. A. Jacobson, and M. D. Freshley. 1988. Hanford Site Groundwater Monitoring for July Through December 1987. PNL-6315-2, Pacific Northwest Laboratory, Richland, Washington.

Evans, J. C., R. W. Bryce, D. J. Bates, and M. L. Kemner. 1990. Hanford Site Ground-Water Surveillance for 1989. PNL-7396, Pacific Northwest Laboratory, Richland, Washington.

Fecht, K. R. 1978. Geology of Gable Mountain--Gable Butte Area. RHO-BWI-LD-5, Rockwell Hanford Operations, Richland, Washington.

Felmy, A. R., D. C. Girvin, and E. A. Jenne. 1984a. MINTEQ: A Computer Program for Calculation of Aqueous Geochemical Equilibria. EPA/600/3-84-032 (NTIS PB84-157148), Prepared for the U.S. Environmental Protection Agency (Athens, Georgia) by Battelle, Pacific Northwest Laboratories, Richland, Washington.

Felmy, A. R., S. M. Brown, Y. Onishi, S. B. Yabusaki and R. S. Argo. 1984b. MEXAMS--The Metals Exposure Analysis Modeling System. EPA-600/3-84-031 (NTIS PB84-157155), Prepared for the U.S. Environmental Protection Agency (Athens, Georgia) by Battelle, Pacific Northwest Laboratories, Richland, Washington.

Freundlich, H. 1926. Colloid and Capillary Chemistry. Methuen, London.

Gary, M., R. McAfee, Jr., and C. L. Wolf. 1974. Glossary of Geology, American Geological Institute, Washington, D. C.

Gephart, R. E., R. C. Arnett, R. G. Baca, L. S. Leonhart, F. A. Spane, Jr., D. A. Palombo, and S. R. Strait. 1979. Hydrologic Studies Within the Columbia Plateau, Washington: An Integration of Current Knowledge. RHO-BWI-ST-5, Rockwell Hanford Operations, Richland, Washington.

Graham, M. J., M. D. Hall, S. R. Strait, and W. R. Brown. 1981. Hydrology of the Separations Area. RHO-ST-42, Rockwell Hanford Operations, Richland, Washington.

Graham, M. J., G. V. Last, and K. R. Fecht. 1984. An Assessment of Aquifer Intercommunication in the B Pond-Gable Mountain Pond Area of the Hanford Site. RHO-RE-ST-12P, Rockwell Hanford Operations, Richland, Washington.

Gupta, S. K., C. T. Kincaid, P. R. Meyer, C. A. Newbill, and C. R. Cole. 1982. A Multi-Dimensional Finite Element Code for the Analysis of Coupled Fluid, Energy, and Solute Transport (CFEST). PNL-4260, Pacific Northwest Laboratory, Richland, Washington.

Gupta, S. K., C. R. Cole, C. T. Kincaid, and A. M. Monti. 1987. Coupled Fluid, Energy, and Solute Transport (CFEST) Model: Formulation and User's Manual. BMI/ONWI-660, Office of Nuclear Waste Isolation, Battelle Memorial Institute, Columbus, Ohio.

Jacobson, E. A. 1985. A Statistical Parameter Estimation Method Using Singular Value Decomposition With Application to Avra Valley Aquifer in Southern Arizona. Dissertation, Department of Hydrology and Water Resources, University of Arizona.

Jacobson, E. A., and M. D. Freshley. 1990. An Initial Inverse Calibration of the Groundwater Flow Model for the Hanford Unconfined Aquifer. PNL-7144, Pacific Northwest Laboratory, Richland, Washington.

Jensen, E. J. 1987. An Evaluation of Aquifer Intercommunication Between the Unconfined and Rattlesnake Ridge Aquifers on the Hanford Site. PNL-6313, Pacific Northwest Laboratory, Richland, Washington.

Kasza, G. L., M. J. Hartman, F. N. Hodges, and D. C. Weekes. 1991. Ground Water Maps of the Hanford Site, June 1991. WHC-EP-0394-3, Westinghouse Hanford Company, Richland, Washington.

Kipp, K. L, A. E. Reisenauer, C. R. Cole, and L. A. Bryan. 1972. Variable Thickness Transient Groundwater Flow Model: Theory and Numerical Implementation. BNWL-1703, Pacific Northwest Laboratory, Richland, Washington.

Langmuir, D. 1918. "The Adsorption of Gases on Plane Surfaces of Glass, Mica, and Platinum." J. Am. Chem. Soc. 40:1361-1403.

LaSala, A. M., Jr., and G. C. Doty. 1975. Geology and Hydrology of Radioactive Solid-Waste Burial Grounds at the Hanford Reservation, Washington. U. S. Geological Survey Open File Report 75-625, U.S. Government Printing Office, Washington, D.C.

Last, G. V., B. N. Bjornstad, M. P. Bergeron, D. W. Wallace, D. R. Newcomer, J. A. Schramke, M. A. Chamness, C. S. Cline, S. P. Airhart, and J. S. Wilbur. 1989. Hydrogeology of the 200 Areas Low-Level Burial Grounds--An Interim Report. PNL-6820, Pacific Northwest Laboratory, Richland, Washington.

Lindsey, K. A. 1991. Revised Stratigraphy for the Ringold Formation, Hanford Site, South-Central Washington. WHC-SD-EE-004, Westinghouse Hanford Company, Richland, Washington.

Lindsey, K. A., B. N. Bjornstad, J. W. Lindberg, and K. Hoffman. 1992. Geologic Setting of the 200 East Area: An Update. WHC-SD-EN-TI-012, Westinghouse Hanford Company, Richland, Washington.

Lum, W. E., J. L. Smoot, and D. R. Ralston. 1990. Geohydrology and Numerical Model Analysis of Groundwater Flow in the Pullman-Moscow Area, Washington and Idaho. Water-Resources Investigations Report 89-4103, U. S. Geological Survey, Tacoma, Washington.

Malde, H. E. 1968. The Catastrophic Late Pleistocene Bonneville Flood in the Snake River Plain, Idaho. U.S. Geological Survey Professional Paper 596, U.S. Government Printing Office, Washington, D.C.

Matthes, G. H. 1947. "Macroturbulence in Stream Flow." American Geophysical Union Transactions 28:255-262.

McKee, E. H., D. A. Swanson, and T. L. Wright. 1977. Duration and Volume of the Columbia River Basalt Volcanism: Washington, Oregon, and Idaho. Geological Society of America, Abstracts with Programs, pp. 463-464.

Muller, A. B., D. Langmuir, and L. E. Duda. 1983. "The Formulation of an Integrated Physicochemical-Hydrologic Model for Predicting Waste Nuclide Retardation in Geologic Media." In Scientific Basis for Nuclear Waste Management VI, Proceedings of Materials Research Society Symposia, ed. D. G. Brookings, pp. 547-564. North Holland, New York.

Mullineaux, D. R., R. E. Wilcox, W. F. Ebaugh, R. Fryxell, and M. Rubin. 1978. "Age of the Last Major Scabland Flood of the Columbia Plateau in Eastern Washington." Quaternary Research 10:171-180.

Neuman, S. P. 1980. "A Statistical Approach to the Inverse Problem of Aquifer Hydrology: 3. Improved Solution Method and Added Perspective." Water Resour. Res. 16(2):331-346.

Newcombe, R. C., J. R. Strand, and F. J. Frank. 1972. Geology and Groundwater Characteristics of the Hanford Reservation of the U.S. Atomic Energy Commission, Washington. U.S. Geological Survey Professional Paper 717, U.S. Geological Survey, Denver, Colorado.

Nordstrom D. K., L. N. Plummer, T. M. L. Wigley, T. J. Wolery, J. W. Ball, E. A. Jenne, R. L. Bassett, D. A. Crerar, T. M. Florence, B. Fritz, M. Hoffman, G. R. Holdren, Jr., G. M. Lafon, S. V. Mattigod, R. E. McDuff, F. Morel, M. M. Reddy, G. Sposito and J. Thrailkill. 1979. "A Comparison of Computerized Chemical Models for Equilibrium Calculations in Aqueous Systems." In: Chemical Modeling in Aqueous Systems (E. A. Jenne, ed.), ACS Symposium Series 93. American Chemical Society, Washington, D. C.

Poston, T. M., K. L. Price, and D. R. Newcomer. 1991. An Evaluation of the Chemical, Radiological, and Ecological Conditions of West Lake on the Hanford Site. PNL-7662, Pacific Northwest Laboratory, Richland, Washington.

Reidel S. P., K. R. Fecht, M. C. Hagood, and T. L. Tolan. 1989. "The Geologic Evolution of the Central Columbia Plateau." In Volcanism and Tectonism in the Columbia River Flood-Basalt Province, eds. S. P. Reidel and P. R. Hooper, pp. 247-264. Special Paper 239, Geological Society of America, Boulder, Colorado.

Reisenauer, A. E. 1979a. Variable Thickness Transient Ground-Water Flow Model: Volume 1. Formulation. PNL-3160-1, Pacific Northwest Laboratory, Richland, Washington.

Reisenauer, A. E. 1979b. Variable Thickness Transient Ground-Water Flow Model: Volume 2. Users' Manual. PNL-3160-2, Pacific Northwest Laboratory, Richland, Washington.

Reisenauer, A. E. 1979c. Variable Thickness Transient Ground-Water Flow Model: Volume 3. Program Listings. PNL-3160-3, Pacific Northwest Laboratory, Richland, Washington.

Salter, P. F., L. L. Ames, and J. E. McGarrah. 1981a. The Sorption Behavior of Selected Radionuclides on Columbia River Basalts. RHO-BWI-LD-48, Rockwell Hanford Operations, Richland, Washington.

Salter, P. F., L. L.Ames, and J. E. McGarrah. 1981b. Sorption of Selected Radionuclides on Secondary Minerals Associated with the Columbia River Basalts. RHO-BWI-LD-43, Rockwell Hanford Operations, Richland, Washington.

Schatz, A. L., and J. J. Ammerman. 1988. Ground-Water Maps of the Hanford Site Separations Area-December 1987. WHC-EP-0142, Westinghouse Hanford Company, Richland, Washington.

Scott, W. E., W. D. McCoy, R. R. Schroba, and M. Rubin. 1983. "Reinterpretation of the Exposed Record of the Last Two Cycles of Lake Bonneville, Western United States." Quaternary Research 20:261-285.

Serne, R. J. and A. B. Muller. 1987. "A Perspective on Adsorption of Radionuclides Onto Geologic Media." In The Geological Disposal of High Level Radioactive Wastes, pp. 407-443. Theophrastus Publications, S. A., Athens, Greece.

Serne, R. J., and J. F. Relyea. 1983. "The Status of Radionuclide Sorption-Desorption Studies Performed by the WRIT Program." In The Technology of High-Level Nuclear Waste Disposal, Vol. 1, pp. 203-254. DOE/TIC-621, Technical Information Center, U.S. Department of Energy, Oak Ridge, Tennessee.

Silling, S. A. 1983. Final Technical Position on Documentation of Computer Codes for High-Level Waste Management. NUREG-0856, Division of Waste Management, Office of Nuclear Material Safety and Safeguards, U. S. Nuclear Regulatory Commission, Washington, D. C.

Simmons, C. S., C. T. Kincaid, and A. E. Reisenauer. 1986. A Simplified Model for Radioactive Contaminant Transport: The TRANSS Code. PNL-6029, Pacific Northwest Laboratory, Richland, Washington.

Strait, S. R., and B. A. Moore. 1982. Geohydrology of the Rattlesnake Ridge Interbed in the Gable Mountain Pond Area. RHO-ST-38, Rockwell Hanford Operations, Richland, Washington.

Tallman, A. M., K. R. Fecht, M. C. Marratt, and G. V. Last. 1979. Geology of the Separation Areas, Hanford Site, South-Central Washington. RHO-ST-23, Rockwell Hanford Operations, Richland, Washington.

Tolan, T. L., S. P. Reidel, M. H. Beeson, J. L. Anderson, K. R. Fecht, and D. A. Swanson. 1989. "Revisions to the Extent of and Volume of the Columbia River Basalt Group." In Volcanism and Tectonism in the Columbia River Flood-Basalt Province, eds. S. P. Reidel and P. R. Hooper, pp. 1-20. Special Paper 239, Geological Society of America, Boulder, Colorado.

U.S. Department of Energy (DOE). 1987. Disposal of Hanford Defense High-Level, Transuranic and Tank Wastes. Final Environmental Impact Statement. DOE/EIS-0113, Vol. 1-5, Assistant Secretary for Defense Programs, Washington, D.C.

U. S. Department of Energy (DOE). 1988. Consultation Draft, Site Characterization Plan, Reference Repository Location, Hanford Site, Washington. DOE/RW-0164, v. 1, U.S. Department of Energy, Washington, D.C.

U. S. Department of Energy (DOE). 1990a. Quarterly Report of RCRA Groundwater Monitoring Data for Period April 1, 1990 Through June 30, 1990. DOE/RL-90-36, prepared by the Geosciences Group, Westinghouse Hanford Company, for the U.S. Department of Energy, Richland, Washington.

U. S. Department of Energy (DOE). 1990b. Quarterly Report of RCRA Groundwater Monitoring Data for Period July 1, 1990 Through September 30, 1990. DOE/RL-90-46, prepared by the Geosciences Group, Westinghouse Hanford Company, for the U.S. Department of Energy, Richland, Washington.

Waitt, R. B., Jr. 1980. "About Forty Last-Glacial Lake Missoula Jokulhlaups Through Southern Washington." Journal of Geology 88:653-679.

Westinghouse Hanford Company (WHC). 1991. Hanford Environmental Information System (HEIS) Operators' Manual. WHC-SP-0660, Westinghouse Hanford Company, Richland, Washington.

APPENDIX B

FIELD AND LABORATORY DATA

CONTENTS - APPENDIX B

APPENDIX B
Part 1

HYDRAULIC CONDUCTIVITY, MOISTURE CONTENT, AND BULK DENSITY ANALYSES OF SAMPLES FROM THE 218-E-12B BURIAL GROUND

WATER_BD 9R x 3C

SAMPLE	HYDRAULIC CONDUCTIVITY (cm/sec)	FIELD WATER CONTENT (g/g)	BULK DENSITY (g/cm**3)
#2 (horiz)	0.001570	0.1239	
#2 (vert)	0.000539		1.46
#3	0.003500	0.1606	1.37
#6	0.022200	0.0525	1.36
#14	0.014200	0.2937	1.54
#15	0.033100	0.0289	1.68
#18	0.019300	0.0518	1.30
#19	0.030700	0.0368	1.84
#20	0.010000	0.0154	1.84

APPENDIX B
Part 2

CLAY MINERAL IDENTIFICATION OF SELECTED SAMPLES FROM THE 218-E-12B BURIAL GROUND

Mineralogical/Textural Analyses of Sediment Samples

. Amonette 24-Feb-92

Mineral	Sample Identification										
	Trench Sample Number					Well 299-E35-1					
	13	14	16	17	21	20 Ft	35 Ft	49 Ft	75 Ft	115 Ft	180 Ft
TEXTURE OF <8mm FRACTION	wt %										
Gravel (2-8 mm)	50	--*	17	2	< 1	33	9	< 1	10	23	35
Sand (53-2000 um)	32	81	62	43	51	48	61	76	56	53	43
Silt (2-53 um)	16	16	18	52	46	16	22	21	28	20	19
Clay (<2 um)**	2	4	3	3	4	3	8	3	7	4	3
CLAY FRACTION MINERALOGY	wt %										
Illite	13	8	16	20	13	4	5	9	3	4	3
Talc	--	1	--	--	--	--	--	1	--	--	--
Hornblende	1	1	1	< 1	--	2	2	1	2	2	1
Kaolinite	2	3	4	4	10	< 1	< 1	2	1	< 1	1
Chlorite	2	2	3	4	1	2	2	2	3	3	2
Vermiculite	6	8	5	2	5	2	2	4	3	2	4
Smectite	49	53	45	36	64	35	49	63	41	38	35
Quartz	8	5	8	12	3	15	10	7	12	11	14
Plagioclase	20	20	19	23	3	40	31	11	36	39	41
Layer Silicates Only	wt %										
Illite	18	11	22	31	14	10	9	11	6	8	6
Talc	--	2	--	--	--	--	--	1	--	--	--
Kaolinite	3	4	5	5	10	1	1	3	1	1	2
Chlorite	2	3	4	7	1	6	4	3	6	5	5
Vermiculite	9	11	7	2	5	4	3	5	6	5	9
Smectite	69	71	62	55	69	[illegible]	[illegible]	[illegible]	81	81	79

* none detected
** Calculated by difference (100-%Gravel-%Sand-%Silt = %Clay)

APPENDIX B
Part 3

PARTICLE SIZE DISTRIBUTION BY HYDROMETER OF SELECTED SAMPLES FROM THE 218-E-12B BURIAL GROUND

Model for Comput.tion of Particle Size Ordinates

0	sample weight 1	Ps & HMP 2	Time 3	Temp 4	Soil and Sieve Wt 5	Sieve Wt 6	Soil or Reading 7	Blank or Soil Sum 8	rhoW & n 9	Theta
1	49.71	2.73						0.00	1.003150	
2	A	5.00			144.69	134.98	9.71	9.71		
3	SAMPLE				125.00	118.45	6.55	16.26		
4					102.84	101.11	1.73	17.99		
5					106.05	104.97	1.08	19.07		
6					115.89	96.42	19.47	38.54		
7					103.56	100.08	3.48	42.02		
8					92.10	90.65	1.45	43.47		
9			1.0	23.3			9.50	4.00	0.009261	51.64
10			3.0	23.3			8.90	4.00	0.009261	51.81
11			10.0	23.3			8.00	4.00	0.009261	52.07
12			29.5	23.3			7.65	4.00	0.009261	52.17
13			60.0	23.3			7.20	4.00	0.009261	52.30
14			90.0	23.3			7.00	4.00	0.009261	52.35
15			120.0	23.3			7.00	4.00	0.009261	52.35
16			1440.0	23.5			6.80	4.20	0.009218	52.41
17				0.0						
18	49.71	2.73						0.00		
19	B				144.69	134.98	9.71	9.71		
20	SAMPLE				125.31	118.45	6.86	16.57		
21					103.14	101.11	2.03	18.60		
22					106.58	104.97	1.61	20.21		
23					115.53	96.42	19.11	39.32		
24					103.38	100.08	3.30	42.62		
25					92.29	90.65	1.64	44.26		
26			1.0	23.3			10.00	4.00	0.009261	51.50
27			3.0	23.3			8.90	4.00	0.009261	51.81
28			10.0	23.3			8.00	4.00	0.009261	52.07
29			29.5	23.3			7.20	4.00	0.009261	52.30
30			60.0	23.3			6.80	4.00	0.009261	52.41
31			90.0	23.3			6.80	4.00	0.009261	52.41
32			120.0	23.3			6.80	4.00	0.009261	52.41
33			1440.0	23.3			6.80	4.20	0.009261	52.41

Model for Computation of Particle Size Ordinates

0	sample weight	10 C	11 X. Part Size	12 P (% <)	13 X. Avg	14 P. Avg	15 TEXTURE ANALYSIS
1	49.71						87% SAND
2	A		2000.000	80.470000	2000.000	80.470	8% SILT
3	SAMPLE		1000.000	67.290000	1000.000	66.980	5% CLAY
4			500.000	63.810000	500.000	63.200	LOAMY SAND
5			250.000	61.640000	250.000	60.490	
6			106.000	22.470000	106.000	21.690	
7			75.000	15.470000	75.000	14.870	
8			53.000	12.550000	53.000	11.760	
9		5.50	51.640	11.064172	51.570	11.570	
10		4.90	29.910	9.857172	29.910	9.857	
11		4.00	16.470	8.046671	16.470	8.047	
12		3.65	9.605	7.342587	9.617	6.890	
13		3.20	6.752	6.437337	6.759	6.035	
14		3.00	5.518	6.035003	5.521	5.834	
15		3.00	4.779	6.035003	4.782	5.834	
16		2.60	1.381	5.230336	1.381	5.230	
17							
18	49.71						
19	B		2000.000	80.470000			
20	SAMPLE		1000.000	66.670000			
21			500.000	62.580000			
22			250.000	59.340000			
23			106.000	20.900000			
24			75.000	14.260000			
25			53.000	10.960000			
26		6.00	51.500	12.070006			
27		4.90	29.910	9.857172			
28		4.00	16.470	8.046671			
29		3.20	9.629	6.437337			
30		2.80	6.766	5.632669			
31		2.80	5.524	5.632669			
32		2.80	4.784	5.632669			
33		2.60	1.381	5.230336			

PARTICLE SIZE ANALYSIS
SUBPIT SAMPLE #3

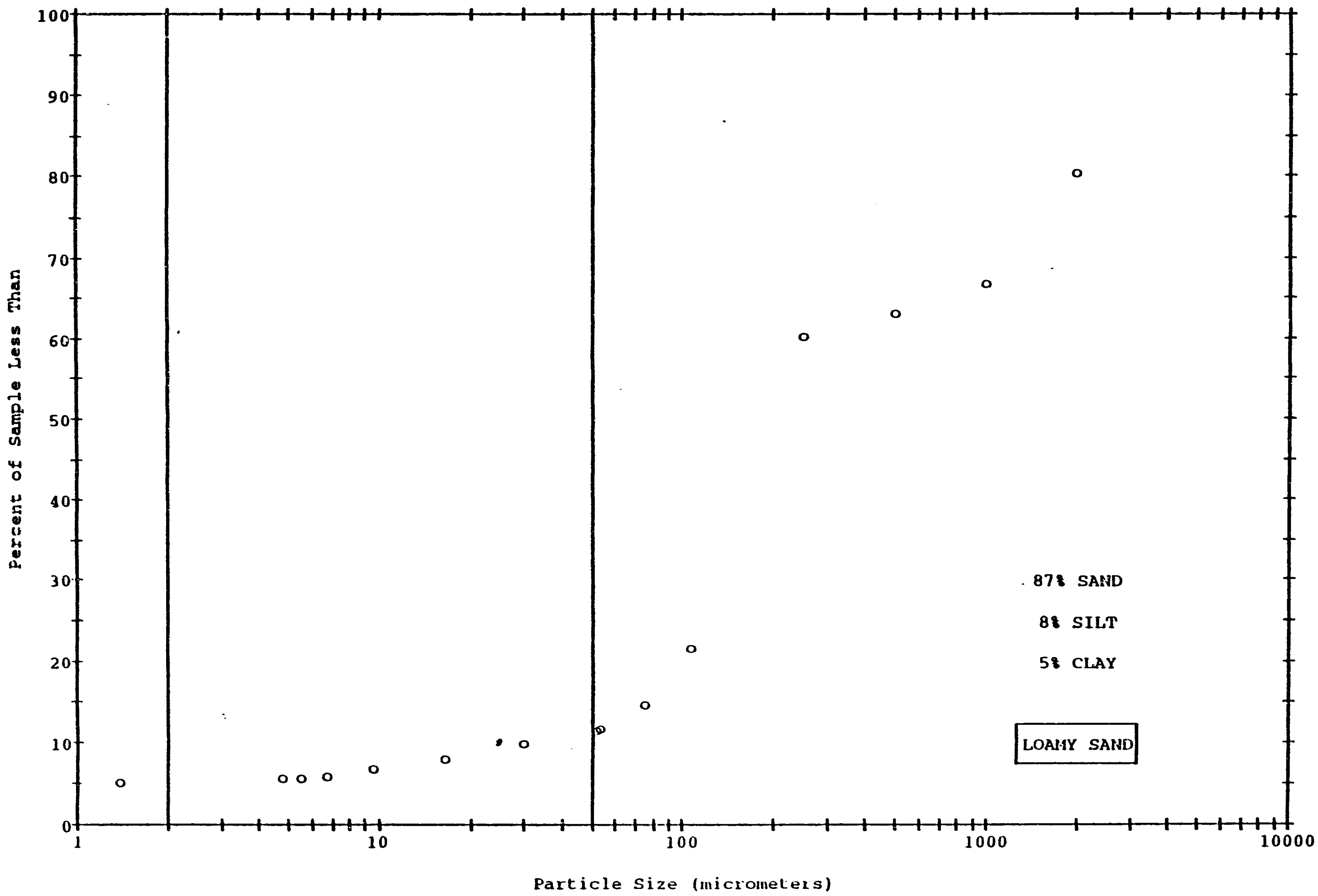

Model for Computation of Particle Size Ordinates

0	sample weight 1	Ps & HMP 2	Time 3	Temp	4 Soil and Sieve Wt	5 Sieve Wt 6	Soil or Reading	7 Blank or Soil Sum	8 rhoW & n 9	Theta
1	529.8	2.73						0.00	1.003150	
2	A	5.00			624.78	134.98	489.80	489.80		
3	SAMPLE				124.46	118.45	6.01	495.81		
4					106.87	101.11	5.76	501.57		
5					112.25	104.97	7.28	508.85		
6					103.28	96.42	6.86	515.71		
7					101.45	100.08	1.37	517.08		
8					91.49	90.65	0.84	517.92		
9			1.0	23.3			16.20	4.00	0.009261	49.68
10			3.0	23.3			15.30	4.00	0.009261	49.94
11			10.0	23.3			14.20	4.00	0.009261	50.27
12			29.5	23.3			12.50	4.00	0.009261	50.77
13			60.0	23.3			12.00	4.00	0.009261	50.92
14			90.0	23.3			11.50	4.00	0.009261	51.06
15			120.0	23.3			11.00	4.00	0.009261	51.21
16			1440.0	23.5			8.90	4.20	0.009218	51.81
17				0.0						
18	529.8	2.73						0.00		
19	B				624.78	134.98	489.80	489.80		
20	SAMPLE				124.36	118.45	5.91	495.71		
21					106.86	101.11	5.75	501.46		
22					112.32	104.97	7.35	508.81		
23					103.52	96.42	7.10	515.91		
24					101.37	100.08	1.29	517.20		
25					91.47	90.65	0.82	518.02		
26			1.0	23.3			16.80	4.00	0.009261	49.50
27			3.0	23.3			16.00	4.00	0.009261	49.74
28			10.0	23.3			15.00	4.00	0.009261	50.03
29			29.5	23.3			13.00	4.00	0.009261	50.62
30			60.0	23.3			12.50	4.00	0.009261	50.77
31			90.0	23.3			11.00	4.00	0.009261	51.21
32			120.0	23.3			11.00	4.00	0.009261	51.21
33			1440.0	23.3			9.00	4.20	0.009261	51.78

Model for Computation of Particle Size Ordinates

0	sample weight	10 C	11 X. Part Size	12 P (% <)	13 X. Avg	14 P. Avg	15 TEXTURE ANALYSIS
1	529.8						98% SAND
2	A		2000.000	7.550000	2000.000	7.5500	1% SILT
3	SAMPLE		1000.000	6.416000	1000.000	6.4260	1% CLAY
4			500.000	5.328000	500.000	5.3390	SAND
5			250.000	3.954000	250.000	3.9580	
6			106.000	2.659000	106.000	2.6410	
7			75.000	2.401000	75.000	2.3900	
8			53.000	2.242000	53.000	2.2330	
9		12.2	49.680	2.302756	49.590	2.3590	
10		11.3	28.830	2.132880	28.780	2.1990	
11		10.2	15.900	1.925255	15.860	2.0010	
12		8.5	9.348	1.604379	9.334	1.6520	
13		8.0	6.574	1.510004	6.564	1.5570	
14		7.5	5.382	1.415629	5.390	1.3680	
15		7.0	4.675	1.321253	4.675	1.3210	
16		4.7	1.365	0.887127	1.365	0.8966	
17							
18	529.8						
19	B		2000.000	7.550000			
20	SAMPLE		1000.000	6.435000			
21			500.000	5.349000			
22			250.000	3.962000			
23			106.000	2.622000			
24			75.000	2.378000			
25			53.000	2.223000			
26		12.8	49.500	2.416006			
27		12.0	28.720	2.265006			
28		11.0	15.820	2.076255			
29		9.0	9.320	1.698754			
30		8.5	6.554	1.604379			
31		7.0	5.398	1.321253			
32		7.0	4.675	1.321253			
33		4.8	1.365	0.906002			

PARTICLE SIZE ANALYSIS
SUBPIT SAMPLE #7

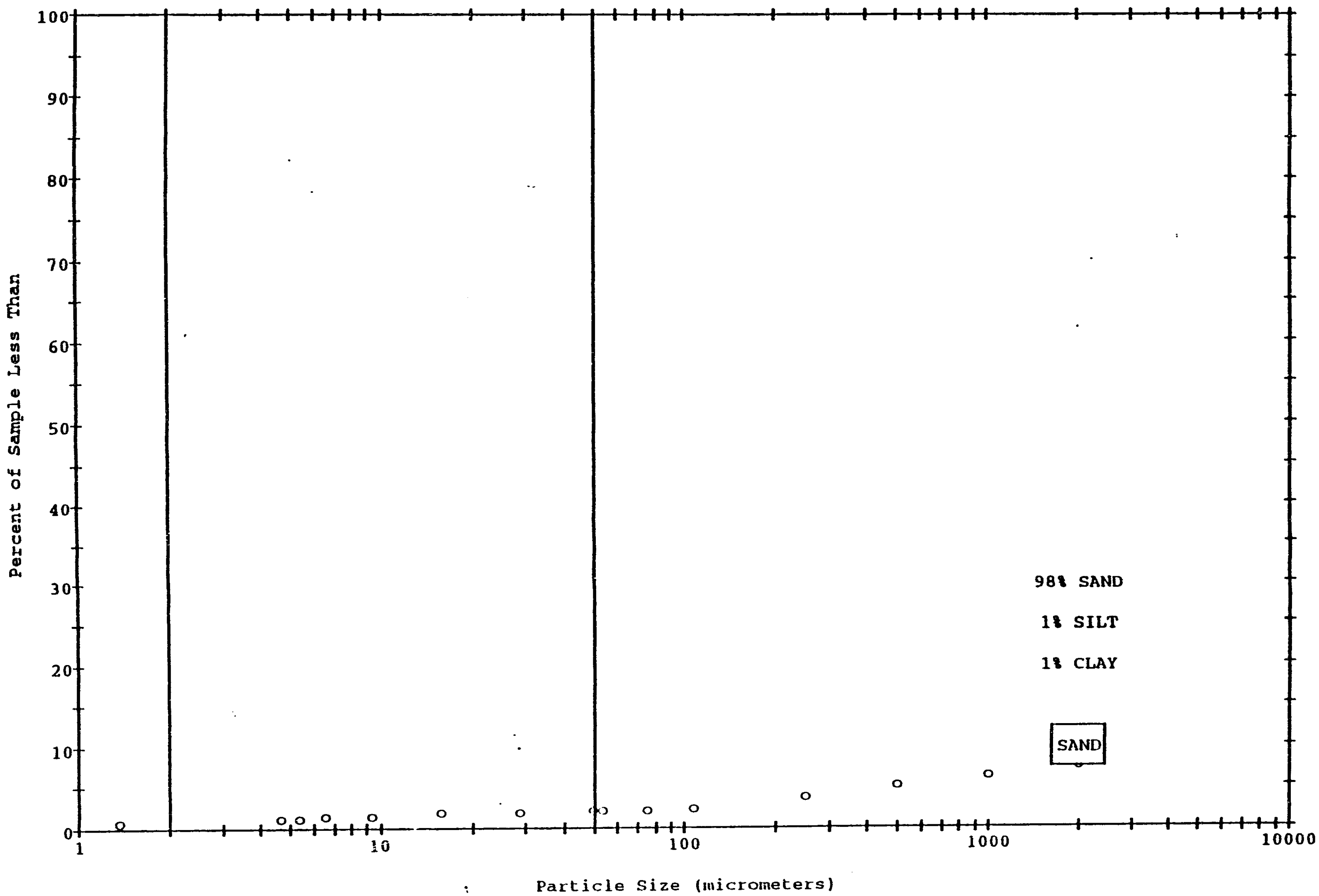

Model for Computation of Particle Size Ordinates

0	sample weight 1	Ps & HMP 2	Time 3	Temp 4	Soil and Sieve Wt 5	Sieve Wt 6	Soil or Reading 7	Blank or Soil Sum 8	rhoW & n 9	Theta
1	100.88	2.73						0.000	1.003150	
2	A	5.00			195.860	134.98	60.880	60.880		
3	SAMPLE				131.010	118.45	12.560	73.440		
4					110.190	101.11	9.080	82.520		
5					113.640	104.97	8.670	91.190		
6					101.580	96.42	5.160	96.350		
7					100.690	100.08	0.610	96.960		
8					90.890	90.65	0.240	97.200		
9			1.0	23.3			9.000	4.000	0.009261	51.78
10			3.0	23.3			9.000	4.000	0.009261	51.78
11			10.0	23.3			9.000	4.000	0.009261	51.78
12			29.5	23.3			8.500	4.000	0.009261	51.93
13			60.0	23.3			8.000	4.000	0.009261	52.07
14			90.0	23.3			8.000	4.000	0.009261	52.07
15			120.0	23.3			8.000	4.000	0.009261	52.07
16			1440.0	23.5			7.200	4.200	0.009218	52.30
17				0.0				0.000		
18	100.88	2.73								
19	B				195.860	134.98	60.880	60.880		
20	SAMPLE				133.430	118.45	14.980	75.860		
21					109.360	101.11	8.250	84.110		
22					113.156	104.97	8.186	92.296		
23					100.820	96.42	4.400	96.696		
24					100.570	100.08	0.490	97.186		
25					90.830	90.65	0.180	97.366		
26			1.0	23.3			9.000	4.000	0.009261	51.78
27			3.0	23.3			9.000	4.000	0.009261	51.78
28			10.0	23.3			9.000	4.000	0.009261	51.78
29			29.5	23.3			8.800	4.000	0.009261	51.84
30			60.0	23.3			8.800	4.000	0.009261	51.84
31			90.0	23.3			8.200	4.000	0.009261	52.01
32			120.0	23.3			8.200	4.000	0.009261	52.01
33			1440.0	23.3			7.800	4.200	0.009261	52.13

Model for Computation of Particle Size Ordinates

0	sample weight	10 C	11 X. Part Size	12 P (% <)	13 X. Avg	14 P. Avg	15 TEXTURE ANALYSIS
1	100.88						96% SAND
2	A		2000.000	39.650000	2000.000	39.650	1% SILT
3	SAMPLE		1000.000	27.200000	1000.000	26.000	3% CLAY
4			500.000	18.200000	500.000	17.410	SAND
5			250.000	9.605000	250.000	9.057	
6			106.000	4.490000	106.000	4.319	
7			75.000	3.886000	75.000	3.774	
8			53.000	3.648000	53.000	3.566	
9		5.0	51.780	4.956384	51.780	4.956	
10		5.0	29.900	4.956384	29.900	4.956	
11		5.0	16.370	4.956384	16.370	4.956	
12		4.5	9.561	4.460745	9.553	4.609	
13		4.0	6.722	3.965107	6.708	4.362	
14		4.0	5.489	3.965107	5.486	4.064	
15		4.0	4.753	3.965107	4.751	4.064	
16		3.0	1.378	2.973830	1.376	3.271	
17							
18	100.88						
19	B		2000.000	39.650000			
20	SAMPLE		1000.000	24.800000			
21			500.000	16.620000			
22			250.000	8.509000			
23			106.000	4.148000			
24			75.000	3.662000			
25			53.000	3.483000			
26		5.0	51.780	4.956384			
27		5.0	29.900	4.956384			
28		5.0	16.370	4.956384			
29		4.8	9.545	4.758128			
30		4.8	6.693	4.758128			
31		4.2	5.482	4.163362			
32		4.2	4.748	4.163362			
33		3.6	1.374	3.568596			

PARTICLE SIZE ANALYSIS
SUBPIT SAMPLE #9

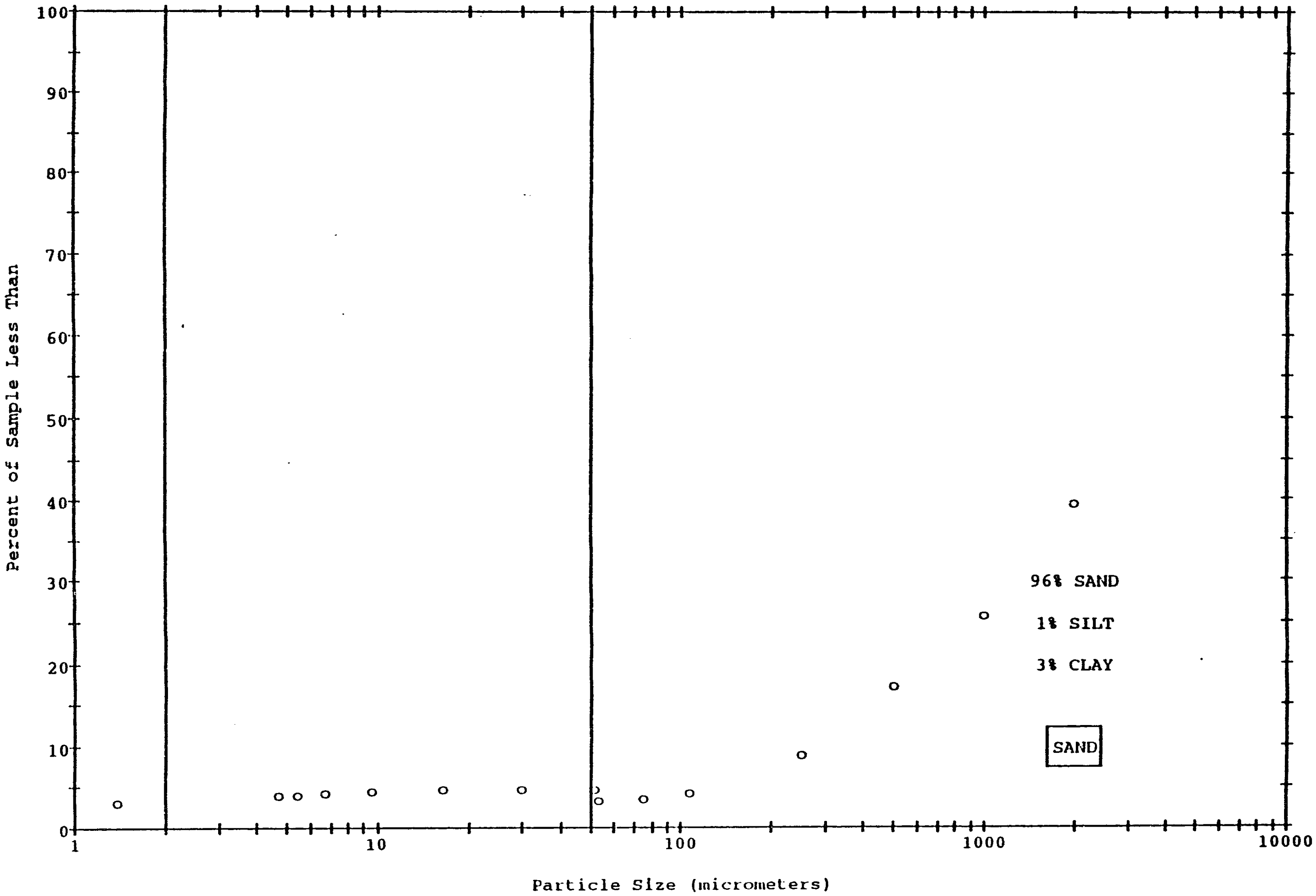

Model for Computation of Particle Size Ordinates

0 sample weight	1 Ps & HMP	2 Time	3 Temp	4 Soil and Sieve Wt	5 Sieve Wt	6 Soil or Reading	7 Blank or Soil Sum	8 rhoW & n	9 Theta
1 489.6	2.73						0.00	1.003150	
2 A	5.00			584.58	134.98	449.60	449.60		
3 SAMPLE				123.15	118.45	4.70	454.30		
4				106.23	101.11	5.12	459.42		
5				112.33	104.97	7.36	466.78		
6				102.93	96.42	6.51	473.29		
7				101.48	100.08	1.40	474.69		
8				91.58	90.65	0.93	475.62		
9		1.0	23.3			18.00	4.00	0.009261	49.14
10		3.0	23.3			17.00	4.00	0.009261	49.44
11		10.0	23.3			15.20	4.00	0.009261	49.97
12		29.5	23.3			13.80	4.00	0.009261	50.39
13		60.0	23.3			12.50	4.00	0.009261	50.77
14		90.0	23.3			12.00	4.00	0.009261	50.92
15		120.0	23.3			11.50	4.00	0.009261	51.06
16		1440.0	23.5			9.00	4.20	0.009218	51.78
17			0.0						
18 489.6	2.73						0.00		
19 B				584.58	134.98	449.60	449.60		
20 SAMPLE				124.50	118.45	6.05	455.65		
21				106.37	101.11	5.26	460.91		
22				111.97	104.97	7.00	467.91		
23				102.85	96.42	6.43	474.34		
24				101.22	100.08	1.14	475.48		
25				91.43	90.65	0.78	476.26		
26		1.0	23.3			17.90	4.00	0.009261	49.17
27		3.0	23.3			16.20	4.00	0.009261	49.68
28		10.0	23.3			15.50	4.00	0.009261	49.88
29		29.5	23.3			13.30	4.00	0.009261	50.54
30		60.0	23.3			12.50	4.00	0.009261	50.77
31		90.0	23.3			12.00	4.00	0.009261	50.92
32		120.0	23.3			11.90	4.00	0.009261	50.95
33		1440.0	23.3			9.00	4.20	0.009261	51.78

Model for Computation of Particle Size Ordinates

0	sample weight	10 C	11 X. Part Size	12 P (% <)	13 X. Avg	14 P. Avg	15 TEXTURE ANALYSIS
1	489.6						97% SAND
2	A		2000.000	8.170000	2000.000	8.1700	2% SILT
3	SAMPLE		1000.000	7.210000	1000.000	7.0720	1% CLAY
4			500.000	6.164000	500.000	6.0120	SAND
5			250.000	4.661000	250.000	4.5460	
6			106.000	3.331000	106.000	3.2240	
7			75.000	3.045000	75.000	2.9650	
8			53.000	2.855000	53.000	2.7900	
9		14.0	49.140	2.859477	49.160	2.8490	
10		13.0	28.540	2.655229	28.610	2.5740	
11		11.2	15.800	2.287582	15.790	2.3180	
12		9.8	9.278	2.001634	9.292	1.9510	
13		8.5	6.554	1.736111	6.554	1.7360	
14		8.0	5.367	1.633987	5.367	1.6340	
15		7.5	4.661	1.531863	4.656	1.5730	
16		4.8	1.365	0.980392	1.365	0.9804	
17							
18	489.6						
19	B		2000.000	8.170000			
20	SAMPLE		1000.000	6.934000			
21			500.000	5.860000			
22			250.000	4.430000			
23			106.000	3.117000			
24			75.000	2.884000			
25			53.000	2.725000			
26		13.9	49.170	2.839052			
27		12.2	28.680	2.491830			
28		11.5	15.770	2.348856			
29		9.3	9.305	1.899510			
30		8.5	6.554	1.736111			
31		8.0	5.367	1.633987			
32		7.9	4.651	1.613562			
33		4.8	1.365	0.980392			

PARTICLE SIZE ANALYSIS
SUBPIT SAMPLE #10

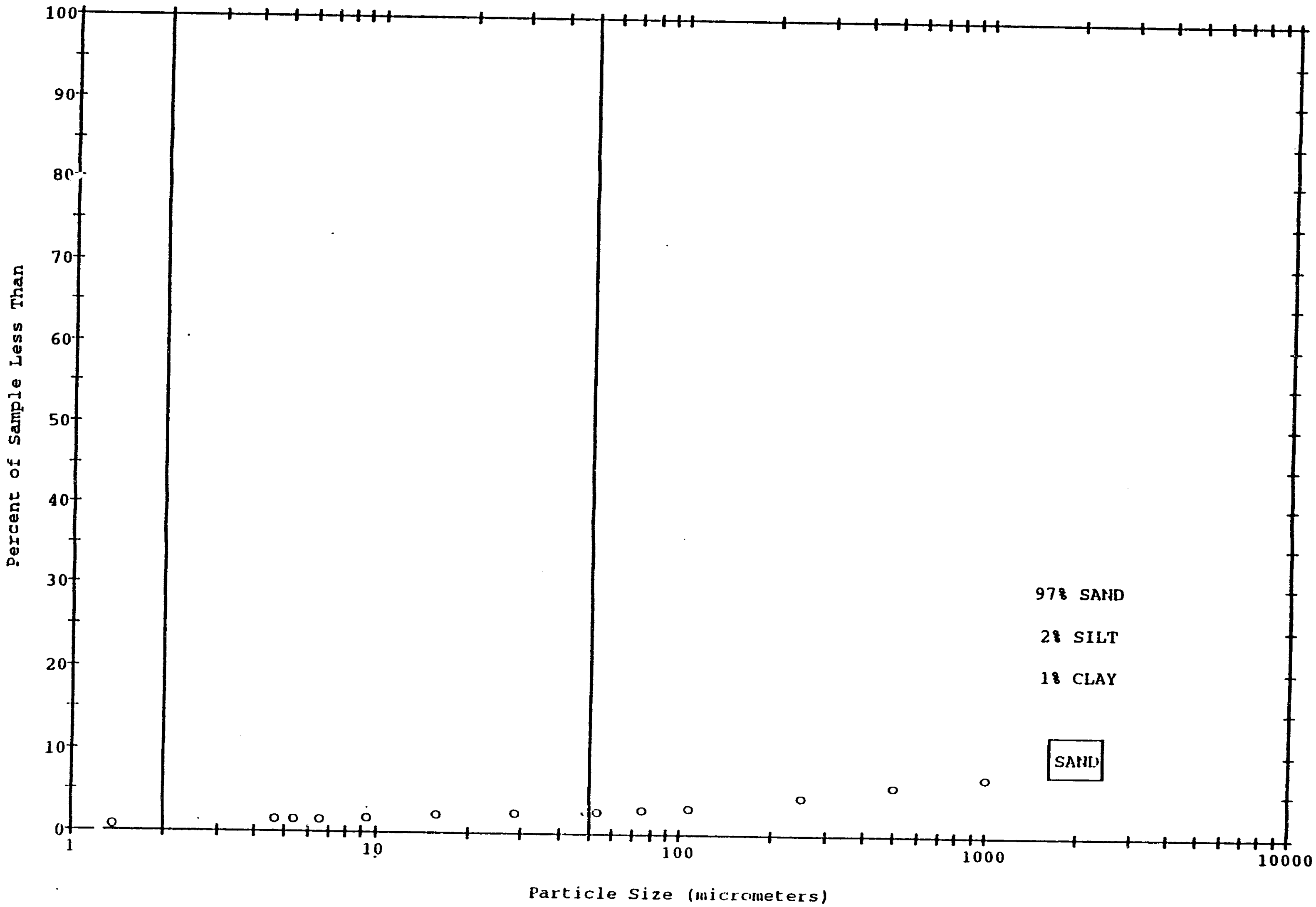

Model for Computation of Particle Size Ordinates

0	sample weight	1 Ps & HMP	2 Time	3 Temp	4 Soil and Sieve Wt	5 Sieve Wt	6 Soil or Reading	7 Blank or Soil Sum	8 rhoW & n	9 Theta
1	40.08	2.73						0.00	1.003150	
2	A	5.00			135.06	134.98	0.08	0.08		
3	SAMPLE				119.54	118.45	1.09	1.17		
4					103.57	101.11	2.46	3.63		
5					110.86	104.97	5.89	9.52		
6					116.18	96.42	19.76	29.28		
7					104.66	100.08	4.58	33.86		
8					92.80	90.65	2.15	36.01		
9			1.0	23.3			8.50	4.00	0.009261	51.93
10			3.0	23.3			8.00	4.00	0.009261	52.07
11			10.0	23.3			8.00	4.00	0.009261	52.07
12			29.5	23.3			7.20	4.00	0.009261	52.30
13			60.0	23.3			7.00	4.00	0.009261	52.35
14			90.0	23.3			7.00	4.00	0.009261	52.35
15			120.0	23.3			7.00	4.00	0.009261	52.35
16			1440.0	23.5			7.20	4.20	0.009218	52.30
17				0.0						
18	40.08	2.73						0.00		
19	B				135.06	134.98	0.08	0.08		
20	SAMPLE				119.61	118.45	1.16	1.24		
21					103.16	101.11	2.05	3.29		
22					111.25	104.97	6.28	9.57		
23					116.59	96.42	20.17	29.74		
24					104.05	100.08	3.97	33.71		
25					92.52	90.65	1.87	35.58		
26			1.0	23.3			8.50	4.00	0.009261	51.93
27			3.0	23.3			8.20	4.00	0.009261	52.01
28			10.0	23.3			8.20	4.00	0.009261	52.01
29			29.5	23.3			7.80	4.00	0.009261	52.13
30			60.0	23.3			7.20	4.00	0.009261	52.30
31			90.0	23.3			7.20	4.00	0.009261	52.30
32			120.0	23.3			7.20	4.00	0.009261	52.30
33			1440.0	23.3			7.20	4.20	0.009261	52.30

Model for Computation of Particle Size Ordinates

0	sample weight	10 C	11 X. Part Size	12 P (% <)	13 X. Avg	14 P. Avg	15 TEXTURE ANALYSIS
1	40.08						90% SAND
2	A		2000.000	99.800000	2000.000	99.800	2% SILT
3	SAMPLE		1000.000	97.080000	1000.000	97.000	8% CLAY
4			500.000	90.940000	500.000	91.370	SAND
5			250.000	76.250000	250.000	76.190	
6			106.000	26.950000	106.000	26.380	
7			75.000	15.520000	75.000	15.710	
8			53.000	10.150000	53.000	10.690	
9		4.5	51.930	11.227545	51.930	11.230	
10		4.0	30.060	9.980040	30.050	10.230	
11		4.0	16.470	9.980040	16.460	10.230	
12		3.2	9.629	7.984032	9.614	8.733	
13		3.0	6.758	7.485030	6.755	7.735	
14		3.0	5.518	7.485030	5.516	7.735	
15		3.0	4.779	7.485030	4.777	7.735	
16		3.0	1.378	7.485030	1.378	7.485	
17							
18	40.08						
19	B		2000.000	99.800000			
20	SAMPLE		1000.000	96.910000			
21			500.000	91.790000			
22			250.000	76.120000			
23			106.000	25.800000			
24			75.000	15.890000			
25			53.000	11.230000			
26		4.5	51.930	11.227545			
27		4.2	30.030	10.479042			
28		4.2	16.450	10.479042			
29		3.8	9.598	9.481038			
30		3.2	6.752	7.984032			
31		3.2	5.513	7.984032			
32		3.2	4.774	7.984032			
33		3.0	1.378	7.485030			

NSP11G

18-FEB-92 16:41 Page 1

PARTICLE SIZE ANALYSIS
SUBPIT SAMPLE #11

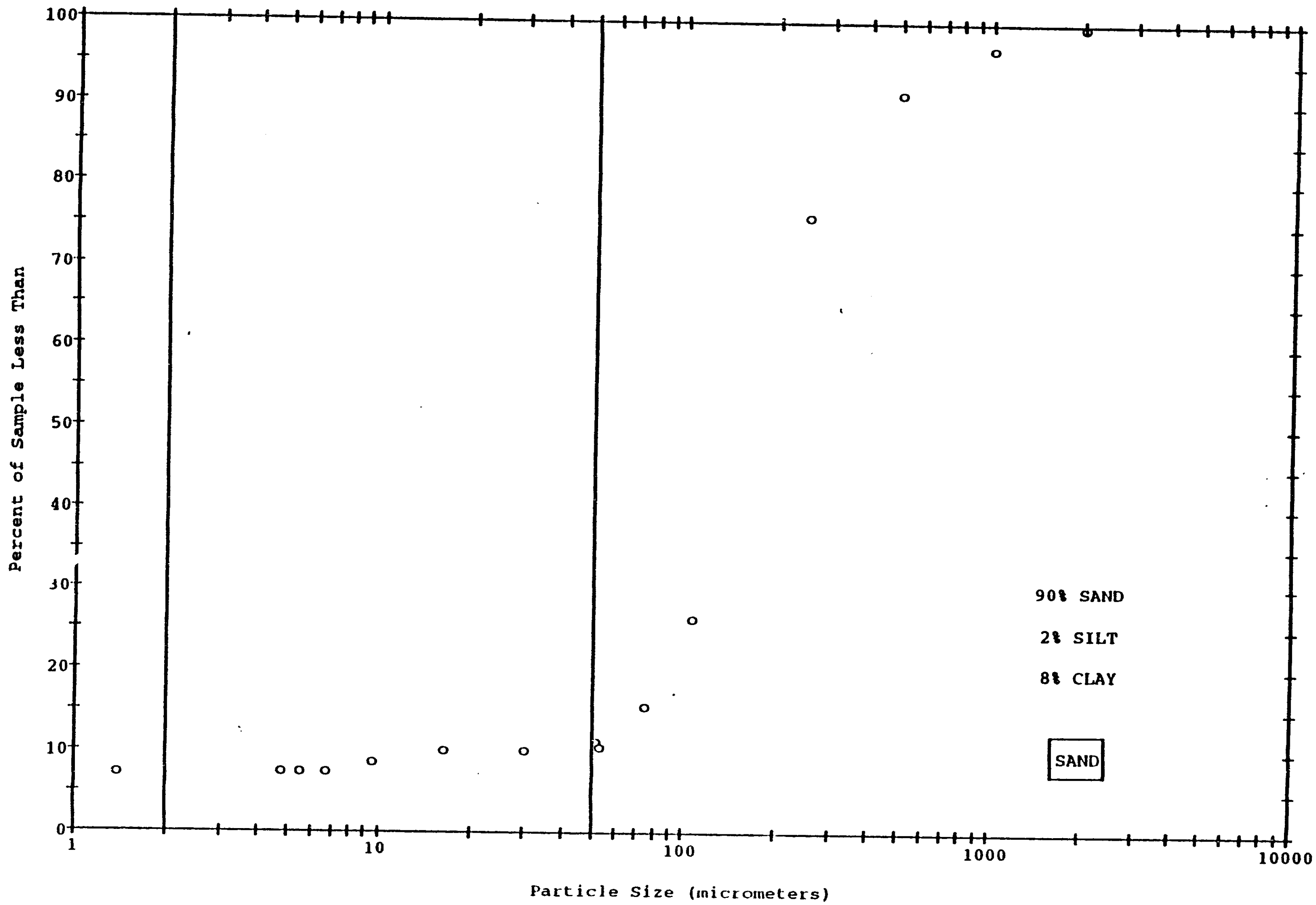

NSP12 33R x 15C

18-FEB-92 16:42 Page 1

Model for Computation of Particle Size Ordinates

0	sample weight	1 Ps & HMP	2 Time	3 Temp	4 Soil and Sieve Wt	5 Sieve Wt	6 Soil or Reading	7 Blank or Soil Sum	8 rhoW & n	9 Theta
1	40.57	2.73						0.00	1.003150	
2	A	5.00			135.55	134.98	0.57	0.57		
3	SAMPLE				119.69	118.45	1.24	1.81		
4					102.78	101.11	1.67	3.48		
5					118.33	104.97	13.36	16.84		
6					107.91	96.42	11.49	28.33		
7					102.89	100.08	2.81	31.14		
8					93.72	90.65	3.07	34.21		
9			1.0	23.3			8.00	4.00	0.009261	52.07
10			3.0	23.3			8.00	4.00	0.009261	52.07
11			10.0	23.3			8.00	4.00	0.009261	52.07
12			29.5	23.3			8.00	4.00	0.009261	52.07
13			60.0	23.3			8.00	4.00	0.009261	52.07
14			90.0	23.3			8.00	4.00	0.009261	52.07
15			120.0	23.3			8.00	4.00	0.009261	52.07
16			1440.0	23.5			8.00	4.20	0.009218	52.07
17				0.0						
18	40.57	2.73						0.00		
19	B				135.55	134.98	0.57	0.57		
20	SAMPLE				119.65	118.45	1.20	1.77		
21					102.85	101.11	1.74	3.51		
22					118.19	104.97	13.22	16.73		
23					107.82	96.42	11.40	28.13		
24					102.94	100.08	2.86	30.99		
25					93.71	90.65	3.06	34.05		
26			1.0	23.3			9.90	4.00	0.009261	51.52
27			3.0	23.3			8.80	4.00	0.009261	51.84
28			10.0	23.3			8.20	4.00	0.009261	52.01
29			29.5	23.3			8.10	4.00	0.009261	52.04
30			60.0	23.3			8.00	4.00	0.009261	52.07
31			90.0	23.3			8.00	4.00	0.009261	52.07
32			120.0	23.3			8.00	4.00	0.009261	52.07
33			1440.0	23.3			8.00	4.20	0.009261	52.07

Model for Computation of Particle Size Ordinates

0	sample weight	10 C	11 X. Part Size	12 P (% <)	13 X. Avg	14 P. Avg	15 TEXTURE ANALYSIS
1	40.57						84% SAND
2	A		2000.000	98.600000	2000.000	98.600	6% SILT
3	SAMPLE		1000.000	95.540000	1000.000	95.590	10% CLAY
4			500.000	91.420000	500.000	91.390	LOAMY SAND
5			250.000	58.490000	250.000	58.630	
6			106.000	30.170000	106.000	30.420	
7			75.000	23.240000	75.000	23.430	
8			53.000	15.680000	53.000	15.880	
9		4.0	52.070	9.859502	51.800	12.200	
10		4.0	30.060	9.859502	30.000	10.850	
11		4.0	16.470	9.859502	16.460	10.110	
12		4.0	9.587	9.859502	9.584	9.983	
13		4.0	6.722	9.859502	6.722	9.860	
14		4.0	5.489	9.859502	5.489	9.860	
15		4.0	4.753	9.859502	4.753	9.860	
16		3.8	1.372	9.366527	1.372	9.367	
17							
18	40.57						
19	B		2000.000	98.600000			
20	SAMPLE		1000.000	95.640000			
21			500.000	91.350000			
22			250.000	58.760000			
23			106.000	30.660000			
24			75.000	23.610000			
25			53.000	16.070000			
26		5.9	51.520	14.542766			
27		4.8	29.930	11.831403			
28		4.2	16.450	10.352477			
29		4.1	9.581	10.105990			
30		4.0	6.722	9.859502			
31		4.0	5.489	9.859502			
32		4.0	4.753	9.859502			
33		3.8	1.372	9.366527			

NSP12G

PARTICLE SIZE ANALYSIS
SUBPIT SAMPLE #12

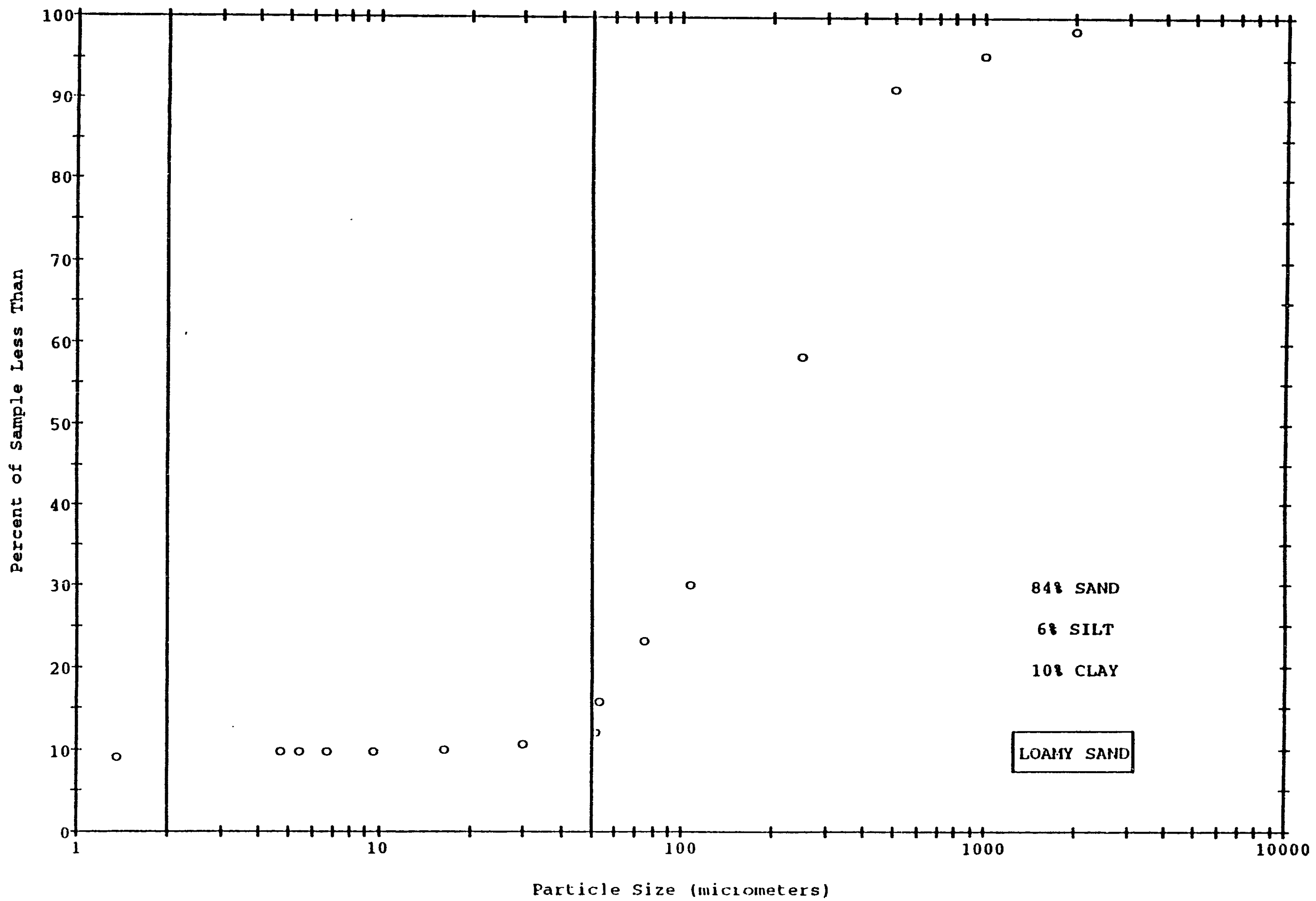

NSP14 33R x 15C

Model for Computation of Particle Size Ordinates

0	sample weight	1	Ps & HMP	2 Time	3 Temp	4 Soil and Sieve Wt	5 Sieve Wt	6 Soil or Reading	7 Blank or Soil Sum	8 rhoW & n	9 Theta
1		40	2.73						0.000	1.003150	
2	A		5.00			134.987	134.98	0.007	0.007		
3	SAMPLE					118.710	118.45	0.260	0.267		
4						101.430	101.11	0.320	0.587		
5						105.370	104.97	0.400	0.987		
6						104.040	96.42	7.620	8.607		
7						107.440	100.08	7.360	15.967		
8						96.510	90.65	5.860	21.827		
9				1.0	23.3			19.500	4.000	0.009261	48.68
10				3.0	23.3			13.000	4.000	0.009261	50.62
11				10.0	23.3			10.800	4.000	0.009261	51.26
12				29.5	23.3			9.000	4.000	0.009261	51.78
13				60.0	23.3			8.500	4.000	0.009261	51.93
14				90.0	23.3			8.200	4.000	0.009261	52.01
15				120.0	23.3			8.000	4.000	0.009261	52.07
16				1440.0	23.5			7.200	4.200	0.009218	52.30
17					0.0						
18		40	2.73						0.000		
19	B					134.980	134.98	0.000	0.000		
20	SAMPLE					118.690	118.45	0.240	0.240		
21						101.450	101.11	0.340	0.580		
22						105.330	104.97	0.360	0.940		
23						103.880	96.42	7.460	8.400		
24						107.270	100.08	7.190	15.590		
25						96.400	90.65	5.750	21.340		
26				1.0	23.3			20.000	4.000	0.009261	48.53
27				3.0	23.3			14.000	4.000	0.009261	50.33
28				10.0	23.3			11.000	4.000	0.009261	51.21
29				29.5	23.3			9.200	4.000	0.009261	51.73
30				60.0	23.3			9.000	4.000	0.009261	51.78
31				90.0	23.3			8.900	4.000	0.009261	51.81
32				120.0	23.3			8.500	4.000	0.009261	51.93
33				1440.0	23.5			7.500	4.200	0.009261	52.21

Model for Computation of Particle Size Ordinates

0	sample	weight	10 C	11 X. Part Size	12 P (% <)	13 X. Avg	14 P. Avg	15 TEXTURE ANALYSIS
1		40						55% SAND
2	A			2000.000	99.98	2000.000	99.990	36% SILT
3	SAMPLE			1000.000	99.33	1000.000	99.370	9% CLAY
4				500.000	98.53	500.000	98.540	SANDY LOAM
5				250.000	97.53	250.000	97.590	
6				106.000	78.48	106.000	78.740	
7				75.000	60.08	75.000	60.560	
8				53.000	45.43	53.000	46.040	
9			15.5	48.680	38.75	48.610	39.380	
10			9.0	29.230	22.50	29.150	23.750	
11			6.8	16.210	17.00	16.200	17.250	
12			5.0	9.533	12.50	9.529	12.750	
13			4.5	6.704	11.25	6.695	11.880	
14			4.2	5.482	10.50	5.472	11.370	
15			4.0	4.753	10.00	4.747	10.630	
16			3.0	1.378	7.50	1.377	7.875	
17								
18		40						
19	B			2000.000	100.00			
20	SAMPLE			1000.000	99.40			
21				500.000	98.55			
22				250.000	97.65			
23				106.000	79.00			
24				75.000	61.03			
25				53.000	46.65			
26			16.0	48.530	40.00			
27			10.0	29.060	25.00			
28			7.0	16.190	17.50			
29			5.2	9.524	13.00			
30			5.0	6.685	12.50			
31			4.9	5.461	12.25			
32			4.5	4.741	11.25			
33			3.3	1.376	8.25			

NSP14G 18-FEB-92 16:47 Page 1

PARTICLE SIZE ANALYSIS
SUBPIT SAMPLE #14

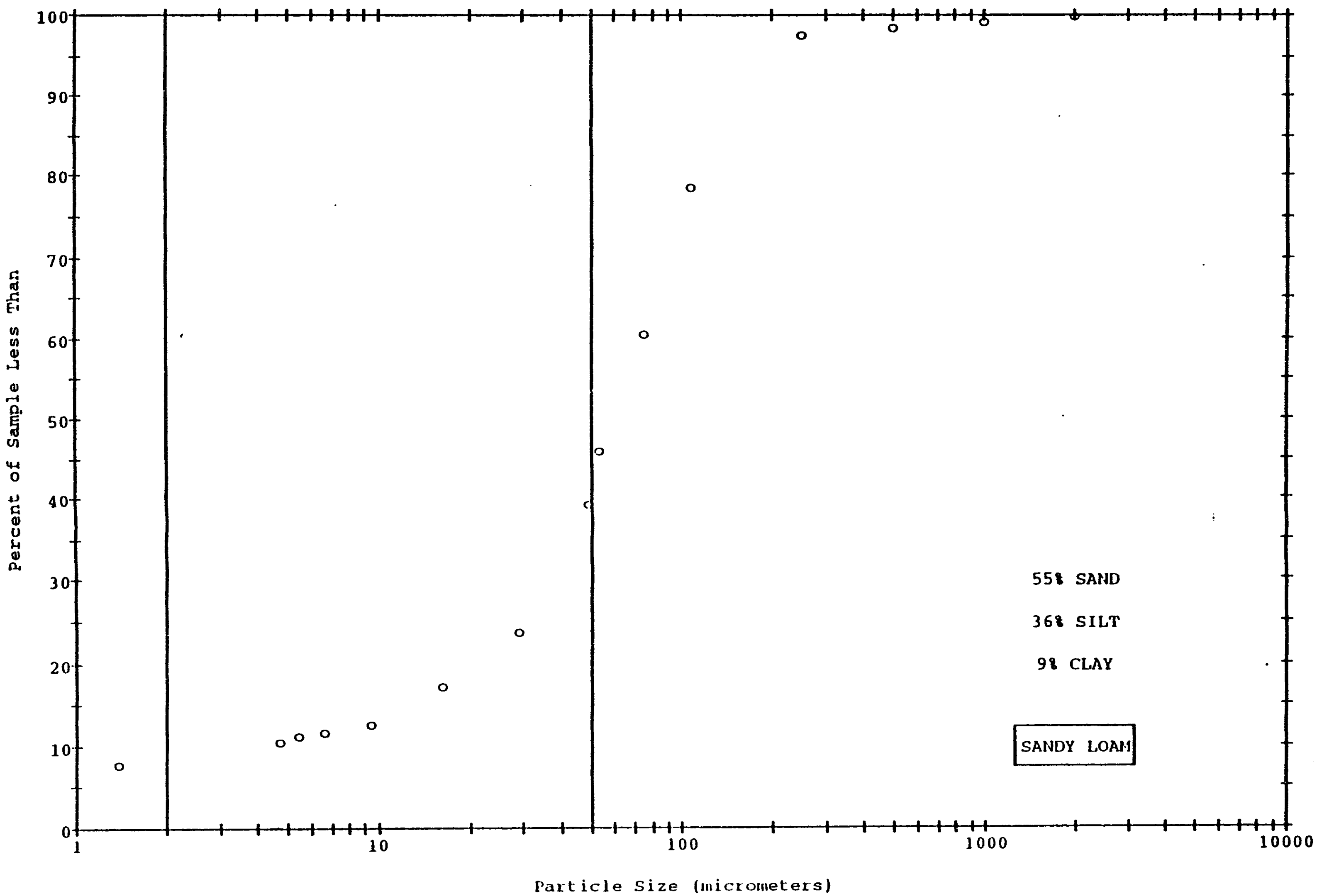

Model for Computation of Particle Size Ordinates

	0 sample weight	Ps & HMP	Time 3	Temp	4 Soil and Sieve Wt	5 Sieve Wt	6 Soil or Reading	7 Blank or Soil Sum	8 rhoW & n	9 Theta
1	60.66	2.73						0.000	1.003150	
2	A	5.00			145.640	134.98	10.660	10.660		
3	SAMPLE				142.570	118.45	24.120	34.780		
4					117.030	101.11	15.920	50.700		
5					110.240	104.97	5.270	55.970		
6					98.880	96.42	2.460	58.430		
7					100.380	100.08	0.300	58.730		
8					90.770	90.65	0.120	58.850		
9			1.0	23.3			6.900	4.000	0.009261	52.38
10			3.0	23.3			6.900	4.000	0.009261	52.38
11			10.0	23.3			6.900	4.000	0.009261	52.38
12			29.5	23.3			6.800	4.000	0.009261	52.41
13			60.0	23.3			6.800	4.000	0.009261	52.41
14			90.0	23.3			6.800	4.000	0.009261	52.41
15			120.0	23.3			6.800	4.000	0.009261	52.41
16			1440.0	23.5			6.800	4.200	0.009218	52.41
17				0.0						
18	60.66	2.73						0.000		
19	B				145.640	134.98	10.660	10.660		
20	SAMPLE				142.780	118.45	24.330	34.990		
21					116.340	101.11	15.230	50.220		
22					110.420	104.97	5.450	55.670		
23					99.130	96.42	2.710	58.380		
24					100.456	100.08	0.376	58.756		
25					90.840	90.65	0.190	58.946		
26			1.0	23.3			6.800	4.000	0.009261	52.41
27			3.0	23.3			6.800	4.000	0.009261	52.41
28			10.0	23.3			6.800	4.000	0.009261	52.41
29			29.5	23.3			6.800	4.000	0.009261	52.41
30			60.0	23.3			6.800	4.000	0.009261	52.41
31			90.0	23.3			6.800	4.000	0.009261	52.41
32			120.0	23.3			6.800	4.000	0.009261	52.41
33			1440.0	23.3			6.800	4.200	0.009261	52.41

NSP15 33R x 15C

Model for Computation of Particle Size Ordinates

0	sample weight	10 C	11 X. Part Size	12 P (% <)	13 X. Avg	14 P. Avg	15 TEXTURE ANALYSIS
1	60.66						
2	A		2000.000	82.430000	2000.000	82.430	97% SAND
3	SAMPLE		1000.000	42.660000	1000.000	42.490	-1% SILT
4			500.000	16.420000	500.000	16.820	4% CLAY
5			250.000	7.732000	250.000	7.979	SAND
6			106.000	3.676000	106.000	3.717	
7			75.000	3.182000	75.000	3.161	
8			53.000	2.984000	53.000	2.905	
9		2.9	52.380	4.780745	52.400	4.698	
10		2.9	30.240	4.780745	30.250	4.698	
11		2.9	16.560	4.780745	16.570	4.698	
12		2.8	9.649	4.615892	9.649	4.616	
13		2.8	6.766	4.615892	6.766	4.616	
14		2.8	5.524	4.615892	5.524	4.616	
15		2.8	4.784	4.615892	4.784	4.616	
16		2.6	1.381	4.286185	1.381	4.286	
17							
18	60.66						
19	B		2000.000	82.430000			
20	SAMPLE		1000.000	42.320000			
21			500.000	17.210000			
22			250.000	8.226000			
23			106.000	3.759000			
24			75.000	3.139000			
25			53.000	2.826000			
26		2.8	52.410	4.615892			
27		2.8	30.260	4.615892			
28		2.8	16.570	4.615892			
29		2.8	9.649	4.615892			
30		2.8	6.766	4.615892			
31		2.8	5.524	4.615892			
32		2.8	4.784	4.615892			
33		2.6	1.381	4.286185			

PARTICLE SIZE ANALYSIS
SUBPIT SAMPLE #15

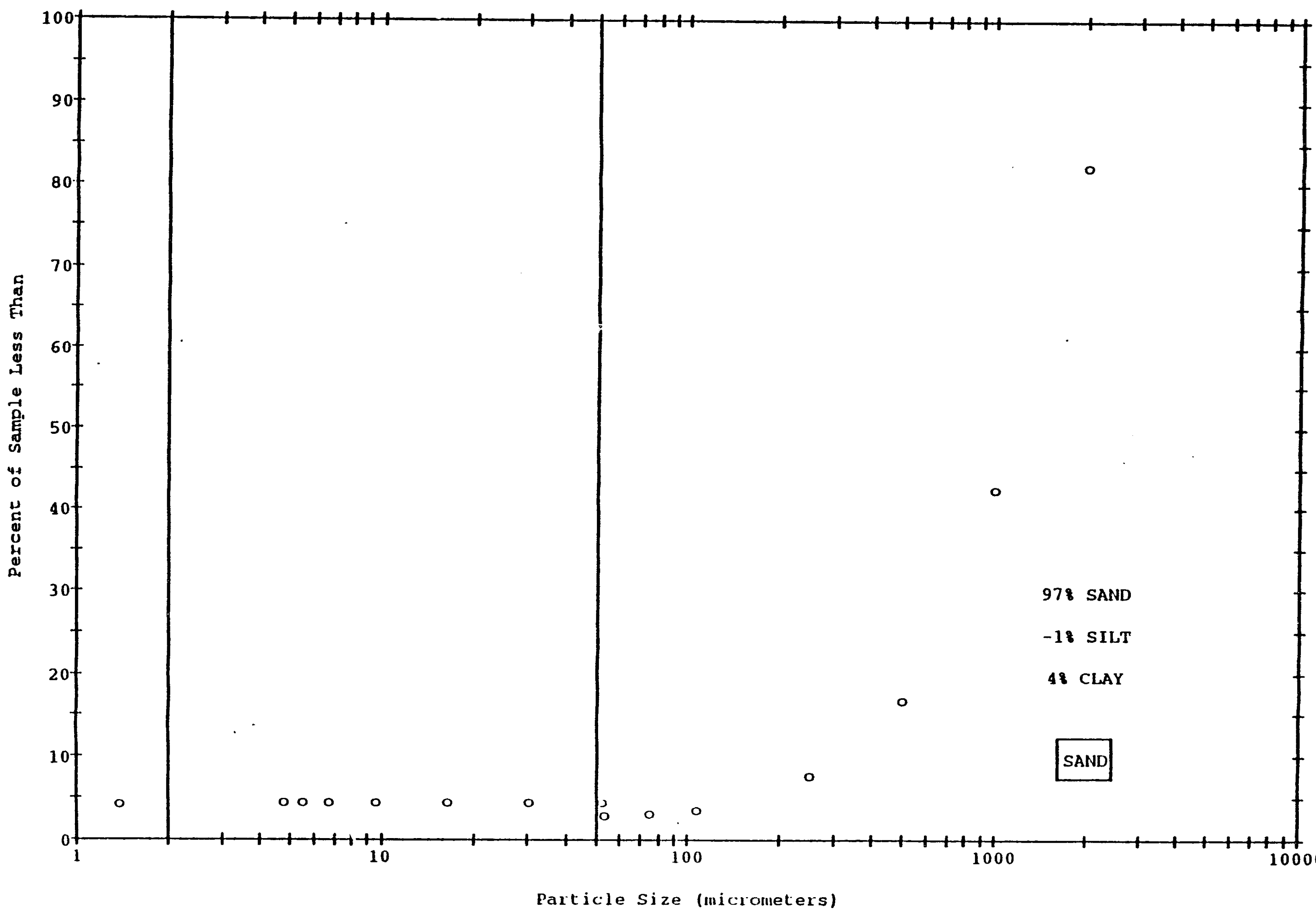

APPENDIX B
Part 4

PARTICLE SIZE DISTRIBUTION BY SIEVING OF SELECTED SAMPLES FROM THE 218-E-12B BURIAL GROUND AND WELLS 299-E34-7 AND 299-E35-1

Model
for Computation of
Sieve Analysis

Name	Sample & Total Wt	Mesh Size	Sieve Wt	Sieve & Soil Wt	Soil Wt	Cumultiv Soil Wt	Percent Less Than
		4.000	460.56	477.26	16.70	16.70	98.30
		2.000	440.17	446.47	6.30	23.00	97.66
	#2	1.000	322.01	333.04	11.03	34.03	96.53
	981.03	0.500	289.75	321.65	31.90	65.93	93.28
		0.250	260.20	390.95	130.75	196.68	79.95
		0.125	242.82	405.11	162.29	358.97	63.41
		0.063	246.10	562.50	316.40	675.37	31.16
		0.045	243.20	304.89	61.69	737.06	24.87
			286.15	510.55	224.40	961.46	1.99
						0.00	
		4.000	460.56	460.41	-0.15	-0.15	100.02
		2.000	440.17	440.25	0.08	-0.07	100.01
	#18	1.000	322.01	322.09	0.08	0.01	100.00
	677.52	0.500	289.75	318.61	28.86	28.87	95.74
		0.250	260.20	616.85	356.65	385.52	43.10
		0.125	242.82	462.55	219.73	605.25	10.67
		0.063	246.10	302.74	56.64	661.89	2.31
		0.045	243.20	253.34	10.14	672.03	0.81
			286.15	290.94	4.79	676.82	0.10
						0.00	
		4.000	460.56	2164.82	1704.26	1704.26	17.08
		2.000	440.17	600.99	160.82	1865.08	9.25
	#20	1.000	322.01	388.89	66.88	1931.96	6.00
	2055.23	0.500	289.75	357.75	68.00	1999.96	2.69
		0.250	260.20	297.81	37.61	2037.57	0.86
		0.125	242.82	251.50	8.68	2046.25	0.44
		0.063	246.10	249.01	2.91	2049.16	0.30
		0.045	243.20	244.51	1.31	2050.47	0.23
			286.15	289.87	3.72	2054.19	0.05
						0.00	
		4.000	460.56	501.57	41.01	41.01	94.76
		2.000	440.17	554.94	114.77	155.78	80.10
	#5	1.000	322.01	469.30	147.29	303.07	61.28

Model
for Computation of
Sieve Analysis

Name	Sample & Total Wt	Mesh Size	Sieve Wt	Sieve & Soil Wt	Soil Wt	Cumultiv Soil Wt	Percent Less Than
	782.67	0.500	289.75	360.12	70.37	373.44	52.29
		0.250	260.20	295.44	35.24	408.68	47.78
		0.125	242.82	312.05	69.23	477.91	38.94
		0.063	246.10	387.71	141.61	619.52	20.85
		0.045	243.20	288.23	45.03	664.55	15.09
			286.15	400.99	114.84	779.39	0.42
						0.00	
		4.000	460.56	543.65	83.09	83.09	83.68
		2.000	440.17	453.27	13.10	96.19	81.10
	e34-7_5'	1.000	322.01	341.14	19.13	115.32	77.34
	509.01	0.500	289.75	315.05	25.30	140.62	72.37
		0.250	260.20	292.68	32.48	173.10	65.99
		0.125	242.82	319.08	76.26	249.36	51.01
		0.063	246.10	429.34	183.24	432.60	15.01
		0.045	243.20	283.19	39.99	472.59	7.16
			286.15	320.44	34.29	506.88	0.42
						0.00	
		4.000	460.56	931.78	471.22	471.22	33.42
		2.000	440.17	482.86	42.69	513.91	27.39
	e34-7_10'	1.000	322.01	349.95	27.94	541.85	23.44
	707.73	0.500	289.75	326.49	36.74	578.59	18.25
		0.250	260.20	301.99	41.79	620.38	12.34
		0.125	242.82	270.01	27.19	647.57	8.50
		0.063	246.10	265.00	18.90	666.47	5.83
		0.045	243.20	251.29	8.09	674.56	4.69
			286.15	318.14	31.99	706.55	0.17
						0.00	
		4.000	460.56	737.98	277.42	277.42	68.38
		2.000	440.17	504.70	64.53	341.95	61.02
	e34-7_15'	1.000	322.01	367.38	45.37	387.32	55.85
	877.22	0.500	289.75	346.36	56.61	443.93	49.39
		0.250	260.20	402.60	142.40	586.33	33.16
		0.125	242.82	371.66	128.84	715.17	18.47

Model
for Ccmputation of
Sieve Analysis

Name	Sample & Total Wt	Mesh Size	Sieve Wt	Sieve & Soil Wt	Soil Wt	Cumultiv Soil Wt	Percent Less Than
		0.063	246.10	312.98	66.88	782.05	10.85
		0.045	243.20	268.62	25.42	807.47	7.95
			286.15	353.44	67.29	874.76	0.28
						0.00	
		4.000	460.56	612.24	151.68	151.68	80.83
		2.000	440.17	545.67	105.50	257.18	67.49
	e34-7_20'	1.000	322.01	404.96	82.95	340.13	57.00
	791.03	0.500	289.75	372.61	82.86	422.99	46.53
		0.250	260.20	381.41	121.21	544.20	31.20
		0.125	242.82	356.67	113.85	658.05	16.81
		0.063	246.10	303.63	57.53	715.58	9.54
		0.045	243.20	267.97	24.77	740.35	6.41
			286.15	331.06	44.91	785.26	0.73

Model
for Computation of
Sieve Analysis

NAME	Sample & Total Wt	Mesh Size	Sieve Wt	Sieve & Soil Wt	Soil Wt	Cumultiv Soil Wt	Percent Less Than
		4.000	460.56	460.56	0.00	0.00	100.00
		2.000	440.17	441.10	0.93	0.93	99.80
	#11	1.000	322.01	330.82	8.81	9.74	97.94
	473.85	0.500	289.75	320.01	30.26	40.00	91.56
		0.250	260.20	343.12	82.92	122.92	74.06
		0.125	242.82	472.47	229.65	352.57	25.59
		0.063	246.10	344.86	98.76	451.33	4.75
		0.045	243.20	253.52	10.32	461.65	2.57
			286.15	297.80	11.65	473.30	0.12
						0.00	
		4.000	460.56	462.28	1.72	1.72	99.71
		2.000	440.17	446.93	6.76	8.48	98.59
	#12	1.000	322.01	332.82	10.81	19.29	96.80
	602.37	0.500	289.75	333.71	43.96	63.25	89.50
		0.250	260.20	537.10	276.90	340.15	43.53
		0.125	242.82	386.47	143.65	483.80	19.68
		0.063	246.10	334.87	88.77	572.57	4.95
		0.045	243.20	263.90	20.70	593.27	1.51
			286.15	295.36	9.21	602.48	-0.02
						0.00	
		4.000	460.56	2908.81	2448.25	2448.25	8.25
		2.000	440.17	458.90	18.73	2466.98	7.55
	#7	1.000	322.01	348.57	26.56	2493.54	6.55
	2668.42	0.500	289.75	320.34	30.59	2524.13	5.41
		0.250	260.20	309.14	48.94	2573.07	3.57
		0.125	242.82	284.56	41.74	2614.81	2.01
		0.063	246.10	267.27	21.17	2635.98	1.22
		0.045	243.20	250.91	7.71	2643.69	0.93
			286.15	311.64	25.49	2669.18	-0.03
						0.00	
		4.000	460.56	973.74	513.18	513.18	59.04
		2.000	440.17	683.09	242.92	756.10	39.65
	#9	1.000	322.01	501.41	179.40	935.50	25.34

Model
for Computation of
Sieve Analysis

NAME	Sample & Total Wt	Mesh Size	Sieve Wt	Sieve & Soil Wt	Soil Wt	Cumultiv Soil Wt	Percent Less Than
	1252.94	0.500	289.75	412.46	122.71	1058.21	15.54
		0.250	260.20	397.06	136.86	1195.07	4.62
		0.125	242.82	285.20	42.38	1237.45	1.24
		0.063	246.10	255.85	9.75	1247.20	0.46
		0.045	243.20	244.76	1.56	1248.76	0.33
			286.15	289.34	3.19	1251.95	0.08
						0.00	
		4.000	460.56	2209.31	1748.75	1748.75	9.38
		2.000	440.17	463.52	23.35	1772.10	8.17
	#10	1.000	322.01	341.55	19.54	1791.64	7.16
	1929.75	0.500	289.75	308.96	19.21	1810.85	6.16
		0.250	260.20	294.17	33.97	1844.82	4.40
		0.125	242.82	271.39	28.57	1873.39	2.92
		0.063	246.10	266.86	20.76	1894.15	1.84
		0.045	243.20	250.90	7.70	1901.85	1.45
			286.15	309.86	23.71	1925.56	0.22
						0.00	
		4.000	460.56	518.00	57.44	57.44	93.60
		2.000	440.17	558.15	117.98	175.42	80.46
	#3	1.000	322.01	439.02	117.01	292.43	67.42
	897.63	0.500	289.75	335.15	45.40	337.83	62.36
		0.250	260.20	294.53	34.33	372.16	58.54
		0.125	242.82	597.03	354.21	726.37	19.08
		0.063	246.10	379.36	133.26	859.63	4.23
		0.045	243.20	259.12	15.92	875.55	2.46
			286.15	310.18	24.03	899.58	-0.22
						0.00	
		4.000	460.56	739.56	279.00	279.00	73.80
		2.000	440.17	691.19	251.02	530.02	50.23
	#4	1.000	322.01	611.52	289.51	819.53	23.04
	1064.94	0.500	289.75	477.82	188.07	1007.60	5.38
		0.250	260.20	304.99	44.79	1052.39	1.18
		0.125	242.82	249.66	6.84	1059.23	0.54

Model
for Computation of
Sieve Analysis

NAME	Sample & Total Wt	Mesh Size	Sieve Wt	Sieve & Soil Wt	Soil Wt	Cumultiv Soil Wt	Percent Less Than
		0.063	246.10	248.56	2.46	1061.69	0.31
		0.045	243.20	244.27	1.07	1062.76	0.20
			286.15	287.93	1.78	1064.54	0.04
						0.00	
		4.000	460.56	486.37	25.81	25.81	98.06
		2.000	440.17	647.99	207.82	233.63	82.43
	#15	1.000	322.01	927.93	605.92	839.55	36.86
	1329.62	0.500	289.75	635.27	345.52	1185.07	10.87
		0.250	260.20	355.27	95.07	1280.14	3.72
		0.125	242.82	275.27	32.45	1312.59	1.28
		0.063	246.10	256.17	10.07	1322.66	0.52
		0.045	243.20	245.78	2.58	1325.24	0.33
			286.15	290.47	4.32	1329.56	0.00

Model
for Computation of
Sieve Analysis

Name	Sample & Total Wt	Mesh Size	Sieve Wt	Sieve & Soil Wt	Soil Wt	Cumultiv Soil Wt	Percent Less Than
		4.000	460.40	497.46	37.06	37.06	94.38
		2.000	440.27	605.73	165.46	202.52	69.28
	e34-7_25'	1.000	322.09	537.64	215.55	418.07	36.58
	659.25	0.500	289.75	388.36	98.61	516.68	21.63
		0.250	260.21	307.66	47.45	564.13	14.43
		0.125	242.81	277.34	34.53	598.66	9.19
		0.063	246.15	266.46	20.31	618.97	6.11
		0.045	243.22	251.38	8.16	627.13	4.87
			286.14	312.58	26.44	653.57	0.86
						0.00	
		4.000	460.40	545.77	85.37	85.37	86.95
		2.000	440.27	591.62	151.35	236.72	63.82
	e34-7_30'	1.000	322.09	414.98	92.89	329.61	49.62
	654.24	0.500	289.75	360.84	71.09	400.70	38.75
		0.250	260.21	325.33	65.12	465.82	28.80
		0.125	242.81	303.75	60.94	526.76	19.49
		0.063	246.15	291.14	44.99	571.75	12.61
		0.045	243.22	262.73	19.51	591.26	9.63
			286.14	347.31	61.17	652.43	0.28
						0.00	
		4.000	460.40	490.38	29.98	29.98	95.68
		2.000	440.27	524.00	83.73	113.71	83.63
	e34-7_35'	1.000	322.09	409.42	87.33	201.04	71.06
	694.63	0.500	289.75	368.34	78.59	279.63	59.74
		0.250	260.21	369.80	109.59	389.22	43.97
		0.125	242.81	345.15	102.34	491.56	29.23
		0.063	246.15	334.68	88.53	580.09	16.49
		0.045	243.22	277.21	33.99	614.08	11.60
			286.14	355.29	69.15	683.23	1.64
						0.00	
		4.000	460.40	644.24	183.84	183.84	73.99
		2.000	440.27	562.33	122.06	305.90	56.73
	e34-7_40'	1.000	322.09	407.21	85.12	391.02	44.68

Model
for Computation of
Sieve Analysis

Name	Sample & Total Wt	Mesh Size	Sieve Wt	Sieve & Soil Wt	Soil Wt	Cumultiv Soil Wt	Percent Less Than
	706.88	0.500	289.75	365.46	75.71	466.73	33.97
		0.250	260.21	331.47	71.26	537.99	23.89
		0.125	242.81	303.13	60.32	598.31	15.36
		0.063	246.15	289.86	43.71	642.02	9.18
		0.045	243.22	259.19	15.97	657.99	6.92
			286.14	333.18	47.04	705.03	0.26
						0.00	
		4.000	460.40	537.37	76.97	76.97	90.15
		2.000	440.27	585.85	145.58	222.55	71.52
	e34-7_45'	1.000	322.09	435.76	113.67	336.22	56.98
	781.49	0.500	289.75	398.34	108.59	444.81	43.08
		0.250	260.21	341.36	81.15	525.96	32.70
		0.125	242.81	311.39	68.58	594.54	23.92
		0.063	246.15	310.97	64.82	659.36	15.63
		0.045	243.22	275.68	32.46	691.82	11.47
			286.14	374.54	88.40	780.22	0.16
						0.00	
		4.000	460.40	574.58	114.18	114.18	83.24
		2.000	440.27	560.07	119.80	233.98	65.65
	e34-7_50'	1.000	322.09	422.33	100.24	334.22	50.93
	681.10	0.500	289.75	375.32	85.57	419.79	38.37
		0.250	260.21	326.34	66.13	485.92	28.66
		0.125	242.81	307.21	64.40	550.32	19.20
		0.063	246.15	290.35	44.20	594.52	12.71
		0.045	243.22	274.84	31.62	626.14	8.07
			286.14	339.66	53.52	679.66	0.21
						0.00	
		4.000	460.40	616.10	155.70	155.70	76.85
		2.000	440.27	535.14	94.87	250.57	62.74
	e34-7_55'	1.000	322.09	393.86	71.77	322.34	52.07
	672.47	0.500	289.75	366.43	76.68	399.02	40.66
		0.250	260.21	322.23	62.02	461.04	31.44
		0.125	242.81	294.82	52.01	513.05	23.71

Model
for Computation of
Sieve Analysis

Name	Sample & Total Wt	Mesh Size	Sieve Wt	Sieve & Soil Wt	Soil Wt	Cumultiv Soil Wt	Percent Less Than
		0.063	246.15	299.09	52.94	565.99	15.83
		0.045	243.22	265.35	22.13	588.12	12.54
			286.14	365.85	79.71	667.83	0.69
						0.00	
		4.000	460.40	683.87	223.47	223.47	70.97
		2.000	440.27	602.33	162.06	385.53	49.92
	e34-7_60'	1.000	322.09	417.63	95.54	481.07	37.51
	769.78	0.500	289.75	356.20	66.45	547.52	28.87
		0.250	260.21	308.97	48.76	596.28	22.54
		0.125	242.81	290.53	47.72	644.00	16.34
		0.063	246.15	291.07	44.92	688.92	10.50
		0.045	243.22	262.21	18.99	707.91	8.04
			286.14	348.56	62.42	770.33	-0.07

Model
for Computation of
Sieve Analysis

Name	Sample & Total Wt	Mesh Size	Sieve Wt	Sieve & Soil Wt	Soil Wt	Cumultiv Soil Wt	Percent Less Than
		4.000	460.34	464.75	4.41	4.41	99.22
		2.000	439.96	479.54	39.58	43.99	92.26
	e35_1-35'	1.000	321.88	428.20	106.32	150.31	73.55
	568.34	0.500	289.48	417.78	128.30	278.61	50.98
		0.250	260.18	337.53	77.35	355.96	37.37
		0.125	242.80	302.72	59.92	415.88	26.83
		0.063	246.13	306.09	59.96	475.84	16.28
		0.045	243.14	274.39	31.25	507.09	10.78
			286.09	347.34	61.25	568.34	0.00
						0.00	
		4.000	460.34	790.23	329.89	329.89	51.62
		2.000	439.96	466.89	26.93	356.82	47.67
	e35_1-50'	1.000	321.88	352.92	31.04	387.86	43.12
	681.85	0.500	289.48	429.64	140.16	528.02	22.56
		0.250	260.18	333.60	73.42	601.44	11.79
		0.125	242.80	275.36	32.56	634.00	7.02
		0.063	246.13	271.88	25.75	659.75	3.24
		0.045	243.14	250.11	6.97	666.72	2.22
			286.09	301.48	15.39	682.11	-0.04
						0.00	
		4.000	460.34	679.54	219.20	219.20	72.00
		2.000	439.96	573.99	134.03	353.23	54.88
	e35_1-60'	1.000	321.88	426.48	104.60	457.83	41.52
	782.82	0.500	289.48	354.28	64.80	522.63	33.24
		0.250	260.18	309.21	49.03	571.66	26.97
		0.125	242.80	290.24	47.44	619.10	20.91
		0.063	246.13	295.90	49.77	668.87	14.56
		0.045	243.14	271.91	28.77	697.64	10.88
			286.09	361.73	75.64	773.28	1.22
						0.00	
		4.000	460.34	470.09	9.75	9.75	98.11
		2.000	439.96	511.86	71.90	81.65	84.19
	e35_1-65'	1.000	321.88	429.35	107.47	189.12	63.37

Model
for Computation of
Sieve Analysis

Name	Sample & Total Wt	Mesh Size	Sieve Wt	Sieve & Soil Wt	Soil Wt	Cumultiv Soil Wt	Percent Less Than
	516.33	0.500	289.48	372.68	83.20	272.32	47.26
		0.250	260.18	325.00	64.82	337.14	34.70
		0.125	242.80	305.11	62.31	399.45	22.64
		0.063	246.13	289.59	43.46	442.91	14.22
		0.045	243.14	259.88	16.74	459.65	10.98
			286.09	343.41	57.32	516.97	-0.12
						0.00	
		4.000	460.34	464.07	3.73	3.73	99.26
		2.000	439.96	479.70	39.74	43.47	91.36
	e35_1-75'	1.000	321.88	448.72	126.84	170.31	66.16
	503.32	0.500	289.48	385.53	96.05	266.36	47.08
		0.250	260.18	309.14	48.96	315.32	37.35
		0.125	242.80	298.61	55.81	371.13	26.26
		0.063	246.13	308.12	61.99	433.12	13.95
		0.045	243.14	271.01	27.87	460.99	8.41
			286.09	325.18	39.09	500.08	0.64
						0.00	
		4.000	460.34	519.44	59.10	59.10	90.51
		2.000	439.96	495.37	55.41	114.51	81.61
	e35_1-90'	1.000	321.88	381.54	59.66	174.17	72.03
	622.72	0.500	289.48	358.32	68.84	243.01	60.98
		0.250	260.18	338.69	78.51	321.52	48.37
		0.125	242.80	344.29	101.49	423.01	32.07
		0.063	246.13	321.83	75.70	498.71	19.91
		0.045	243.14	266.74	23.60	522.31	16.12
			286.09	381.90	95.81	618.12	0.74
						0.00	
		4.000	460.34	509.72	49.38	49.38	90.31
		2.000	439.96	518.71	78.75	128.13	74.86
	e35_1-180'	1.000	321.88	389.45	67.57	195.70	61.61
	509.72	0.500	289.48	357.66	68.18	263.88	48.23
		0.250	260.18	316.31	56.13	320.01	37.22
		0.125	242.80	288.23	45.43	365.44	28.31

Model
for Computation of
Sieve Analysis

Name	Sample & Total Wt	Mesh Size	Sieve Wt	Sieve & Soil Wt	Soil Wt	Cumultiv Soil Wt	Percent Less Than
		0.063	246.13	296.23	50.10	415.54	18.48
		0.045	243.14	267.24	24.10	439.64	13.75
			286.09	355.73	69.64	509.28	0.09
						0.00	
		4.000	460.34	460.34	0.00	0.00	100.00
		2.000	439.96	439.96	0.00	0.00	100.00
		1.000	321.88	321.88	0.00	0.00	100.00
	1.00	0.500	289.48	289.48	0.00	0.00	100.00
		0.250	260.18	260.18	0.00	0.00	100.00
		0.125	242.80	242.80	0.00	0.00	100.00
		0.063	246.13	246.13	0.00	0.00	100.00
		0.045	243.14	243.14	0.00	0.00	100.00
			286.09	286.09	0.00	0.00	100.00

APPENDIX B
Part 5

BULK GEOCHEMICAL ANALYSES OF SELECTED SAMPLES FROM THE 218-E-12B BURIAL GROUND AND WELL 299-E35-1

REPORT # 0798
RESULTS OF PIXE ANALYSIS ON: SUB PIT SAMPLES SP13

ELEMENT	CONCENTRATION	ERROR	DET LIMIT	PK AREA	XRY YIELD			OXIDE	CONCENTRATION	FILT
	----------------	PPM ----------------		-- CTS --	- CTS/PPM -				--- PPM ---	
NA	14254.	755.	1589.	1956.	.1373			Na2O	19214.	NON
MG	13898.	521.	1111.	4534.	.3262			MgO	23047.	NON
AL	78516.	555.	938.	42757.	.5445			Al2O3	148356.	NON
SI	273673.	677.	575.	189048.	.6908			SiO2	585468.	NON
P	2456.	456.	1048.	1046.	.4260			P2O5	5628.	NON
S	76.	109.	251.	40.	.5170	****	CONCN BELOW DET LIM	SO3	191.	NON
CL	638.	100.	219.	365.	.5721			Cl	638.	NON
K	12777.	117.	129.	15613.	1.2220			K2O	15391.	AL
CA	31083.	227.	393.	41251.	1.3272			CaO	43491.	AL
SC	0.	0.	249.	0.	.0000	******	ELEMENT NOT DETECTED	Sc2O3	0.	AL
TI	9383.	105.	178.	16926.	1.8039			TiO2	15651.	AL
V	163.	61.	139.	300.	1.8327	**	CONCN NEAR DET LIM	VO2	265.	AL
CR	17.	25.	58.	31.	1.7700	****	CONCN BELOW DET LIM	Cr2O3	25.	AL
MN	931.	46.	92.	1460.	1.5685			MnO2	1474.	AL
FE	61916.	302.	499.	85757.	1.3851			Fe2O3	88521.	AL
CO	25.	114.	263.	76.	2.9201	****	CONCN BELOW DET LIM	Co2O3	36.	AMC
NI	8.	15.	36.	39.	4.8916	****	CONCN BELOW DET LIM	NiO	11.	AMC
CU	17.	5.	10.	122.	7.0835	**	CONCN NEAR DET LIM	CuO	21.	AMC
ZN	87.	5.	10.	808.	9.3031			ZnO	108.	AMC
GA	17.	3.	7.	182.	10.5016			Ga2O3	23.	AMC
GE	2.	3.	7.	28.	11.1414	****	CONCN BELOW DET LIM	GeO2	2.	AMC
AS	7.	3.	5.	71.	11.1338	**	CONCN NEAR DET LIM	As2O5	10.	AMC
SE	5.	2.	5.	51.	10.3362	**	CONCN NEAR DET LIM	SeO3	8.	AMC
BR	0.	0.	5.	0.	.0000	******	ELEMENT NOT DETECTED	Br	0.	AMC
RB	71.	5.	10.	513.	7.1403			Rb2O	78.	AMC
SR	283.	10.	19.	1708.	6.0172			SrO	335.	AMC
Y	25.	7.	14.	127.	5.0340	**	CONCN NEAR DET LIM	Y2O3	32.	AMC
ZR	260.	15.	29.	1067.	4.1020			ZrO2	351.	AMC
NB	14.	7.	15.	45.	3.3390	****	CONCN BELOW DET LIM	Nb2O3	17.	AMC
MO	5.	12.	25.	12.	2.6554	****	CONCN BELOW DET LIM	MoO3	8.	AMC
CD	44.	29.	64.	26.	.5953	****	CONCN BELOW DET LIM	CdO	50.	AMC
IN	36.	36.	81.	16.	.4550	****	CONCN BELOW DET LIM	In2O3	43.	AMC
SN	80.	47.	103.	27.	.3421	****	CONCN BELOW DET LIM	SnO2	101.	AMC
SB	85.	59.	134.	22.	.2582	****	CONCN BELOW DET LIM	Sb2O3	102.	AMC
I	148.	98.	219.	22.	.1469	****	CONCN BELOW DET LIM	I	148.	AMC
BA	1002.	293.	616.	61.	.0609	**	CONCN NEAR DET LIM	BaO	1119.	AMC
TAL	5.	12.	27.	15.	3.0328	****	CONCN BELOW DET LIM	Ta2O5	6.	AMC
WL	0.	0.	29.	0.	.0000	******	ELEMENT NOT DETECTED	WO3	0.	AMC
PBL	8.	5.	10.	45.	5.5842	****	CONCN BELOW DET LIM	PbO	9.	AMC
								OXIDE SUM =	949976.	

REPORT # 0792

RESULTS OF PIXE ANALYSIS ON: SUB PIT SAMPLES SP14

ELEMENT	CONCENTRATION	ERROR	DET LIMIT	PK AREA	XRY YIELD			OXIDE	CONCENTRATION	FILT
	----------------	PPM ----------------		-- CTS --	- CTS/PPM -				--- PPM ---	
NA	18527.	674.	1367.	3126.	.1687			Na2O	24974.	NON
MG	10726.	466.	1016.	4273.	.3984			MgO	17788.	NON
AL	80194.	506.	858.	53697.	.6696			Al2O3	151526.	NON
SI	294727.	632.	512.	248019.	.8415			SiO2	630510.	NON
P	1399.	438.	1011.	697.	.4981	**	CONCN NEAR DET LIM	P2O5	3207.	NON
S	0.	0.	218.	0.	.0000	******	ELEMENT NOT DETECTED	SO3	0.	NON
CL	612.	89.	195.	410.	.6696			Cl	612.	NON
K	12838.	106.	115.	18499.	1.4409			K2O	15465.	AL
CA	25108.	191.	331.	39338.	1.5667			CaO	35132.	AL
SC	0.	0.	204.	0.	.0000	******	ELEMENT NOT DETECTED	Sc2O3	0.	AL
TI	5117.	74.	127.	10995.	2.1485			TiO2	8536.	AL
V	54.	42.	99.	116.	2.1807	****	CONCN BELOW DET LIM	VO2	87.	AL
CR	76.	21.	47.	161.	2.1138	**	CONCN NEAR DET LIM	Cr2O3	112.	AL
MN	786.	37.	74.	8470.	1.8708			MnO2	1244.	AL
FE	40888.	225.	372.	67472.	1.6501			Fe2O3	58458.	AL
CO	44.	83.	194.	155.	3.5349	****	CONCN BELOW DET LIM	Co2O3	62.	AHC
NI	23.	8.	20.	136.	5.9935	**	CONCN NEAR DET LIM	NiO	29.	AHC
CU	16.	4.	10.	138.	8.6543	**	CONCN NEAR DET LIM	CuO	19.	AHC
ZN	66.	4.	8.	756.	11.3399			ZnO	83.	AHC
GA	11.	3.	6.	152.	12.7770	**	CONCN NEAR DET LIM	Ga2O3	15.	AHC
GE	0.	3.	6.	6.	13.5349	******	ELEMENT NOT DETECTED	GeO2	0.	AHC
AS	3.	3.	6.	41.	13.5089	****	CONCN BELOW DET LIM	As2O5	4.	AHC
SE	3.	1.	4.	33.	12.5287	****	CONCN BELOW DET LIM	SeO2	4.	AHC
BR	1.	1.	4.	11.	11.5910	****	CONCN BELOW DET LIM	Br	1.	AHC
RB	59.	4.	8.	516.	8.6367			Rb2O	65.	AHC
SR	335.	10.	17.	2442.	7.2748			SrO	396.	AHC
Y	23.	6.	11.	138.	6.0837	**	CONCN NEAR DET LIM	Y2O3	29.	AHC
ZR	274.	14.	27.	1362.	4.9557			ZrO2	370.	AHC
NB	10.	6.	14.	42.	4.0328	****	CONCN BELOW DET LIM	Nb2O3	12.	AHC
MO	0.	0.	24.	0.	.0000	******	ELEMENT NOT DETECTED	MoO3	0.	AHC
CD	0.	0.	48.	0.	.0000	******	ELEMENT NOT DETECTED	CdO	0.	AHC
IN	52.	31.	68.	28.	.5490	****	CONCN BELOW DET LIM	In2O3	63.	AHC
SN	54.	38.	85.	22.	.4126	****	CONCN BELOW DET LIM	SnO2	68.	AHC
SB	96.	48.	105.	30.	.3114	****	CONCN BELOW DET LIM	Sb2O3	115.	AHC
I	112.	75.	165.	20.	.1771	****	CONCN BELOW DET LIM	I	112.	AHC
BA	800.	228.	471.	59.	.0735	**	CONCN NEAR DET LIM	BaO	893.	AHC
TAL	0.	0.	24.	0.	.0000	******	ELEMENT NOT DETECTED	Ta2O5	0.	AHC
WL	0.	0.	24.	0.	.0000	******	ELEMENT NOT DETECTED	WO3	0.	AHC
PBL	11.	4.	8.	76.	6.7767	**	CONCN NEAR DET LIM	PbO	12.	AHC
								OXIDE SUM =	950003.	

REPORT # 0791

RESULTS OF PIXE ANALYSIS ON: SUB PIT SAMPLES SP14 REP

ELEMENT	CONCENTRATION	ERROR	DET LIMIT	PK AREA	XRY YIELD			OXIDE	CONCENTRATION	FILT
	---------------- PPM	----------------		-- CTS --	- CTS/PPM -				--- PPM ---	
NA	16154.	701.	1448.	2531.	.1567			Na2O	21775.	NON
MG	11148.	483.	1051.	4143.	.3716			MgO	18487.	NON
AL	79113.	526.	900.	49353.	.6238			Al2O3	149484.	NON
SI	300539.	660.	535.	235834.	.7847			SiO2	642943.	NON
P	1704.	465.	1072.	782.	.4588	**	CONCN NEAR DET LIM	P2O5	3904.	NON
S	0.	0.	235.	0.	.0000	******	ELEMENT NOT DETECTED	SO3	0.	NON
CL	715.	95.	206.	441.	.6170			Cl	715.	NON
K	12548.	108.	112.	16994.	1.3544			K2O	15115.	AL
CA	23835.	191.	333.	35131.	1.4740			CaO	33350.	AL
SC	0.	0.	204.	0.	.0000	******	ELEMENT NOT DETECTED	Sc2O3	0.	AL
TI	4855.	73.	126.	9832.	2.0248			TiO2	8099.	AL
V	44.	42.	100.	90.	2.0547	****	CONCN BELOW DET LIM	VO2	72.	AL
CR	56.	23.	50.	111.	1.9920	**	CONCN NEAR DET LIM	Cr2O3	82.	AL
MN	647.	38.	74.	1141.	1.7626			MnO2	1023.	AL
FE	37160.	221.	367.	57763.	1.5544			Fe2O3	53127.	AL
CO	6.	83.	195.	21.	3.3035	****	CONCN BELOW DET LIM	Co2O3	9.	AHC
NI	21.	11.	26.	118.	5.6127	****	CONCN BELOW DET LIM	NiO	27.	AHC
CU	12.	5.	9.	99.	8.1006	**	CONCN NEAR DET LIM	CuO	15.	AHC
ZN	62.	5.	9.	653.	10.6104			ZnO	77.	AHC
GA	11.	3.	6.	129.	11.9513	**	CONCN NEAR DET LIM	Ga2O3	14.	AHC
GE	0.	0.	6.	0.	.0000	******	ELEMENT NOT DETECTED	GeO2	0.	AHC
AS	3.	2.	5.	45.	12.6304	****	CONCN BELOW DET LIM	As2O5	5.	AHC
SE	6.	2.	5.	64.	11.7119	**	CONCN NEAR DET LIM	SeO2	9.	AHC
BR	2.	2.	5.	13.	10.8339	****	CONCN BELOW DET LIM	Br	2.	AHC
RB	61.	5.	9.	491.	8.0710			Rb2O	66.	AHC
SR	310.	11.	18.	2110.	6.7978			SrO	367.	AHC
Y	12.	6.	12.	72.	5.6844	**	CONCN NEAR DET LIM	Y2O3	15.	AHC
ZR	254.	14.	27.	1179.	4.6302			ZrO2	344.	AHC
NB	12.	6.	14.	46.	3.7677	****	CONCN BELOW DET LIM	Nb2O3	15.	AHC
MO	0.	0.	24.	0.	.0000	******	ELEMENT NOT DETECTED	MoO3	0.	AHC
CD	0.	0.	56.	0.	.0000	******	ELEMENT NOT DETECTED	CdO	0.	AHC
IN	0.	0.	70.	0.	.0000	******	ELEMENT NOT DETECTED	In2O3	0.	AHC
SN	0.	0.	92.	0.	.0000	******	ELEMENT NOT DETECTED	SnO2	0.	AHC
SB	0.	0.	114.	0.	.0000	******	ELEMENT NOT DETECTED	Sb2O3	0.	AHC
I	132.	94.	209.	22.	.1655	****	CONCN BELOW DET LIM	I	132.	AHC
BA	635.	250.	538.	44.	.0686	**	CONCN NEAR DET LIM	BaO	709.	AHC
TAL	0.	11.	24.	2.	3.4686	******	ELEMENT NOT DETECTED	Ta2O5	0.	AHC
WL	0.	0.	24.	0.	.0000	******	ELEMENT NOT DETECTED	WO3	0.	AHC
PBL	0.	0.	9.	0.	.0000	******	ELEMENT NOT DETECTED	PbO	0.	AHC
								OXIDE SUM =	949981.	

REPORT # 0797

RESULTS OF PIXE ANALYSIS ON: SUB PIT SAMPLES SP15

ELEMENT	CONCENTRATION (PPM)	ERROR (PPM)	DET LIMIT (PPM)	PK AREA -- CTS --	XRY YIELD - CTS/PPM -			OXIDE	CONCENTRATION --- PPM ---	FILT
NA	24854.	686.	1342.	4454.	.1792			Na2O	33504.	NON
MG	10047.	464.	1019.	4204.	.4185			MgO	16661.	NON
AL	85518.	497.	823.	60227.	.7042			Al2O3	161587.	NON
SI	286501.	612.	507.	251165.	.8767			SiO2	612911.	NON
P	1568.	417.	962.	828.	.5287	**	CONCN NEAR DET LIM	P2O5	3592.	NON
S	57.	89.	205.	37.	.6418	****	CONCN BELOW DET LIM	SO3	142.	NON
CL	1308.	90.	186.	929.	.7106			Cl	1308.	NON
K	11675.	98.	107.	18329.	1.5698			K2O	14064.	AL
CA	26186.	184.	320.	44779.	1.7100			CaO	36639.	AL
SC	0.	0.	200.	0.	.0000	******	ELEMENT NOT DETECTED	Sc2O3	0.	AL
TI	5072.	68.	117.	11866.	2.3395			TiO2	8460.	AL
V	0.	0.	92.	0.	.0000	******	ELEMENT NOT DETECTED	VO2	0.	AL
CR	0.	0.	44.	0.	.0000	******	ELEMENT NOT DETECTED	Cr2O3	0.	AL
MN	615.	34.	68.	1253.	2.0363			MnO2	974.	AL
FE	40548.	214.	356.	72821.	1.7959			Fe2O3	57972.	AL
CO	27.	79.	182.	104.	3.8585	****	CONCN BELOW DET LIM	Co2O3	38.	AMC
NI	10.	10.	25.	69.	6.5435	****	CONCN BELOW DET LIM	NiO	13.	AMC
CU	12.	4.	8.	107.	9.4481	**	CONCN NEAR DET LIM	CuO	15.	AMC
ZN	62.	4.	8.	770.	12.3797			ZnO	77.	AMC
GA	13.	3.	5.	176.	13.9481			Ga2O3	17.	AMC
GE	0.	0.	5.	0.	.0000	******	ELEMENT NOT DETECTED	GeO2	0.	AMC
AS	6.	3.	5.	97.	14.7468	**	CONCN NEAR DET LIM	As2O5	10.	AMC
SE	1.	1.	4.	18.	13.6765	****	CONCN BELOW DET LIM	SeO3	2.	AMC
BR	0.	0.	4.	0.	.0000	******	ELEMENT NOT DETECTED	Br	0.	AMC
RB	49.	4.	8.	457.	9.4278			Rb2O	54.	AMC
SR	405.	10.	18.	3215.	7.9412			SrO	479.	AMC
Y	15.	5.	10.	106.	6.6408	**	CONCN NEAR DET LIM	Y2O3	20.	AMC
ZR	117.	12.	25.	635.	5.4095			ZrO2	159.	AMC
NB	4.	5.	13.	17.	4.4021	****	CONCN BELOW DET LIM	Nb2O3	5.	AMC
MO	0.	0.	18.	0.	.0000	******	ELEMENT NOT DETECTED	MoO3	0.	AMC
CD	0.	0.	49.	0.	.0000	******	ELEMENT NOT DETECTED	CdO	0.	AMC
IN	0.	0.	63.	0.	.0000	******	ELEMENT NOT DETECTED	In2O3	0.	AMC
SN	0.	0.	83.	0.	.0000	******	ELEMENT NOT DETECTED	SnO2	0.	AMC
SB	31.	48.	108.	11.	.3399	****	CONCN BELOW DET LIM	Sb2O3	37.	AMC
I	85.	80.	179.	16.	.1933	****	CONCN BELOW DET LIM	I	85.	AMC
BA	1045.	221.	440.	84.	.0802			BaO	1167.	AMC
TAL	0.	0.	21.	0.	.0000	******	ELEMENT NOT DETECTED	Ta2O5	0.	AMC
WL	0.	0.	22.	0.	.0000	******	ELEMENT NOT DETECTED	WO3	0.	AMC
PBL	0.	0.	8.	0.	.0000	******	ELEMENT NOT DETECTED	PbO	0.	AMC

OXIDE SUM = 949990.

REPORT # 0782
RESULTS OF PIXE ANALYSIS ON: SUB PIT SAMPLES SP16

ELEMENT	CONCENTRATION	ERROR	DET LIMIT	PK AREA	XRY YIELD			OXIDE	CONCENTRATION	FILT
	----------------	PPM	----------------	-- CTS --	- CTS/PPM -				--- PPM ---	
NA	16691.	745.	1539.	2394.	.1434			Na2O	22499.	HON
MG	15425.	499.	1050.	5237.	.3395			MgO	25580.	HON
AL	82613.	546.	908.	46674.	.5650			Al2O3	156097.	NON
SI	271721.	662.	549.	193252.	.7112			SiO2	581294.	HON
P	1927.	435.	1000.	852.	.4419	**	CONCN NEAR DET LIM	P2O5	4416.	HON
S	0.	0.	230.	0.	.0000	******	ELEMENT NOT DETECTED	SO3	0.	NON
CL	432.	92.	205.	256.	.5935			Cl	432.	NON
K	11344.	97.	109.	17594.	1.5509			K2O	13665.	AL
CA	29343.	196.	337.	49550.	1.6887			CaO	41057.	AL
SC	0.	0.	214.	0.	.0000	******	ELEMENT NOT DETECTED	Sc2O3	0.	AL
TI	8696.	89.	150.	19991.	2.2989			TiO2	14505.	AL
V	171.	51.	118.	398.	2.3341	**	CONCN NEAR DET LIM	VO2	278.	AL
CR	0.	0.	51.	0.	.0000	******	ELEMENT NOT DETECTED	Cr2O3	0.	AL
MN	900.	41.	80.	1797.	1.9974			MnO2	1424.	AL
FE	60572.	264.	438.	106786.	1.7630			Fe2O3	86599.	AL
CO	16.	96.	222.	56.	3.6662	****	CONCN BELOW DET LIM	Co2O3	22.	AMC
NI	12.	11.	24.	72.	6.1451	****	CONCN BELOW DET LIM	NiO	15.	AMC
CU	14.	4.	9.	131.	8.8953	**	CONCN NEAR DET LIM	CuO	18.	AMC
ZN	80.	4.	8.	930.	11.6790			ZnO	100.	AMC
GA	13.	3.	5.	178.	13.1804			Ga2O3	18.	AMC
GE	0.	0.	5.	0.	.0000	******	ELEMENT NOT DETECTED	GeO2	0.	AMC
AS	3.	3.	5.	45.	13.9688	****	CONCN BELOW DET LIM	As2O5	4.	AMC
SE	3.	1.	4.	25.	12.9664	****	CONCN BELOW DET LIM	SeO3	4.	AMC
BR	3.	3.	4.	24.	12.0047	****	CONCN BELOW DET LIM	Br	3.	AMC
RB	57.	4.	9.	508.	8.9548			Rb2O	62.	AMC
SR	249.	9.	14.	1875.	7.5458			SrO	294.	AMC
Y	24.	5.	12.	148.	6.3125	**	CONCN NEAR DET LIM	Y2O3	30.	AMC
ZR	263.	13.	25.	1352.	5.1436			ZrO2	355.	AMC
NB	8.	5.	13.	33.	4.1867	****	CONCN BELOW DET LIM	Nb2O3	10.	AMC
MO	0.	0.	22.	0.	.0000	******	ELEMENT NOT DETECTED	MoO3	0.	AMC
CD	20.	22.	50.	14.	.7464	****	CONCN BELOW DET LIM	CdO	23.	AMC
IN	29.	28.	62.	17.	.5705	****	CONCN BELOW DET LIM	In2O3	35.	AMC
SN	0.	0.	78.	0.	.0000	******	ELEMENT NOT DETECTED	SnO2	0.	AMC
SB	63.	47.	105.	21.	.3237	****	CONCN BELOW DET LIM	Sb2O3	76.	AMC
I	0.	0.	171.	0.	.0000	******	ELEMENT NOT DETECTED	I	0.	AMC
BA	959.	230.	468.	73.	.0764			BaO	1071.	AMC
TAL	3.	9.	22.	10.	3.8085	****	CONCN BELOW DET LIM	Ta2O5	3.	AMC
WL	4.	11.	24.	17.	4.3709	****	CONCN BELOW DET LIM	WO3	5.	AMC
PBL	8.	4.	8.	56.	7.0062	**	CONCN NEAR DET LIM	PbO	9.	AMC
								OXIDE SUM =	950003.	

REPORT # 0800

RESULTS OF PIXE ANALYSIS ON: SUB PIT SAMPLES SP17

ELEMENT	CONCENTRATION (PPM)	ERROR (PPM)	DET LIMIT (PPM)	PK AREA -- CTS --	XRY YIELD - CTS/PPM -			OXIDE	CONCENTRATION --- PPM ---	FILT
NA	12469.	717.	1529.	1891.	.1517			Na2O	16808.	HON
MG	14787.	509.	1083.	5349.	.3618			MgO	24521.	HON
AL	88723.	539.	880.	53471.	.6027			Al2O3	167641.	HON
SI	271651.	647.	549.	202938.	.7471			SiO2	581143.	HON
P	2082.	430.	989.	965.	.4636			P2O5	4771.	HON
S	268.	102.	231.	151.	.5626	**	CONCN NEAR DET LIM	SO3	670.	HON
CL	1442.	100.	205.	898.	.6222			Cl	1442.	HON
K	16625.	123.	126.	22226.	1.3369			K2O	20027.	AL
CA	28772.	214.	373.	41525.	1.4433			CaO	40258.	AL
SC	0.	0.	230.	0.	.0000	******	ELEMENT NOT DETECTED	Sc2O3	0.	AL
TI	7407.	89.	153.	14604.	1.9716			TiO2	12354.	AL
V	83.	52.	119.	165.	2.0036	****	CONCN BELOW DET LIM	VO2	135.	AL
CR	26.	23.	54.	50.	1.9393	****	CONCN BELOW DET LIM	Cr2O3	38.	AL
MN	801.	42.	83.	1377.	1.7183			MnO2	1268.	AL
FE	53823.	268.	445.	81649.	1.5170			Fe2O3	76951.	AL
CO	17.	100.	234.	55.	3.2416	****	CONCN BELOW DET LIM	Co2O3	24.	AHC
NI	14.	11.	25.	76.	5.4564	****	CONCN BELOW DET LIM	NiO	18.	AHC
CU	20.	5.	9.	154.	7.8937			CuO	25.	AHC
ZN	85.	5.	9.	882.	10.3590			ZnO	106.	AHC
GA	15.	3.	6.	188.	11.6860			Ga2O3	21.	AHC
GE	0.	0.	6.	0.	.0000	******	ELEMENT NOT DETECTED	GeO2	0.	AHC
AS	8.	3.	6.	97.	12.3778	**	CONCN NEAR DET LIM	As2O5	12.	AHC
SE	6.	2.	5.	65.	11.4872	**	CONCN NEAR DET LIM	SeO2	9.	AHC
BR	3.	3.	6.	30.	10.6333	****	CONCN BELOW DET LIM	Br	3.	AHC
RB	94.	6.	11.	746.	7.9297			Rb2O	103.	AHC
SR	225.	9.	15.	1502.	6.6813			SrO	266.	AHC
Y	26.	6.	14.	143.	5.5888	**	CONCN NEAR DET LIM	Y2O3	33.	AHC
ZR	200.	12.	25.	909.	4.5536			ZrO2	271.	AHC
NB	14.	6.	15.	49.	3.7062	****	CONCN BELOW DET LIM	Nb2O3	17.	AHC
MO	0.	0.	23.	0.	.0000	******	ELEMENT NOT DETECTED	MoO3	0.	AHC
CD	18.	28.	62.	13.	.6605	****	CONCN BELOW DET LIM	CdO	21.	AHC
IN	0.	0.	77.	0.	.0000	******	ELEMENT NOT DETECTED	In2O3	0.	AHC
SN	0.	0.	102.	0.	.0000	******	ELEMENT NOT DETECTED	SnO2	0.	AHC
SB	0.	0.	133.	0.	.0000	******	ELEMENT NOT DETECTED	Sb2O3	0.	AHC
I	0.	0.	216.	0.	.0000	******	ELEMENT NOT DETECTED	I	0.	AHC
BA	895.	267.	561.	60.	.0676	**	CONCN NEAR DET LIM	BaO	1000.	AHC
TAL	0.	0.	26.	0.	.0000	******	ELEMENT NOT DETECTED	Ta2O5	0.	AHC
WL	5.	12.	28.	18.	3.8779	****	CONCN BELOW DET LIM	WO3	6.	AHC
PBL	9.	5.	9.	54.	6.2086	**	CONCN NEAR DET LIM	PbO	10.	AHC
								OXIDE SUM =	949972.	

REPORT # 0799

RESULTS OF PIXE ANALYSIS ON: SUB PIT SAMPLES SP17 REP

ELEMENT	CONCENTRATION	ERROR	DET LIMIT	PK AREA	XRY YIELD			OXIDE	CONCENTRATION	FILT
	PPM			-- CTS --	- CTS/PPM -				--- PPM ---	
NA	12645.	742.	1581.	1797.	.1421			Na2O	17045.	NON
MG	14951.	505.	1069.	5066.	.3388			MgO	24794.	NON
AL	87885.	540.	858.	49591.	.5643			Al2O3	166059.	NON
SI	269973.	667.	563.	189245.	.7010			SiO2	577554.	NON
P	1945.	409.	939.	849.	.4365			P2O5	4457.	NON
S	239.	111.	251.	127.	.5296	****	CONCN BELOW DET LIM	SO3	597.	NON
CL	1426.	107.	221.	835.	.5859			Cl	1426.	NON
K	17100.	130.	134.	21422.	1.2527			K2O	20598.	AL
CA	29837.	224.	393.	40307.	1.3509			CaO	41748.	AL
SC	0.	0.	241.	0.	.0000	******	ELEMENT NOT DETECTED	Sc2O3	0.	AL
TI	7789.	94.	160.	14359.	1.8432			TiO2	12992.	AL
V	124.	54.	125.	232.	1.8736	****	CONCN BELOW DET LIM	VO2	201.	AL
CR	0.	0.	56.	0.	.0000	******	ELEMENT NOT DETECTED	Cr2O3	0.	AL
MN	800.	43.	86.	1286.	1.6072			MnO2	1266.	AL
FE	55719.	282.	469.	79075.	1.4192			Fe2O3	79661.	AL
CO	15.	104.	243.	43.	3.0125	****	CONCN BELOW DET LIM	Co2O3	21.	AMC
NI	12.	12.	26.	62.	5.0653	****	CONCN BELOW DET LIM	NiO	15.	AMC
CU	15.	5.	10.	108.	7.3300	**	CONCN NEAR DET LIM	CuO	19.	AMC
ZN	86.	5.	10.	827.	9.6213			ZnO	107.	AMC
GA	15.	3.	7.	159.	10.8558			Ga2O3	20.	AMC
GE	0.	0.	7.	0.	.0000	******	ELEMENT NOT DETECTED	GeO2	0.	AMC
AS	8.	3.	7.	94.	11.5016	**	CONCN NEAR DET LIM	As2O5	13.	AMC
SE	3.	2.	5.	33.	10.6751	****	CONCN BELOW DET LIM	SeO3	5.	AMC
BR	0.	0.	7.	0.	.0000	******	ELEMENT NOT DETECTED	Br	0.	AMC
RB	96.	7.	12.	711.	7.3706			Rb2O	105.	AMC
SR	233.	10.	16.	1448.	6.2106			SrO	275.	AMC
Y	15.	7.	15.	80.	5.1952	**	CONCN NEAR DET LIM	Y2O3	19.	AMC
ZR	193.	13.	26.	816.	4.2330			ZrO2	261.	AMC
NB	13.	7.	15.	44.	3.4454	****	CONCN BELOW DET LIM	Nb2O3	17.	AMC
MO	0.	0.	23.	0.	.0000	******	ELEMENT NOT DETECTED	MoO3	0.	AMC
CD	0.	0.	63.	0.	.0000	******	ELEMENT NOT DETECTED	CdO	0.	AMC
IN	0.	0.	81.	0.	.0000	******	ELEMENT NOT DETECTED	In2O3	0.	AMC
SN	0.	0.	107.	0.	.0000	******	ELEMENT NOT DETECTED	SnO2	0.	AMC
SB	0.	0.	137.	0.	.0000	******	ELEMENT NOT DETECTED	Sb2O3	0.	AMC
I	0.	0.	231.	0.	.0000	******	ELEMENT NOT DETECTED	I	0.	AMC
BA	665.	262.	563.	42.	.0629	**	CONCN NEAR DET LIM	BaO	742.	AMC
TAL	0.	0.	26.	0.	.0000	******	ELEMENT NOT DETECTED	Ta2O5	0.	AMC
WL	0.	0.	28.	0.	.0000	******	ELEMENT NOT DETECTED	WO3	0.	AMC
PBL	7.	5.	10.	38.	5.7690	****	CONCN BELOW DET LIM	PbO	7.	AMC
								OXIDE SUM =	950023.	

REPORT # 0796

RESULTS OF PIXE ANALYSIS ON: SUB PIT SAMPLES SP18

ELEMENT	CONCENTRATION	ERROR	DET LIMIT	PK AREA	XRY YIELD			OXIDE	CONCENTRATION	FILT
	----------------	PPM ----------------		-- CTS --	- CTS/PPM -				--- PPM ---	
NA	16944.	735.	1514.	2433.	.1436			Na2O	22841.	NON
MG	12145.	498.	1072.	4126.	.3398			MgO	20140.	NON
AL	72976.	533.	917.	41541.	.5693			Al2O3	137889.	NON
SI	273372.	652.	531.	199867.	.7311			SiO2	584825.	NON
P	2203.	442.	1014.	991.	.4499			P2O5	5047.	NON
S	244.	105.	241.	133.	.5458	**	CONCN NEAR DET LIM	SO3	609.	NON
CL	579.	96.	212.	350.	.6036			Cl	579.	NON
K	14120.	118.	129.	18255.	1.2929			K2O	17009.	AL
CA	35727.	238.	408.	50036.	1.4005			CaO	49990.	AL
SC	0.	0.	260.	0.	.0000	******	ELEMENT NOT DETECTED	Sc2O3	0.	AL
TI	9738.	104.	175.	18434.	1.8930			TiO2	16244.	AL
V	93.	59.	137.	179.	1.9253	****	CONCN BELOW DET LIM	VO2	151.	AL
CR	0.	0.	59.	0.	.0000	******	ELEMENT NOT DETECTED	Cr2O3	0.	AL
MN	928.	46.	93.	1532.	1.6501			MnO2	1469.	AL
FE	63601.	298.	494.	92728.	1.4580			Fe2O3	90931.	AL
CO	27.	108.	250.	85.	3.1048	****	CONCN BELOW DET LIM	Co2O3	38.	AMC
NI	0.	0.	33.	0.	.0000	******	ELEMENT NOT DETECTED	NiO	0.	AMC
CU	10.	5.	10.	76.	7.5304	**	CONCN NEAR DET LIM	CuO	12.	AMC
ZN	88.	5.	10.	870.	9.8935			ZnO	109.	AMC
GA	13.	3.	6.	139.	11.1713	**	CONCN NEAR DET LIM	Ga2O3	17.	AMC
GE	0.	3.	6.	8.	11.8548	******	ELEMENT NOT DETECTED	GeO2	0.	AMC
AS	3.	3.	6.	32.	11.8489	****	CONCN BELOW DET LIM	As2O5	5.	AMC
SE	5.	2.	5.	46.	11.0018	**	CONCN NEAR DET LIM	SeO3	8.	AMC
BR	2.	2.	5.	17.	10.1883	****	CONCN BELOW DET LIM	Br	2.	AMC
RB	59.	5.	10.	454.	7.6025			Rb2O	65.	AMC
SR	300.	10.	18.	1923.	6.4072			SrO	355.	AMC
Y	19.	6.	13.	101.	5.3606	**	CONCN NEAR DET LIM	Y2O3	24.	AMC
ZR	140.	13.	26.	615.	4.3684			ZrO2	190.	AMC
NB	13.	6.	14.	44.	3.5560	****	CONCN BELOW DET LIM	Nb2O3	16.	AMC
MO	0.	0.	21.	0.	.0000	******	ELEMENT NOT DETECTED	MoO3	0.	AMC
CD	0.	0.	59.	0.	.0000	******	ELEMENT NOT DETECTED	CdO	0.	AMC
IN	32.	33.	75.	15.	.4847	****	CONCN BELOW DET LIM	In2O3	39.	AMC
SN	80.	45.	99.	29.	.3644	****	CONCN BELOW DET LIM	SnO2	101.	AMC
SB	97.	57.	126.	27.	.2750	****	CONCN BELOW DET LIM	Sb2O3	116.	AMC
I	140.	99.	219.	22.	.1564	****	CONCN BELOW DET LIM	I	140.	AMC
BA	906.	266.	557.	59.	.0649	**	CONCN NEAR DET LIM	BaO	1011.	AMC
TAL	6.	11.	26.	22.	3.2241	****	CONCN BELOW DET LIM	Ta2O5	8.	AMC
WL	0.	0.	27.	0.	.0000	******	ELEMENT NOT DETECTED	WO3	0.	AMC
PBL	13.	5.	10.	71.	5.9427	**	CONCN NEAR DET LIM	PbO	14.	AMC

OXIDE SUM = 949992.

REPORT # 0784
RESULTS OF PIXE ANALYSIS ON: SUB PIT SAMPLES SP19

ELEMENT	CONCENTRATION	ERROR	DET LIMIT	PK AREA	XRY YIELD			OXIDE	CONCENTRATION	FILT
		PPM		-- CTS --	- CTS/PPM -				--- PPM ---	
NA	20355.	718.	1454.	3283.	.1612			Na2O	27439.	NON
MG	16535.	472.	984.	6269.	.3791			MgO	27420.	NON
AL	79627.	507.	838.	50136.	.6296			Al2O3	150455.	NON
SI	249992.	599.	503.	200511.	.8021			SiO2	534807.	NON
P	1967.	381.	877.	1021.	.5190			P2O5	4508.	NON
S	281.	92.	209.	177.	.6294	**	CONCN NEAR DET LIM	SO3	702.	NON
CL	592.	85.	187.	412.	.6954			Cl	592.	NON
K	12152.	106.	124.	17730.	1.4590			K2O	14638.	AL
CA	41207.	238.	405.	65280.	1.5842			CaO	57656.	AL
SC	0.	0.	265.	0.	.0000	******	ELEMENT NOT DETECTED	Sc2O3	0.	AL
TI	10840.	104.	177.	23009.	2.1225			TiO2	18082.	AL
V	194.	60.	138.	419.	2.1595	**	CONCN NEAR DET LIM	VO2	315.	AL
CR	8.	25.	57.	18.	2.0856	****	CONCN BELOW DET LIM	Cr2O3	12.	AL
MN	1147.	46.	92.	2123.	1.8506			MnO2	1816.	AL
FE	76514.	308.	510.	125153.	1.6357			Fe2O3	109392.	AL
CO	26.	113.	263.	91.	3.4326	****	CONCN BELOW DET LIM	Co2O3	37.	AMC
NI	1.	13.	28.	7.	5.7032	****	CONCN BELOW DET LIM	NiO	2.	AMC
CU	13.	4.	10.	102.	8.2754	**	CONCN NEAR DET LIM	CuO	16.	AMC
ZN	100.	6.	10.	1085.	10.8863			ZnO	125.	AMC
GA	13.	3.	7.	158.	12.3050	**	CONCN NEAR DET LIM	Ga2O3	17.	AMC
GE	0.	0.	6.	0.	.0000	******	ELEMENT NOT DETECTED	GeO2	0.	AMC
AS	1.	3.	6.	22.	13.0713	****	CONCN BELOW DET LIM	As2O5	2.	AMC
SE	3.	3.	6.	42.	12.1437	****	CONCN BELOW DET LIM	SeO3	4.	AMC
BR	0.	0.	6.	0.	.0000	******	ELEMENT NOT DETECTED	Br	0.	AMC
RB	61.	4.	10.	509.	8.4014			Rb2O	67.	AMC
SR	319.	10.	18.	2262.	7.0824			SrO	377.	AMC
Y	25.	6.	13.	152.	5.9267	**	CONCN NEAR DET LIM	Y2O3	32.	AMC
ZR	185.	13.	25.	894.	4.8306			ZrO2	250.	AMC
NB	8.	6.	14.	31.	3.9329	****	CONCN BELOW DET LIM	Nb2O3	11.	AMC
MO	0.	0.	21.	0.	.0000	******	ELEMENT NOT DETECTED	MoO3	0.	AMC
CD	0.	0.	52.	0.	.0000	******	ELEMENT NOT DETECTED	CdO	0.	AMC
IN	40.	31.	68.	21.	.5365	****	CONCN BELOW DET LIM	In2O3	49.	AMC
SN	38.	39.	86.	15.	.4033	****	CONCN BELOW DET LIM	SnO2	48.	AMC
SB	65.	49.	107.	20.	.3044	****	CONCN BELOW DET LIM	Sb2O3	78.	AMC
I	120.	88.	194.	21.	.1732	****	CONCN BELOW DET LIM	I	120.	AMC
BA	823.	241.	503.	59.	.0718	**	CONCN NEAR DET LIM	BaO	919.	AMC
TAL	0.	0.	25.	0.	.0000	******	ELEMENT NOT DETECTED	Ta2O5	0.	AMC
WL	0.	0.	28.	0.	.0000	******	ELEMENT NOT DETECTED	WO3	0.	AMC
PBL	8.	4.	8.	51.	6.5551	**	CONCN NEAR DET LIM	PbO	9.	AMC
								OXIDE SUM =	949996.	

REPORT # 0804
RESULTS OF PIXE ANALYSIS ON: SUB PIT SAMPLES SP20

ELEMENT	CONCENTRATION	ERROR	DET LIMIT	PK AREA	XRY YIELD			OXIDE	CONCENTRATION	FILT
	----------------	PPM ----------------		-- CTS --	- CTS/PPM -				--- PPM ---	
NA	23390.	682.	1351.	4282.	.1831			Na2O	31529.	NON
MG	14907.	452.	957.	6386.	.4284			MgO	24720.	NON
AL	87601.	488.	790.	62517.	.7137			Al2O3	165522.	NON
SI	258232.	579.	492.	230121.	.8911			SiO2	552436.	NON
P	1807.	372.	855.	1027.	.5688			P2O5	4140.	NON
S	174.	86.	196.	120.	.6900	****	CONCN BELOW DET LIM	SO3	434.	NON
CL	1599.	89.	178.	1220.	.7630			Cl	1599.	NON
K	10592.	94.	113.	17503.	1.6524			K2O	12759.	AL
CA	36345.	209.	357.	65437.	1.8004			CaO	50854.	AL
SC	0.	0.	232.	0.	.0000	******	ELEMENT NOT DETECTED	Sc2O3	0.	AL
TI	8180.	85.	143.	19848.	2.4266			TiO2	13644.	AL
V	187.	49.	113.	463.	2.4663	**	CONCN NEAR DET LIM	VO2	305.	AL
CR	0.	0.	50.	0.	.0000	******	ELEMENT NOT DETECTED	Cr2O3	0.	AL
MN	920.	40.	79.	1947.	2.1152			MnO2	1456.	AL
FE	62418.	260.	432.	116581.	1.8677			Fe2O3	89239.	AL
CO	26.	92.	215.	105.	4.0577	****	CONCN BELOW DET LIM	Co2O3	36.	AMC
NI	16.	12.	28.	110.	6.7946	****	CONCN BELOW DET LIM	NiO	20.	AMC
CU	16.	4.	9.	153.	9.8394	**	CONCN NEAR DET LIM	CuO	20.	AMC
ZN	78.	4.	9.	1000.	12.9227			ZnO	97.	AMC
GA	16.	2.	5.	231.	14.5876			Ga2O3	21.	AMC
GE	0.	0.	5.	0.	.0000	******	ELEMENT NOT DETECTED	GeO2	0.	AMC
AS	0.	0.	5.	0.	.0000	******	ELEMENT NOT DETECTED	As2O5	0.	AMC
SE	2.	2.	4.	38.	14.3583	****	CONCN BELOW DET LIM	SeO3	4.	AMC
BR	2.	2.	4.	35.	13.2949	****	CONCN BELOW DET LIM	Br	2.	AMC
RB	41.	4.	7.	409.	9.9188			Rb2O	45.	AMC
SR	294.	9.	15.	2461.	8.3588			SrO	348.	AMC
Y	21.	5.	10.	146.	6.9928			Y2O3	26.	AMC
ZR	141.	11.	22.	800.	5.6983			ZrO2	191.	AMC
NB	12.	5.	11.	58.	4.6383	**	CONCN NEAR DET LIM	Nb2O3	15.	AMC
MO	5.	7.	17.	20.	3.6888	****	CONCN BELOW DET LIM	MoO3	7.	AMC
CD	0.	0.	44.	0.	.0000	******	ELEMENT NOT DETECTED	CdO	0.	AMC
IN	0.	0.	58.	0.	.0000	******	ELEMENT NOT DETECTED	In2O3	0.	AMC
SN	0.	0.	77.	0.	.0000	******	ELEMENT NOT DETECTED	SnO2	0.	AMC
SB	0.	0.	98.	0.	.0000	******	ELEMENT NOT DETECTED	Sb2O3	0.	AMC
I	0.	0.	168.	0.	.0000	******	ELEMENT NOT DETECTED	I	0.	AMC
BA	474.	197.	423.	40.	.0846	**	CONCN NEAR DET LIM	BaO	529.	AMC
TAL	0.	0.	22.	0.	.0000	******	ELEMENT NOT DETECTED	Ta2O5	0.	AMC
WL	6.	10.	23.	28.	4.8354	****	CONCN BELOW DET LIM	WO3	8.	AMC
PBL	7.	4.	7.	58.	7.7570	**	CONCN NEAR DET LIM	PbO	8.	AMC
								OXIDE SUM =	950015.	

REPORT # 0785

RESULTS OF PIXE ANALYSIS ON: SUB PIT SAMPLES SP21

ELEMENT	CONCENTRATION (PPM)	ERROR (PPM)	DET LIMIT (PPM)	PK AREA -- CTS --	XRY YIELD - CTS/PPM -			OXIDE	CONCENTRATION --- PPM ---	FILT
NA	13707.	654.	1368.	2292.	.1672			Na2O	18477.	NON
MG	8675.	448.	983.	3455.	.3984			MgO	14385.	NON
AL	83133.	511.	865.	55892.	.6723			Al2O3	157079.	NON
SI	308027.	647.	524.	257396.	.8356			SiO2	658962.	NON
P	1147.	457.	1058.	553.	.4819	**	CONCN NEAR DET LIM	P2O5	2629.	NON
S	0.	0.	224.	0.	.0000	******	ELEMENT NOT DETECTED	SO3	0.	NON
CL	1486.	98.	198.	964.	.6484			Cl	1486.	NON
K	17047.	120.	116.	24536.	1.4393			K2O	20534.	AL
CA	16336.	161.	292.	25410.	1.5555			CaO	22857.	AL
SC	0.	0.	166.	0.	.0000	******	ELEMENT NOT DETECTED	Sc2O3	0.	AL
TI	3776.	64.	112.	8169.	2.1632			TiO2	6298.	AL
V	27.	38.	88.	59.	2.1942	****	CONCN BELOW DET LIM	VO2	44.	AL
CR	33.	18.	42.	69.	2.1282	****	CONCN BELOW DET LIM	Cr2O3	48.	AL
MN	482.	31.	62.	908.	1.8821			MnO2	762.	AL
FE	31055.	195.	323.	51521.	1.6590			Fe2O3	44400.	AL
CO	18.	72.	167.	65.	3.5505	****	CONCN BELOW DET LIM	Co2O3	26.	AHC
NI	8.	7.	18.	53.	6.0539	****	CONCN BELOW DET LIM	NiO	11.	AHC
CU	14.	4.	8.	119.	8.7298	**	CONCN NEAR DET LIM	CuO	18.	AHC
ZN	62.	4.	8.	718.	11.4265			ZnO	78.	AHC
GA	11.	3.	6.	155.	12.8634	**	CONCN NEAR DET LIM	Ga2O3	15.	AHC
GE	0.	0.	4.	0.	.0000	******	ELEMENT NOT DETECTED	GeO2	0.	AHC
AS	6.	3.	6.	86.	13.5829	**	CONCN NEAR DET LIM	As2O5	9.	AHC
SE	3.	1.	4.	39.	12.5914	****	CONCN BELOW DET LIM	SeO3	5.	AHC
BR	0.	0.	4.	0.	.0000	******	ELEMENT NOT DETECTED	Br	0.	AHC
RB	88.	6.	10.	755.	8.6716			Rb2O	96.	AHC
SR	280.	10.	16.	2051.	7.3027			SrO	332.	AHC
Y	18.	6.	13.	111.	6.1058	**	CONCN NEAR DET LIM	Y2O3	23.	AHC
ZR	228.	13.	25.	1137.	4.9730			ZrO2	308.	AHC
NB	4.	6.	13.	18.	4.0463	****	CONCN BELOW DET LIM	Nb2O3	5.	AHC
MO	0.	0.	23.	0.	.0000	******	ELEMENT NOT DETECTED	MoO3	0.	AHC
CD	0.	0.	54.	0.	.0000	******	ELEMENT NOT DETECTED	CdO	0.	AHC
IN	0.	0.	68.	0.	.0000	******	ELEMENT NOT DETECTED	In2O3	0.	AHC
SN	44.	41.	92.	18.	.4138	****	CONCN BELOW DET LIM	SnO2	56.	AHC
SB	0.	0.	110.	0.	.0000	******	ELEMENT NOT DETECTED	Sb2O3	0.	AHC
I	74.	76.	170.	13.	.1776	****	CONCN BELOW DET LIM	I	74.	AHC
BA	848.	237.	489.	62.	.0736	**	CONCN NEAR DET LIM	BaO	947.	AHC
TAL	7.	10.	21.	25.	3.7380	****	CONCN BELOW DET LIM	Ta2O5	9.	AHC
WL	0.	0.	23.	0.	.0000	******	ELEMENT NOT DETECTED	WO3	0.	AHC
PBL	17.	4.	8.	113.	6.8144	**	CONCN NEAR DET LIM	PbO	18.	AHC
								OXIDE SUM =	949988.	

REPORT # 0789

RESULTS OF PIXE ANALYSIS ON: SUB PIT SAMPLES EE10

ELEMENT	CONCENTRATION (PPM)	ERROR (PPM)	DET LIMIT (PPM)	PK AREA -- CTS --	XRY YIELD - CTS/PPM -			OXIDE	CONCENTRATION --- PPM ---	FILT
NA	20755.	686.	1380.	3632.	.1750			Na2O	27978.	NON
MG	15467.	449.	941.	6364.	.4115			MgO	25649.	NON
AL	76752.	490.	831.	52554.	.6847			Al2O3	145023.	NON
SI	276488.	601.	487.	241273.	.8727			SiO2	591490.	NON
P	1447.	374.	861.	776.	.5360	**	CONCN NEAR DET LIM	P2O5	3316.	NON
S	3.	85.	197.	2.	.6505	****	CONCN BELOW DET LIM	SO3	6.	NON
CL	534.	80.	175.	384.	.7197			Cl	534.	NON
K	9324.	90.	107.	14722.	1.5788			K2O	11232.	AL
CA	34345.	207.	353.	59240.	1.7248			CaO	48056.	AL
SC	0.	0.	229.	0.	.0000	******	ELEMENT NOT DETECTED	Sc2O3	0.	AL
TI	7518.	82.	139.	17525.	2.3311			TiO2	12539.	AL
V	139.	48.	110.	329.	2.3682	**	CONCN NEAR DET LIM	VO2	227.	AL
CR	0.	0.	49.	0.	.0000	******	ELEMENT NOT DETECTED	Cr2O3	0.	AL
MN	825.	39.	77.	1675.	2.0305			MnO2	1305.	AL
FE	56598.	254.	420.	101444.	1.7924			Fe2O3	80918.	AL
CO	17.	93.	217.	65.	3.8457	****	CONCN BELOW DET LIM	Co2O3	24.	AMC
NI	1.	9.	22.	9.	6.4622	****	CONCN BELOW DET LIM	NiO	2.	AMC
CU	39.	5.	10.	363.	9.3506			CuO	48.	AMC
ZN	79.	4.	9.	972.	12.2727			ZnO	98.	AMC
GA	9.	3.	6.	125.	13.8468	**	CONCN NEAR DET LIM	Ga2O3	12.	AMC
GE	0.	0.	5.	0.	.0000	******	ELEMENT NOT DETECTED	GeO2	0.	AMC
AS	0.	0.	5.	0.	.0000	******	ELEMENT NOT DETECTED	As2O5	0.	AMC
SE	4.	3.	4.	49.	13.6147	**	CONCN NEAR DET LIM	SeO3	6.	AMC
BR	1.	1.	4.	14.	12.6034	****	CONCN BELOW DET LIM	Br	1.	AMC
RB	41.	4.	8.	386.	9.3997			Rb2O	45.	AMC
SR	273.	9.	15.	2166.	7.9202			SrO	323.	AMC
Y	21.	5.	10.	134.	6.6252	**	CONCN NEAR DET LIM	Y2O3	26.	AMC
ZR	129.	10.	22.	697.	5.3982			ZrO2	174.	AMC
NB	6.	5.	13.	30.	4.3938	****	CONCN BELOW DET LIM	Nb2O3	8.	AMC
MO	0.	0.	18.	0.	.0000	******	ELEMENT NOT DETECTED	MoO3	0.	AMC
CD	41.	21.	45.	32.	.7831	****	CONCN BELOW DET LIM	CdO	47.	AMC
IN	40.	26.	58.	24.	.5986	****	CONCN BELOW DET LIM	In2O3	48.	AMC
SN	31.	36.	81.	14.	.4500	****	CONCN BELOW DET LIM	SnO2	39.	AMC
SB	0.	0.	110.	0.	.0000	******	ELEMENT NOT DETECTED	Sb2O3	0.	AMC
I	0.	0.	179.	0.	.0000	******	ELEMENT NOT DETECTED	I	0.	AMC
BA	720.	218.	455.	58.	.0802	**	CONCN NEAR DET LIM	BaO	804.	AMC
TAL	6.	12.	27.	25.	4.0035	****	CONCN BELOW DET LIM	Ta2O5	8.	AMC
WL	0.	0.	24.	0.	.0000	******	ELEMENT NOT DETECTED	WO3	0.	AMC
PBL	13.	4.	8.	95.	7.3578	**	CONCN NEAR DET LIM	PbO	14.	AMC
								OXIDE SUM =	950001.	

REPORT # 0781
RESULTS OF PIXE ANALYSIS ON: SUB PIT SAMPLES EE20

ELEMENT	CONCENTRATION	ERROR	DET LIMIT	PK AREA	XRY YIELD			OXIDE	CONCENTRATION	FILT
	PPM			-- CTS --	- CTS/PPM -				--- PPM ---	
NA	19189.	551.	1121.	5152.	.2685			Na2O	25867.	NON
MG	13346.	357.	760.	8445.	.6328			MgO	22131.	NON
AL	73875.	392.	676.	78131.	1.0576			Al2O3	139587.	NON
SI	278211.	483.	391.	377033.	1.3552			SiO2	595176.	NON
P	1711.	326.	750.	1416.	.8275			P2O5	3921.	NON
S	96.	76.	175.	96.	1.0040	****	CONCN BELOW DET LIM	SO3	240.	NON
CL	654.	71.	155.	726.	1.1106			Cl	654.	NON
K	13236.	109.	117.	19166.	1.4480			K2O	15944.	AL
CA	33567.	217.	373.	52751.	1.5715			CaO	46967.	AL
SC	0.	0.	237.	0.	.0000	******	ELEMENT NOT DETECTED	Sc2O3	0.	AL
TI	8133.	90.	151.	17327.	2.1303			TiO2	13566.	AL
V	191.	52.	119.	413.	2.1654	**	CONCN NEAR DET LIM	VO2	310.	AL
CR	18.	23.	52.	38.	2.0950	****	CONCN BELOW DET LIM	Cr2O3	27.	AL
MN	846.	41.	80.	1571.	1.8568			MnO2	1336.	AL
FE	57623.	267.	442.	94487.	1.6398			Fe2O3	82383.	AL
CO	0.	0.	229.	0.	.0000	******	ELEMENT NOT DETECTED	Co2O3	0.	AHC
NI	0.	0.	24.	0.	.0000	******	ELEMENT NOT DETECTED	NiO	0.	AHC
CU	32.	4.	10.	265.	8.3153			CuO	41.	AHC
ZN	79.	4.	8.	863.	10.9168			ZnO	98.	AHC
GA	13.	3.	6.	148.	12.3195			Ga2O3	17.	AHC
GE	0.	0.	6.	0.	.0000	******	ELEMENT NOT DETECTED	GeO2	0.	AHC
AS	3.	3.	4.	44.	13.0554	****	CONCN BELOW DET LIM	As2O5	4.	AHC
SE	4.	1.	4.	45.	12.1183	**	CONCN NEAR DET LIM	SeO3	7.	AHC
BR	3.	1.	4.	27.	11.2192	****	CONCN BELOW DET LIM	Br	3.	AHC
RB	45.	4.	8.	374.	8.3685			Rb2O	49.	AHC
SR	256.	8.	16.	1804.	7.0517			SrO	302.	AHC
Y	18.	6.	11.	108.	5.8991	**	CONCN NEAR DET LIM	Y2O3	23.	AHC
ZR	138.	11.	23.	663.	4.8067			ZrO2	187.	AHC
NB	8.	6.	14.	34.	3.9125	****	CONCN BELOW DET LIM	Nb2O3	11.	AHC
MO	0.	0.	20.	0.	.0000	******	ELEMENT NOT DETECTED	MoO3	0.	AHC
CD	0.	0.	52.	0.	.0000	******	ELEMENT NOT DETECTED	CdO	0.	AHC
IN	0.	0.	69.	0.	.0000	******	ELEMENT NOT DETECTED	In2O3	0.	AHC
SN	49.	41.	92.	20.	.4008	****	CONCN BELOW DET LIM	SnO2	63.	AHC
SB	49.	52.	117.	15.	.3025	****	CONCN BELOW DET LIM	Sb2O3	59.	AHC
I	0.	0.	186.	0.	.0000	******	ELEMENT NOT DETECTED	I	0.	AHC
BA	920.	246.	507.	66.	.0714	**	CONCN NEAR DET LIM	BaO	1028.	AHC
TAL	3.	11.	28.	11.	3.5602	****	CONCN BELOW DET LIM	Ta2O5	3.	AHC
WL	0.	0.	25.	0.	.0000	******	ELEMENT NOT DETECTED	WO3	0.	AHC
PBL	0.	0.	8.	0.	.0000	******	ELEMENT NOT DETECTED	PbO	0.	AHC
								OXIDE SUM =	950007.	

REPORT # 0787

RESULTS OF PIXE ANALYSIS ON: SUB PIT SAMPLES EE30

ELEMENT	CONCENTRATION ----------------	ERROR PPM	DET LIMIT ----------------	PK AREA -- CTS --	XRY YIELD - CTS/PPM -			OXIDE	CONCENTRATION --- PPM ---	FILT
NA	20085.	734.	1488.	3134.	.1560			Na2O	27075.	NON
MG	15469.	478.	1003.	5680.	.3672			MgO	25653.	NON
AL	76486.	519.	883.	46737.	.6111			Al2O3	144520.	NON
SI	271696.	631.	518.	211847.	.7797			SiO2	581239.	NON
P	2085.	420.	966.	1007.	.4829			P2O5	4778.	NON
S	219.	101.	229.	128.	.5858	****	CONCN BELOW DET LIM	SO3	547.	NON
CL	702.	93.	204.	455.	.6480			Cl	702.	NON
K	10553.	102.	121.	14649.	1.3879			K2O	12713.	AL
CA	36192.	228.	387.	54746.	1.5126			CaO	50639.	AL
SC	0.	0.	251.	0.	.0000	******	ELEMENT NOT DETECTED	Sc2O3	0.	AL
TI	7917.	90.	154.	16149.	2.0400			TiO2	13205.	AL
V	135.	52.	121.	280.	2.0736	**	CONCN NEAR DET LIM	VO2	219.	AL
CR	0.	0.	53.	0.	.0000	******	ELEMENT NOT DETECTED	Cr2O3	0.	AL
MN	839.	41.	84.	1493.	1.7791			MnO2	1327.	AL
FE	60160.	280.	461.	94508.	1.5710			Fe2O3	86011.	AL
CO	13.	101.	234.	44.	3.3629	****	CONCN BELOW DET LIM	Co2O3	19.	AMC
NI	3.	13.	30.	19.	5.6391	****	CONCN BELOW DET LIM	NiO	4.	AMC
CU	9.	4.	10.	67.	8.1640	****	CONCN BELOW DET LIM	CuO	11.	AMC
ZN	68.	4.	9.	727.	10.7200			ZnO	85.	AMC
GA	10.	3.	6.	120.	12.0991	**	CONCN NEAR DET LIM	Ga2O3	14.	AMC
GE	0.	0.	6.	0.	.0000	******	ELEMENT NOT DETECTED	GeO2	0.	AMC
AS	1.	1.	4.	18.	12.8245	****	CONCN BELOW DET LIM	As2O5	2.	AMC
SE	4.	1.	4.	54.	11.9049	**	CONCN NEAR DET LIM	SeO3	7.	AMC
BR	0.	0.	4.	0.	.0000	******	ELEMENT NOT DETECTED	Br	0.	AMC
RB	38.	4.	9.	314.	8.2225			Rb2O	42.	AMC
SR	259.	9.	16.	1797.	6.9289			SrO	306.	AMC
Y	19.	6.	12.	112.	5.7965	**	CONCN NEAR DET LIM	Y2O3	24.	AMC
ZR	121.	10.	22.	576.	4.7232			ZrO2	164.	AMC
NB	3.	6.	13.	13.	3.8445	****	CONCN BELOW DET LIM	Nb2O3	4.	AMC
MO	0.	0.	19.	0.	.0000	******	ELEMENT NOT DETECTED	MoO3	0.	AMC
CD	0.	0.	50.	0.	.0000	******	ELEMENT NOT DETECTED	CdO	0.	AMC
IN	34.	31.	70.	18.	.5239	****	CONCN BELOW DET LIM	In2O3	41.	AMC
SN	0.	0.	92.	0.	.0000	******	ELEMENT NOT DETECTED	SnO2	0.	AMC
SB	0.	0.	115.	0.	.0000	******	ELEMENT NOT DETECTED	Sb2O3	0.	AMC
I	0.	0.	200.	0.	.0000	******	ELEMENT NOT DETECTED	I	0.	AMC
BA	547.	229.	491.	38.	.0701	**	CONCN NEAR DET LIM	BaO	611.	AMC
TAL	9.	10.	24.	28.	3.4954	****	CONCN BELOW DET LIM	Ta2O5	11.	AMC
WL	0.	0.	25.	0.	.0000	******	ELEMENT NOT DETECTED	WO3	0.	AMC
PBL	4.	4.	9.	32.	6.4323	****	CONCN BELOW DET LIM	PbO	5.	AMC
								OXIDE SUM =	949977.	

REPORT # 0803
RESULTS OF PIXE ANALYSIS ON: SUB PIT SAMPLES EE35

ELEMENT	CONCENTRATION	ERROR	DET LIMIT	PK AREA	XRY YIELD		OXIDE	CONCENTRATION	FILT
	---------------- PPM	----------------	----------------	-- CTS --	- CTS/PPM -			--- PPM ---	
NA	18539.	704.	1440.	3094.	.1668		Na2O	24991.	NON
MG	17061.	480.	1006.	6719.	.3938		MgO	28292.	NON
AL	78373.	504.	853.	51189.	.6532		Al2O3	148086.	NON
SI	270617.	611.	503.	224579.	.8299		SiO2	578931.	NON
P	1567.	406.	936.	808.	.5153 **	CONCN NEAR DET LIM	P2O5	3592.	NON
S	75.	94.	217.	47.	.6252 ****	CONCN BELOW DET LIM	SO3	188.	NON
CL	1546.	97.	197.	1069.	.6916		Cl	1546.	NON
K	10773.	98.	118.	15975.	1.4829		K2O	12977.	AL
CA	37484.	224.	383.	60558.	1.6155		CaO	52448.	AL
SC	0.	0.	249.	0.	.0000 ******	ELEMENT NOT DETECTED	Sc2O3	0.	AL
TI	7243.	85.	143.	15759.	2.1755		TiO2	12081.	AL
V	178.	49.	113.	392.	2.2120 **	CONCN NEAR DET LIM	VO2	289.	AL
CR	100.	25.	53.	214.	2.1427 **	CONCN NEAR DET LIM	Cr2O3	146.	AL
MN	869.	41.	81.	1650.	1.8992		MnO2	1375.	AL
FE	58415.	266.	440.	97969.	1.6771		Fe2O3	83516.	AL
CO	16.	93.	217.	60.	3.6522 ****	CONCN BELOW DET LIM	Co2O3	23.	AHC
NI	16.	10.	23.	105.	6.1313 ****	CONCN BELOW DET LIM	NiO	21.	AHC
CU	25.	4.	10.	215.	8.8752		CuO	31.	AHC
ZN	70.	4.	8.	808.	11.6527		ZnO	87.	AHC
GA	12.	3.	5.	160.	13.1507		Ga2O3	17.	AHC
GE	0.	0.	5.	0.	.0000 ******	ELEMENT NOT DETECTED	GeO2	0.	AHC
AS	0.	0.	5.	0.	.0000 ******	ELEMENT NOT DETECTED	As2O5	0.	AHC
SE	4.	1.	4.	53.	12.9372 **	CONCN NEAR DET LIM	SeO3	7.	AHC
BR	0.	0.	4.	0.	.0000 ******	ELEMENT NOT DETECTED	Br	0.	AHC
RB	46.	4.	8.	409.	8.9346		Rb2O	51.	AHC
SR	280.	10.	15.	2114.	7.5288		SrO	331.	AHC
Y	26.	5.	11.	164.	6.2982		Y2O3	33.	AHC
ZR	134.	11.	22.	685.	5.1319		ZrO2	181.	AHC
NB	8.	5.	12.	36.	4.1772 ****	CONCN BELOW DET LIM	Nb2O3	10.	AHC
MO	0.	0.	18.	0.	.0000 ******	ELEMENT NOT DETECTED	MoO3	0.	AHC
CD	0.	0.	49.	0.	.0000 ******	ELEMENT NOT DETECTED	CdO	0.	AHC
IN	41.	29.	66.	23.	.5692 ****	CONCN BELOW DET LIM	In2O3	50.	AHC
SN	0.	0.	79.	0.	.0000 ******	ELEMENT NOT DETECTED	SnO2	0.	AHC
SB	0.	0.	98.	0.	.0000 ******	ELEMENT NOT DETECTED	Sb2O3	0.	AHC
I	0.	0.	180.	0.	.0000 ******	ELEMENT NOT DETECTED	I	0.	AHC
BA	634.	223.	473.	48.	.0762 **	CONCN NEAR DET LIM	BaO	708.	AHC
TAL	0.	0.	26.	0.	.0000 ******	ELEMENT NOT DETECTED	Ta2O5	0.	AHC
WL	0.	11.	25.	2.	4.3610 ******	ELEMENT NOT DETECTED	WO3	0.	AHC
PBL	10.	4.	8.	65.	6.9905 **	CONCN NEAR DET LIM	PbO	10.	AHC
							OXIDE SUM =	950017.	

REPORT # 0790

RESULTS OF PIXE ANALYSIS ON: SUB PIT SAMPLES EE45

ELEMENT	CONCENTRATION	ERROR	DET LIMIT	PK AREA	XRY YIELD			OXIDE	CONCENTRATION	FILT
	----------------	PPM	----------------	-- CTS --	- CTS/PPM -				--- PPM ---	
NA	27111.	665.	1322.	6156.	.2271			Na2O	36545.	NON
MG	12004.	385.	832.	7207.	.6004			MgO	19906.	NON
AL	81736.	397.	668.	88187.	1.0789			Al2O3	154440.	NON
SI	275113.	472.	389.	389040.	1.4141			SiO2	588549.	NON
P	1895.	309.	712.	1691.	.8922			P2O5	4343.	NON
S	133.	72.	165.	146.	1.0986	****	CONCN BELOW DET LIM	SO3	333.	NON
CL	846.	67.	144.	1038.	1.2267			Cl	846.	NON
K	12931.	112.	124.	17379.	1.3440			K2O	15577.	AL
CA	31515.	219.	377.	46005.	1.4598			CaO	44096.	AL
SC	0.	0.	237.	0.	.0000	******	ELEMENT NOT DETECTED	Sc2O3	0.	AL
TI	6775.	86.	147.	13438.	1.9835			TiO2	11301.	AL
V	29.	49.	115.	60.	2.0153	****	CONCN BELOW DET LIM	VO2	47.	AL
CR	0.	0.	51.	0.	.0000	******	ELEMENT NOT DETECTED	Cr2O3	0.	AL
MN	723.	40.	78.	1250.	1.7284			MnO2	1144.	AL
FE	49237.	256.	424.	75118.	1.5256			Fe2O3	70394.	AL
CO	12.	95.	222.	39.	3.2527	****	CONCN BELOW DET LIM	Co2O3	17.	AHC
NI	0.	0.	29.	0.	.0000	******	ELEMENT NOT DETECTED	NiO	0.	AHC
CU	17.	5.	11.	136.	7.9381	**	CONCN NEAR DET LIM	CuO	21.	AHC
ZN	72.	5.	9.	743.	10.4126			ZnO	90.	AHC
GA	11.	3.	6.	124.	11.7423	**	CONCN NEAR DET LIM	Ga2O3	14.	AHC
GE	2.	3.	6.	13.	12.4477	****	CONCN BELOW DET LIM	GeO2	2.	AHC
AS	2.	2.	5.	28.	12.4309	****	CONCN BELOW DET LIM	As2O5	2.	AHC
SE	3.	2.	5.	40.	11.5342	****	CONCN BELOW DET LIM	SeO3	5.	AHC
BR	0.	0.	5.	0.	.0000	******	ELEMENT NOT DETECTED	Br	0.	AHC
RB	51.	5.	9.	406.	7.9590			Rb2O	55.	AHC
SR	380.	11.	20.	2550.	6.7054			SrO	449.	AHC
Y	15.	5.	12.	88.	5.6086	**	CONCN NEAR DET LIM	Y2O3	19.	AHC
ZR	129.	12.	26.	586.	4.5694			ZrO2	174.	AHC
NB	12.	6.	14.	45.	3.7189	****	CONCN BELOW DET LIM	Nb2O3	15.	AHC
MO	9.	9.	20.	27.	2.9572	****	CONCN BELOW DET LIM	MoO3	14.	AHC
CD	26.	26.	60.	18.	.6626	****	CONCN BELOW DET LIM	CdO	30.	AHC
IN	0.	0.	77.	0.	.0000	******	ELEMENT NOT DETECTED	In2O3	0.	AHC
SN	43.	47.	106.	16.	.3808	****	CONCN BELOW DET LIM	SnO2	54.	AHC
SB	0.	0.	139.	0.	.0000	******	ELEMENT NOT DETECTED	Sb2O3	0.	AHC
I	0.	0.	228.	0.	.0000	******	ELEMENT NOT DETECTED	I	0.	AHC
BA	1322.	288.	587.	90.	.0678			BaO	1476.	AHC
TAL	9.	11.	26.	33.	3.3988	****	CONCN BELOW DET LIM	Ta2O5	11.	AHC
WL	0.	0.	26.	0.	.0000	******	ELEMENT NOT DETECTED	WO3	0.	AHC
PBL	8.	5.	9.	45.	6.2354	****	CONCN BELOW DET LIM	PbO	8.	AHC
								OXIDE SUM =	949980.	

REPORT # 0801

RESULTS OF PIXE ANALYSIS ON: SUB PIT SAMPLES EE49

ELEMENT	CONCENTRATION (PPM)	ERROR (PPM)	DET LIMIT (PPM)	PK AREA (CTS)	XRY YIELD (CTS/PPM)			OXIDE	CONCENTRATION (PPM)	FILT
NA	18569.	738.	1504.	2715.	.1462			Na2O	25031.	NON
MG	10125.	511.	1120.	3502.	.3458			MgO	16790.	NON
AL	84094.	554.	937.	49001.	.5827			Al2O3	158895.	NON
SI	298045.	677.	554.	220770.	.7407			SiO2	637607.	NON
P	1450.	456.	1051.	660.	.4556	**	CONCN NEAR DET LIM	P2O5	3323.	NON
S	0.	0.	243.	0.	.0000	******	ELEMENT NOT DETECTED	SO3	0.	NON
CL	2133.	109.	213.	1304.	.6112			Cl	2133.	NON
K	12231.	107.	114.	16297.	1.3324			K2O	14734.	AL
CA	23230.	192.	334.	33166.	1.4277			CaO	32503.	AL
SC	0.	0.	210.	0.	.0000	******	ELEMENT NOT DETECTED	Sc2O3	0.	AL
TI	4341.	71.	123.	8375.	1.9291			TiO2	7240.	AL
V	99.	43.	98.	196.	1.9654	**	CONCN NEAR DET LIM	VO2	162.	AL
CR	39.	21.	47.	77.	1.9060	****	CONCN BELOW DET LIM	Cr2O3	58.	AL
MN	554.	35.	69.	936.	1.6914			MnO2	876.	AL
FE	33931.	215.	357.	50732.	1.4952			Fe2O3	48511.	AL
CO	16.	80.	186.	49.	3.1770	****	CONCN BELOW DET LIM	Co2O3	22.	AHC
NI	13.	9.	21.	68.	5.3430	****	CONCN BELOW DET LIM	NiO	16.	AHC
CU	11.	5.	9.	88.	7.7375	**	CONCN NEAR DET LIM	CuO	14.	AHC
ZN	54.	5.	8.	539.	10.1623			ZnO	67.	AHC
GA	16.	3.	6.	175.	11.4718			Ga2O3	2[illegible].	AHC
GE	0.	0.	5.	0.	.0000	******	ELEMENT NOT DETECTED	GeO2	0.	AHC
AS	6.	2.	5.	86.	12.1629	**	CONCN NEAR DET LIM	As2O5	10.	AHC
SE	6.	2.	5.	78.	11.2919	**	CONCN NEAR DET LIM	SeO3	10.	AHC
BR	0.	0.	5.	0.	.0000	******	ELEMENT NOT DETECTED	Br	0.	AHC
RB	58.	5.	9.	452.	7.8007			Rb2O	64.	AHC
SR	320.	11.	17.	2110.	6.5738			SrO	379.	AHC
Y	21.	5.	13.	109.	5.4996	**	CONCN NEAR DET LIM	Y2O3	26.	AHC
ZR	211.	14.	27.	945.	4.4814			ZrO2	286.	AHC
NB	11.	6.	14.	43.	3.6479	****	CONCN BELOW DET LIM	Nb2O3	14.	AHC
MO	5.	9.	24.	14.	2.9011	****	CONCN BELOW DET LIM	MoO3	7.	AHC
CD	0.	0.	55.	0.	.0000	******	ELEMENT NOT DETECTED	CdO	0.	AHC
IN	0.	0.	74.	0.	.0000	******	ELEMENT NOT DETECTED	In2O3	0.	AHC
SN	57.	44.	101.	21.	.3737	****	CONCN BELOW DET LIM	SnO2	72.	AHC
SB	0.	0.	128.	0.	.0000	******	ELEMENT NOT DETECTED	Sb2O3	0.	AHC
I	109.	101.	227.	17.	.1604	****	CONCN BELOW DET LIM	I	109.	AHC
BA	898.	256.	532.	60.	.0665	**	CONCN NEAR DET LIM	BaO	1002.	AHC
TAL	0.	0.	24.	0.	.0000	******	ELEMENT NOT DETECTED	Ta2O5	0.	AHC
WL	3.	9.	24.	13.	3.8025	****	CONCN BELOW DET LIM	WO3	4.	AHC
PBL	0.	0.	9.	0.	.0000	******	ELEMENT NOT DETECTED	PbO	0.	AHC
								OXIDE SUM =	949985.	

REPORT # 0794
RESULTS OF PIXE ANALYSIS ON: SUB PIT SAMPLES EE75

ELEMENT	CONCENTRATION	ERROR	DET LIMIT	PK AREA	XRY YIELD			OXIDE	CONCENTRATION	FILT
	----------------	PPM	----------------	-- CTS --	- CTS/PPM -				--- PPM ---	
NA	19177.	698.	1417.	3142.	.1638			Na2O	25850.	NON
MG	12421.	470.	1010.	4797.	.3863			MgO	20597.	NON
AL	73004.	504.	873.	47214.	.6467			Al2O3	137942.	NON
SI	285442.	625.	503.	236711.	.8293			SiO2	610646.	NON
P	1420.	431.	995.	710.	.4996	**	CONCN NEAR DET LIM	P2O5	3254.	NON
S	96.	97.	224.	58.	.6062	****	CONCN BELOW DET LIM	SO3	239.	NON
CL	845.	93.	201.	567.	.6708			Cl	845.	NON
K	11653.	101.	114.	17118.	1.4690			K2O	14037.	AL
CA	30953.	206.	355.	49508.	1.5995			CaO	43309.	AL
SC	0.	0.	226.	0.	.0000	******	ELEMENT NOT DETECTED	Sc2O3	0.	AL
TI	6659.	82.	139.	14482.	2.1747			TiO2	11108.	AL
V	80.	47.	109.	176.	2.2090	****	CONCN BELOW DET LIM	VO2	131.	AL
CR	10.	22.	50.	21.	2.1396	****	CONCN BELOW DET LIM	Cr2O3	14.	AL
MN	740.	39.	78.	1402.	1.8951			MnO2	1171.	AL
FE	55323.	259.	430.	92526.	1.6725			Fe2O3	79095.	AL
CO	24.	96.	222.	83.	3.5770	****	CONCN BELOW DET LIM	Co2O3	33.	AHC
NI	1.	12.	29.	8.	6.0144	****	CONCN BELOW DET LIM	NiO	2.	AHC
CU	14.	4.	8.	121.	8.7006	**	CONCN NEAR DET LIM	CuO	17.	AHC
ZN	76.	4.	8.	870.	11.4176			ZnO	95.	AHC
GA	14.	3.	6.	179.	12.8800			Ga2O3	19.	AHC
GE	1.	3.	6.	19.	13.6574	****	CONCN BELOW DET LIM	GeO2	2.	AHC
AS	7.	3.	4.	96.	13.6420	**	CONCN NEAR DET LIM	As2O5	11.	AHC
SE	3.	1.	4.	40.	12.6603	****	CONCN BELOW DET LIM	SeO3	4.	AHC
BR	0.	0.	6.	0.	.0000	******	ELEMENT NOT DETECTED	Br	0.	AHC
RB	43.	4.	8.	380.	8.7392			Rb2O	47.	AHC
SR	249.	8.	15.	1832.	7.3635			SrO	295.	AHC
Y	19.	6.	11.	122.	6.1594	**	CONCN NEAR DET LIM	Y2O3	25.	AHC
ZR	125.	11.	22.	626.	5.0184			ZrO2	168.	AHC
NB	6.	6.	14.	22.	4.0846	****	CONCN BELOW DET LIM	Nb2O3	7.	AHC
MO	0.	0.	19.	0.	.0000	******	ELEMENT NOT DETECTED	MoO3	0.	AHC
CD	35.	22.	50.	25.	.7279	****	CONCN BELOW DET LIM	CdO	40.	AHC
IN	36.	28.	61.	20.	.5564	****	CONCN BELOW DET LIM	In2O3	44.	AHC
SN	85.	37.	80.	35.	.4183	**	CONCN NEAR DET LIM	SnO2	107.	AHC
SB	0.	0.	94.	0.	.0000	******	ELEMENT NOT DETECTED	Sb2O3	0.	AHC
I	0.	0.	177.	0.	.0000	******	ELEMENT NOT DETECTED	I	0.	AHC
BA	765.	238.	502.	57.	.0745	**	CONCN NEAR DET LIM	BaO	854.	AHC
TAL	0.	0.	24.	0.	.0000	******	ELEMENT NOT DETECTED	Ta2O5	0.	AHC
WL	10.	11.	25.	39.	4.2743	****	CONCN BELOW DET LIM	WO3	12.	AHC
PBL	0.	0.	8.	0.	.0000	******	ELEMENT NOT DETECTED	PbO	0.	AHC
								OXIDE SUM =	950020.	

REPORT # 0788

RESULTS OF PIXE ANALYSIS ON: SUB PIT SAMPLES EE90

ELEMENT	CONCENTRATION	ERROR	DET LIMIT	PK AREA	XRY YIELD			OXIDE	CONCENTRATION	FILT
	----------------	PPM	----------------	-- CTS --	- CTS/PPM -				--- PPM ---	
NA	18938.	699.	1421.	3110.	.1642			Na2O	25529.	NON
MG	12933.	459.	981.	5008.	.3872			MgO	21446.	NON
AL	78335.	507.	857.	50733.	.6477			Al2O3	148013.	NON
SI	276940.	621.	508.	227517.	.8215			SiO2	592459.	NON
P	1829.	418.	960.	921.	.5037	**	CONCN NEAR DET LIM	P2O5	4191.	NON
S	309.	95.	213.	189.	.6112	**	CONCN NEAR DET LIM	SO3	772.	NON
CL	1407.	93.	191.	951.	.6760			Cl	1407.	NON
K	11720.	102.	116.	17186.	1.4664			K2O	14118.	AL
CA	32156.	210.	362.	51309.	1.5956			CaO	44993.	AL
SC	0.	0.	231.	0.	.0000	******	ELEMENT NOT DETECTED	Sc2O3	0.	AL
TI	7375.	85.	145.	15967.	2.1652			TiO2	12302.	AL
V	149.	50.	114.	329.	2.2000	**	CONCN NEAR DET LIM	VO2	242.	AL
CR	22.	22.	50.	48.	2.1295	****	CONCN BELOW DET LIM	Cr2O3	33.	AL
MN	845.	40.	79.	1594.	1.8865			MnO2	1337.	AL
FE	56792.	263.	436.	94582.	1.6654			Fe2O3	81196.	AL
CO	19.	99.	231.	71.	3.5639	****	CONCN BELOW DET LIM	Co2O3	27.	AHC
NI	8.	13.	29.	49.	5.9878	****	CONCN BELOW DET LIM	NiO	11.	AHC
CU	15.	4.	10.	127.	8.6647	**	CONCN NEAR DET LIM	CuO	19.	AHC
ZN	84.	4.	8.	942.	11.3733			ZnO	104.	AHC
GA	15.	3.	6.	190.	12.8325			Ga2O3	21.	AHC
GE	0.	0.	6.	0.	.0000	******	ELEMENT NOT DETECTED	GeO2	0.	AHC
AS	4.	3.	6.	55.	13.5958	****	CONCN BELOW DET LIM	As2O5	6.	AHC
SE	3.	1.	4.	38.	12.6188	****	CONCN BELOW DET LIM	SeO3	4.	AHC
BR	0.	0.	4.	0.	.0000	******	ELEMENT NOT DETECTED	Br	0.	AHC
RB	54.	4.	8.	467.	8.7125			Rb2O	59.	AHC
SR	271.	10.	15.	1994.	7.3413			SrO	321.	AHC
Y	21.	6.	11.	129.	6.1410	**	CONCN NEAR DET LIM	Y2O3	27.	AHC
ZR	156.	11.	24.	780.	5.0037			ZrO2	211.	AHC
NB	13.	6.	13.	51.	4.0727	**	CONCN NEAR DET LIM	Nb2O3	16.	AHC
MO	0.	0.	19.	0.	.0000	******	ELEMENT NOT DETECTED	MoO3	0.	AHC
CD	25.	25.	56.	18.	.7259	****	CONCN BELOW DET LIM	CdO	29.	AHC
IN	0.	0.	70.	0.	.0000	******	ELEMENT NOT DETECTED	In2O3	0.	AHC
SN	36.	40.	92.	15.	.4172	****	CONCN BELOW DET LIM	SnO2	46.	AHC
SB	0.	0.	120.	0.	.0000	******	ELEMENT NOT DETECTED	Sb2O3	0.	AHC
I	0.	0.	206.	0.	.0000	******	ELEMENT NOT DETECTED	I	0.	AHC
BA	955.	257.	539.	71.	.0743	**	CONCN NEAR DET LIM	BaO	1066.	AHC
TAL	0.	0.	24.	0.	.0000	******	ELEMENT NOT DETECTED	Ta2O5	0.	AHC
WL	4.	11.	25.	16.	4.2571	****	CONCN BELOW DET LIM	WO3	5.	AHC
PBL	7.	4.	8.	47.	6.8193	****	CONCN BELOW DET LIM	PbO	7.	AHC
								OXIDE SUM =	950016.	

REPORT # 0793
RESULTS OF PIXE ANALYSIS ON: SUB PIT SAMPLES EE90 REP

ELEMENT	CONCENTRATION	ERROR	DET LIMIT	PK AREA	XRY YIELD			OXIDE	CONCENTRATION	FILT
	----------------	PPM	----------------	-- CTS --	- CTS/PPM -				--- PPM ---	
NA	17902.	753.	1554.	2660.	.1486			Na2O	24132.	NON
MG	12724.	500.	1075.	4467.	.3510			MgO	21101.	NON
AL	76435.	531.	909.	44894.	.5873			Al2O3	144425.	NON
SI	276974.	650.	533.	207104.	.7477			SiO2	592531.	NON
P	2336.	443.	1018.	1068.	.4573			P2O5	5353.	NON
S	290.	103.	234.	161.	.5548	**	CONCN NEAR DET LIM	SO3	724.	NON
CL	2302.	109.	209.	1412.	.6136			Cl	2302.	NON
K	12394.	111.	125.	16353.	1.3195			K2O	14930.	AL
CA	33306.	226.	388.	47758.	1.4339			CaO	46601.	AL
SC	0.	0.	248.	0.	.0000	******	ELEMENT NOT DETECTED	Sc2O3	0.	AL
TI	7517.	90.	154.	14610.	1.9437			TiO2	12539.	AL
V	140.	53.	122.	276.	1.9755	**	CONCN NEAR DET LIM	VO2	228.	AL
CR	0.	0.	55.	0.	.0000	******	ELEMENT NOT DETECTED	Cr2O3	0.	AL
MN	817.	42.	86.	1385.	1.6950			MnO2	1292.	AL
FE	57380.	279.	463.	85871.	1.4965			Fe2O3	82036.	AL
CO	25.	106.	245.	78.	3.1855	****	CONCN BELOW DET LIM	Co2O3	35.	AMC
NI	5.	14.	33.	29.	5.3501	****	CONCN BELOW DET LIM	NiO	6.	AMC
CU	9.	5.	9.	71.	7.7432	**	CONCN NEAR DET LIM	CuO	12.	AMC
ZN	75.	5.	9.	753.	10.1649			ZnO	93.	AMC
GA	12.	3.	6.	141.	11.4702	**	CONCN NEAR DET LIM	Ga2O3	17.	AMC
GE	0.	0.	6.	0.	.0000	******	ELEMENT NOT DETECTED	GeO2	0.	AMC
AS	3.	3.	6.	31.	12.1542	****	CONCN BELOW DET LIM	As2O5	5.	AMC
SE	3.	3.	5.	44.	11.2814	****	CONCN BELOW DET LIM	SeO3	5.	AMC
BR	0.	0.	5.	0.	.0000	******	ELEMENT NOT DETECTED	Br	0.	AMC
RB	50.	5.	9.	388.	7.7900			Rb2O	55.	AMC
SR	260.	9.	17.	1707.	6.5642			SrO	308.	AMC
Y	25.	6.	12.	139.	5.4911	**	CONCN NEAR DET LIM	Y2O3	32.	AMC
ZR	168.	12.	25.	750.	4.4742			ZrO2	227.	AMC
NB	11.	6.	14.	37.	3.6418	****	CONCN BELOW DET LIM	Nb2O3	14.	AMC
MO	0.	0.	22.	0.	.0000	******	ELEMENT NOT DETECTED	MoO3	0.	AMC
CD	30.	26.	61.	19.	.6491	****	CONCN BELOW DET LIM	CdO	34.	AMC
IN	25.	33.	76.	13.	.4962	****	CONCN BELOW DET LIM	In2O3	30.	AMC
SN	53.	44.	97.	20.	.3730	****	CONCN BELOW DET LIM	SnO2	67.	AMC
SB	0.	0.	125.	0.	.0000	******	ELEMENT NOT DETECTED	Sb2O3	0.	AMC
I	0.	0.	212.	0.	.0000	******	ELEMENT NOT DETECTED	I	0.	AMC
BA	759.	265.	566.	50.	.0664	**	CONCN NEAR DET LIM	BaO	847.	AMC
TAL	0.	0.	25.	0.	.0000	******	ELEMENT NOT DETECTED	Ta2O5	0.	AMC
WL	0.	11.	26.	0.	3.8045	******	ELEMENT NOT DETECTED	WO3	0.	AMC
PBL	11.	5.	9.	63.	6.0962	**	CONCN NEAR DET LIM	PbO	12.	AMC

OXIDE SUM = 949992.

REPORT # 0805

RESULTS OF PIXE ANALYSIS ON: SUB PIT SAMPLES EE115

ELEMENT	CONCENTRATION	ERROR	DET LIMIT	PK AREA	XRY YIELD			OXIDE	CONCENTRATION	FILT
	PPM	PPM	PPM	CTS	CTS/PPM				PPM	
NA	21716.	688.	1376.	3869.	.1782			Na2O	29273.	NON
MG	14631.	451.	955.	6119.	.4183			MgO	24263.	NON
AL	81438.	492.	820.	56780.	.6972			Al2O3	153877.	NON
SI	271735.	594.	492.	239121.	.8800			SiO2	581322.	NON
P	1614.	393.	905.	882.	.5463	**	CONCN NEAR DET LIM	P2O5	3698.	NON
S	179.	88.	203.	119.	.6629	****	CONCN BELOW DET LIM	SO3	448.	NON
CL	1629.	92.	183.	1195.	.7333			Cl	1629.	NON
K	9956.	92.	110.	15864.	1.5934			K2O	11993.	AL
CA	32950.	203.	348.	57291.	1.7387			CaO	46103.	AL
SC	0.	0.	224.	0.	.0000	******	ELEMENT NOT DETECTED	Sc2O3	0.	AL
TI	7056.	81.	138.	16612.	2.3545			TiO2	11769.	AL
V	128.	47.	109.	305.	2.3917	**	CONCN NEAR DET LIM	VO2	208.	AL
CR	32.	21.	49.	74.	2.3150	****	CONCN BELOW DET LIM	Cr2O3	46.	AL
MN	838.	39.	77.	1717.	2.0506			MnO2	1326.	AL
FE	57473.	254.	421.	104017.	1.8099			Fe2O3	82169.	AL
CO	29.	88.	206.	113.	3.9400	****	CONCN BELOW DET LIM	Co2O3	41.	AMC
NI	6.	11.	27.	41.	6.6159	****	CONCN BELOW DET LIM	NiO	8.	AMC
CU	13.	4.	9.	126.	9.5737	**	CONCN NEAR DET LIM	CuO	16.	AMC
ZN	72.	4.	8.	900.	12.5665			ZnO	90.	AMC
GA	14.	3.	5.	199.	14.1789			Ga2O3	19.	AMC
GE	0.	3.	5.	6.	15.0373	******	ELEMENT NOT DETECTED	GeO2	0.	AMC
AS	1.	3.	5.	13.	15.0223	****	CONCN BELOW DET LIM	As2O5	2.	AMC
SE	4.	1.	4.	55.	13.9428	**	CONCN NEAR DET LIM	SeO3	6.	AMC
BR	0.	0.	4.	0.	.0000	******	ELEMENT NOT DETECTED	Br	0.	AMC
RB	40.	4.	8.	385.	9.6268			Rb2O	44.	AMC
SR	278.	9.	15.	2260.	8.1116			SrO	329.	AMC
Y	19.	5.	10.	128.	6.7855	**	CONCN NEAR DET LIM	Y2O3	24.	AMC
ZR	121.	10.	20.	672.	5.5288			ZrO2	164.	AMC
NB	9.	5.	11.	41.	4.5001	****	CONCN BELOW DET LIM	Nb2O3	11.	AMC
MO	0.	0.	16.	0.	.0000	******	ELEMENT NOT DETECTED	MoO3	0.	AMC
CD	0.	0.	44.	0.	.0000	******	ELEMENT NOT DETECTED	CdO	0.	AMC
IN	0.	0.	56.	0.	.0000	******	ELEMENT NOT DETECTED	In2O3	0.	AMC
SN	62.	37.	80.	28.	.4609	****	CONCN BELOW DET LIM	SnO2	79.	AMC
SB	0.	0.	97.	0.	.0000	******	ELEMENT NOT DETECTED	Sb2O3	0.	AMC
I	0.	0.	173.	0.	.0000	******	ELEMENT NOT DETECTED	I	0.	AMC
BA	939.	214.	430.	77.	.0821			BaO	1048.	AMC
TAL	0.	0.	21.	0.	.0000	******	ELEMENT NOT DETECTED	Ta2O5	0.	AMC
WL	0.	0.	23.	0.	.0000	******	ELEMENT NOT DETECTED	WO3	0.	AMC
PBL	9.	4.	8.	65.	7.5348	**	CONCN NEAR DET LIM	PbO	10.	AMC
								OXIDE SUM =	950014.	

REPORT # 0806
RESULTS OF PIXE ANALYSIS ON: SUB PIT SAMPLES EE115 REP

ELEMENT	CONCENTRATION	ERROR	DET LIMIT	PK AREA	XRY YIELD			OXIDE	CONCENTRATION	FILT
	----------------	PPM ----------------		-- CTS --	- CTS/PPM -				--- PPM ---	
NA	21270.	668.	1339.	3964.	.1864			Na2O	28672.	HON
MG	14688.	440.	930.	6430.	.4376			MgO	24357.	HON
AL	81583.	478.	797.	59518.	.7295			Al2O3	154152.	HON
SI	268532.	578.	479.	247386.	.9213			SiO2	574470.	HON
P	1488.	379.	873.	857.	.5757	**	CONCN NEAR DET LIM	P2O5	3410.	HON
S	140.	85.	194.	98.	.6986	****	CONCN BELOW DET LIM	SO3	346.	HON
CL	1618.	88.	177.	1251.	.7727			Cl	1618.	HON
K	10212.	91.	109.	17113.	1.6757			K2O	12302.	AL
CA	33957.	200.	343.	62062.	1.8277			CaO	47512.	AL
SC	0.	0.	223.	0.	.0000	******	ELEMENT NOT DETECTED	Sc2O3	0.	AL
TI	7281.	80.	136.	17994.	2.4715			TiO2	12144.	AL
V	179.	47.	107.	450.	2.5111	**	CONCN NEAR DET LIM	VO2	291.	AL
CR	31.	21.	50.	75.	2.4308	****	CONCN BELOW DET LIM	Cr2O3	45.	AL
MN	852.	38.	76.	1834.	2.1536			MnO2	1348.	AL
FE	61158.	255.	423.	116265.	1.9011			Fe2O3	87437.	AL
CO	44.	87.	202.	183.	4.1805	****	CONCN BELOW DET LIM	Co2O3	62.	AMC
NI	8.	10.	21.	56.	7.0044	****	CONCN BELOW DET LIM	NiO	11.	AMC
CU	18.	4.	8.	182.	10.1404			CuO	22.	AMC
ZN	72.	4.	7.	960.	13.3152			ZnO	89.	AMC
GA	17.	2.	5.	255.	15.0280			Ga2O3	22.	AMC
GE	1.	2.	5.	19.	15.9416	****	CONCN BELOW DET LIM	GeO2	2.	AMC
AS	4.	2.	5.	54.	15.9288	****	CONCN BELOW DET LIM	As2O5	5.	AMC
SE	4.	1.	4.	50.	14.7864	**	CONCN NEAR DET LIM	SeO3	6.	AMC
BR	2.	2.	4.	35.	13.6903	****	CONCN BELOW DET LIM	Br	2.	AMC
RB	37.	4.	7.	373.	10.2126			Rb2O	40.	AMC
SR	284.	8.	14.	2440.	8.6059			SrO	336.	AMC
Y	20.	5.	10.	142.	7.1994			Y2O3	26.	AMC
ZR	131.	10.	20.	769.	5.8663			ZrO2	177.	AMC
NB	6.	5.	11.	29.	4.7751	****	CONCN BELOW DET LIM	Nb2O3	8.	AMC
MO	0.	0.	17.	0.	.0000	******	ELEMENT NOT DETECTED	MoO3	0.	AMC
CD	0.	0.	41.	0.	.0000	******	ELEMENT NOT DETECTED	CdO	0.	AMC
IN	23.	24.	52.	15.	.6508	****	CONCN BELOW DET LIM	In2O3	27.	AMC
SN	63.	33.	72.	31.	.4892	****	CONCN BELOW DET LIM	SnO2	80.	AMC
SB	105.	43.	93.	39.	.3692	**	CONCN NEAR DET LIM	Sb2O3	126.	AMC
I	0.	0.	161.	0.	.0000	******	ELEMENT NOT DETECTED	I	0.	AMC
BA	756.	208.	433.	66.	.0871	**	CONCN NEAR DET LIM	BaO	844.	AMC
TAL	0.	0.	20.	0.	.0000	******	ELEMENT NOT DETECTED	Ta2O5	0.	AMC
WL	2.	10.	21.	14.	4.9829	****	CONCN BELOW DET LIM	WO3	3.	AMC
PBL	6.	4.	7.	44.	7.9893	****	CONCN BELOW DET LIM	PbO	6.	AMC
								OXIDE SUM =	950004.	

REPORT # 0783

RESULTS OF PIXE ANALYSIS ON: SUB PIT SAMPLES EE180

ELEMENT	CONCENTRATION	ERROR	DET LIMIT	PK AREA	XRY YIELD			OXIDE	CONCENTRATION	FILT
	----------------	PPM	----------------	-- CTS --	- CTS/PPM -				--- PPM ---	
NA	15467.	829.	1726.	1741.	.1126			Na2O	20850.	NON
MG	11575.	561.	1215.	3091.	.2670			MgO	19195.	NON
AL	74266.	603.	1031.	33263.	.4479			Al2O3	140326.	NON
SI	276267.	741.	603.	158245.	.5728			SiO2	591019.	NON
P	2322.	503.	1156.	813.	.3500			P2O5	5320.	NON
S	582.	121.	266.	247.	.4247			SO3	1454.	NON
CL	2928.	130.	240.	1375.	.4694			Cl	2928.	NON
K	13135.	121.	136.	15695.	1.1950			K2O	15822.	AL
CA	36105.	247.	425.	46820.	1.2967			CaO	50518.	AL
SC	0.	0.	273.	0.	.0000	******	ELEMENT NOT DETECTED	Sc2O3	0.	AL
TI	7978.	98.	168.	13976.	1.7519			TiO2	13307.	AL
V	0.	0.	130.	0.	.0000	******	ELEMENT NOT DETECTED	VO2	0.	AL
CR	0.	0.	59.	0.	.0000	******	ELEMENT NOT DETECTED	Cr2O3	0.	AL
MN	864.	47.	93.	1321.	1.5294			MnO2	1367.	AL
FE	60139.	301.	499.	81247.	1.3509			Fe2O3	85981.	AL
CO	35.	111.	257.	97.	2.8006	****	CONCN BELOW DET LIM	Co2O3	49.	AMC
NI	5.	12.	28.	24.	4.6971	****	CONCN BELOW DET LIM	NiO	7.	AMC
CU	9.	5.	10.	64.	6.8016	****	CONCN BELOW DET LIM	CuO	11.	AMC
ZN	76.	5.	10.	683.	8.9327			ZnO	95.	AMC
GA	16.	3.	7.	158.	10.0834			Ga2O3	21.	AMC
GE	0.	3.	7.	7.	10.6976	******	ELEMENT NOT DETECTED	GeO2	0.	AMC
AS	5.	2.	5.	63.	10.6901	**	CONCN NEAR DET LIM	As2O5	8.	AMC
SE	9.	2.	5.	91.	9.9243	**	CONCN NEAR DET LIM	SeO3	14.	AMC
BR	2.	2.	5.	12.	9.1892	****	CONCN BELOW DET LIM	Br	2.	AMC
RB	55.	5.	10.	380.	6.8556			Rb2O	60.	AMC
SR	299.	10.	19.	1728.	5.7773			SrO	353.	AMC
Y	26.	7.	14.	122.	4.8332	**	CONCN NEAR DET LIM	Y2O3	33.	AMC
ZR	147.	14.	28.	582.	3.9384			ZrO2	198.	AMC
NB	5.	7.	16.	19.	3.2058	****	CONCN BELOW DET LIM	Nb2O3	7.	AMC
MO	0.	0.	24.	0.	.0000	******	ELEMENT NOT DETECTED	MoO3	0.	AMC
CD	0.	0.	59.	0.	.0000	******	ELEMENT NOT DETECTED	CdO	0.	AMC
IN	36.	36.	79.	16.	.4369	****	CONCN BELOW DET LIM	In2O3	44.	AMC
SN	50.	47.	104.	17.	.3284	****	CONCN BELOW DET LIM	SnO2	64.	AMC
SB	0.	0.	133.	0.	.0000	******	ELEMENT NOT DETECTED	Sb2O3	0.	AMC
I	0.	0.	235.	0.	.0000	******	ELEMENT NOT DETECTED	I	0.	AMC
BA	838.	271.	568.	49.	.0585	**	CONCN NEAR DET LIM	BaO	935.	AMC
TAL	0.	0.	28.	0.	.0000	******	ELEMENT NOT DETECTED	Ta2O5	0.	AMC
WL	0.	0.	29.	0.	.0000	******	ELEMENT NOT DETECTED	WO3	0.	AMC
PBL	0.	0.	10.	0.	.0000	******	ELEMENT NOT DETECTED	PbO	0.	AMC

OXIDE SUM = 949988.

APPENDIX B
Part 6

AS-BUILT DIAGRAMS AND WELL COMPLETION REPORTS FOR WELLS 299-E34-7 AND 299-E35-1

Battelle
Pacific Northwest Laboratories

AS-BUILT DIAGRAM

Well Number 299-E34-7

Geologist S. Brandenberger, T. Gilmore, M. Chamness, B. Biornstad, L. Kennedy, R. Miller, E. Jensen

Page 1 of 2

Well Started: 08/03/89

Reviewed by V. L. McGhan 10-10-89 Date Well Completed: 10/17/89

Construction Data

Description

- Cement Pad (+0.5 - 2.0')
- 12" dia. carbon steel casing (0' - 19.75') - removed
- Cement Grout (2.0' - 20.2')
- Casing Centralizer
- Casing Joint
- 8" dia. carbon steel casing (0' - 205.5') - removed
- 4" dia. stainless steel final casing (+1.5' - 193.9')
- 8 - 20 mesh bentonite crumbles (20.2' - 186.3')

DB = Drive Barrel
HT = Hard Tool

Diagram

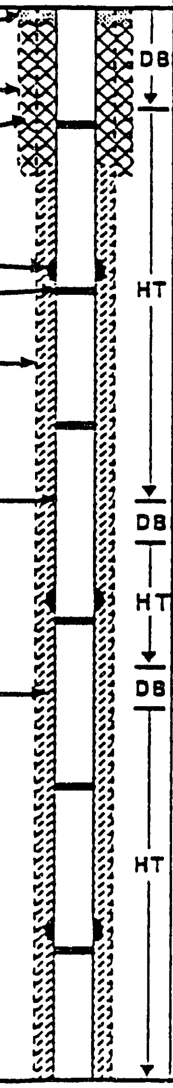

Geologic/Hydrologic Data

Sample Type: o Drive Barrel; ● Hard Tool; ▲ Split Spoon

Depth in Feet	Sample Type	Lithologic Description
5	o	Gravelly Sand
10	o	Sandy Gravel
15	●	" "
20	●	Muddy Sandy Gravel
25	●	" " "
30	●	" " "
35	●	" " "
40	●	Sandy Gravel
45	●	" "
50	●	" "
55	●	" "
60	●	Muddy Sandy Gravel
65	o	" " "
70	●	Sandy Gravel
75	●	" "
80	●	" "
85	o	" "
90	●	" "
95	●	" "
100	●	Muddy Sandy Gravel
105	●	Sandy Gravel
110	●	Muddy Sandy Gravel
115	●	Sandy Gravel
120	●	" "
125	●	Muddy Sandy Gravel
130	●	Sandy Gravel

A-1800-186 (3/87)

Battelle
Pacific Northwest Laboratories

AS-BUILT DIAGRAM

Well Number 299-E34-7
Geologist S. Brandenberger, T. Gilmore, M. Chamness, B. Bjornstad, L. Kennedy, R. Miller, E. Jensen
Page 2 of 2

Reviewed by V. L. McGhan 10-10-89 Date Well Started: 08/03/89 Well Completed: 10/17/89

Construction Data

Description

8" dia. carbon steel casing (0' - 205.5') - removed

4" dia. stainless steel final casing (+1.5' - 193.9')

8 - 20 mesh bentonite crumbles (20.2' - 186.3')

DB = Drive Barrel
HT = Hard Tool

3/8" Volclay pellets (186.3' - 189.3')

20 - 40 mesh Colorado silica sand (189.3' - 204.05')

Static Water Table (195.2') - 8/22/89 -

4" dia. stainless steel Johnson continuous wrap, 10 slot screen (193.9' - 204.55')

Bottom of well = 204.55'
Backfill (204.05' - 205.5')

Diagram

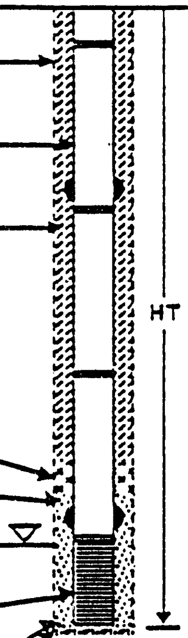

Well Completion Symbols (as per PNL-6392)

- Cement Grout
- Granular Bentonite
- Bentonite Pellets
- Sand Pack
- Backfill

Geologic/Hydrologic Data

Sample Type: O Drive Barrel; ● Hard Tool; ▲ Split Spoon

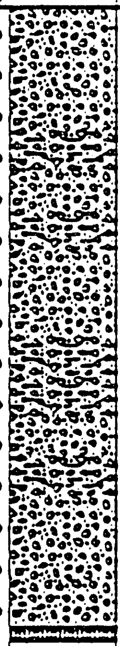

Depth in Feet	Sample Type	Lithologic Description
135	●	Sandy Gravel
140	●	" "
145	●	" "
150	●	Muddy Sandy Gravel
155	●	Sandy Gravel
160	●	Muddy Sandy Gravel
165	●	Sandy Gravel
170	●	" "
175	●	Muddy Sandy Gravel
180	●	" " "
185	●	Sandy Gravel
190	●	Muddy Sandy Gravel
195	●	Sandy Gravel
200	●	" "
205	●	" "
		Basalt

A-1800-188 (3/87)

WELL COMPLETION/INSPECTION REPORT (governing procedure DO-1, RO)

Specification No. WHC-S-014 Rev. No. 3
Project W-017 Low Level Burial Ground
Location 200 East Area
Drilling Co. [illegible] Drilling
Driller [illegible] / Robert [illegible]
Other (companies) NONE
Geologist(s) S. Brandenburger T. Gilmore M. Chamness S. Bjornstad, E. Kennedy, R. Miller E. Jensen

Well No. 299 E34 7 Temp. Well No. E-34-MW0
Coordinates
Casing Elev. Ground Elev.

DRILLING METHOD
Rotary Air N/A Mud N/A
Cable Tool D 0-15' 50-55 20-65 H 15'-60 65-80 85-205'
Drilling Fluid 200 EAST RAW H2O SUPPLY
Other NONE

GEOPHYSICAL LOGGING

Sondes	Interval	Date
Gross gamma	0 - 203	8/22/89

COMPLETION DATA
Drilled Depth 205.5'
Completed Depth 204.55'
Date Started 8/3/89
Date Completed 10/17/89
Static Water Level/Date 195.8' 8/22/89

AQUIFER TESTING
Type Slug withdrawal
Length of Test
Volume Pumped
Drawdown
Date of Test 10/5/89

INSPECTION RESULTS

CLEANING
Inspection Method Visual
Acceptance Criteria As per section 7.6

	Accept	Reject	Date
Drilling Tools/Rig	[initials]		8/3/89
Temporary Materials	[initials]		8/22/89
Permanent Materials	[initials]		8/25/89

MATERIAL STORAGE/PACKING
Inspection Method Visual
Acceptance Criteria As per section 7.3

	Accept	Reject	Date
Mtl. Handling/Storage	[initials]		8/25/89
Material Packing	[initials]		8/25/89

SCREEN

Type	Length	Slot Size
Johnson Div Type 304 Continuous slot stainless steel (4")	10.65	10
—	—	—

Depth(s) 204.55 - 193.9'

Inspection Method Visual
Acceptance Criteria As per section 4.2.3
Accept [initials] Reject Date 8/22/89

LUBRICANTS/ADDITIVES
Inspection Method Visual
Acceptance Criteria As per section 7.2

	Identity	Accept	Reject	Date
Additives	N/A	N/A	N/A	N/A
Lubricants	Chevron Poly FM	[initials]		8/10/89

STRAIGHTNESS TEST
Inspection Method 23' long 7" diameter bailer
Acceptance Criteria As per section 8.3
Accept [initials] Reject Date 8/22/89

CASING (permanent)

Type	Size	Placement
Johnson Div. type 304 stainless steel	4"	193.9' - +1.5'
—	—	—

Inspection Method Visual
Acceptance Criteria As per section 4.2.4
Accept [initials] Reject Date 8/22/89

WELL PROTECTION
Inspection Method Visual
Acceptance Criteria As per section 4.2.9-4.2.10

	Accept	Reject	Date
Protective Posts	MAC		11/1/89
Locks	BNB		[illegible]

ANNULAR SEAL
Inspection Method Measured w/steel tape
Acceptance Criteria As per section 4.2.6-4.2.9

Type	Interval	Volume	Accept	Reject	Date
20-40 Colorado Silica Sand	204.05' - 189.3'	1.68 ft3	[initials]		8/22/89
3/8" Volclay pellets	189.3 - 186.3	1.24 ft3	[initials]		8/23/89
8-20 Bentonite granules	186.3 - 20.2'	31.77 ft3	MAC		8/24/89
Cement grout	20.2 - 2'	17.16 ft3	MAC		8/25/89
[illegible]	2 - +3	3	[illegible]		10/[illegible]

OTHER (initial if performed)
N/A Well Abandonment [initials] Downhole TV Inspection _____ Complete As-Built Diagram, Driller's/Geologist's Logs
[initials] Well Development

Reviewed by V L McKim 10-10-89

For all blanks mark N/A if not applicable.

Battelle
Pacific Northwest Laboratories

AS-BUILT DIAGRAM

Well Number 299-E35-1

Geologist S. Brandenberger, T. Gilmore, E. Jensen, B. Bjornstad, M. Chamness, L. Kennedy, R. Biegan, R. Miller

Page 1 of 2

Well Started: 08/07/89

Reviewed by V. L. McGhan 10-10-89 Date Well Completed: 12/14/89

Construction Data

Description

Cement Pad (0.5' - 2.0')

12" dia. carbon steel casing (0' - 20.0') - removed

Cement Grout (2.0' - 20.0')

8" dia. carbon steel casing (0' - 191.55') - removed

4" dia. stainless steel final casing (+2.03' - 181.45')

Casing Centralizer

Casing Joint

8-20 mesh bentonite crumbles (20.0' - 173.4')

DB = Drive Barrel
HT = Hard Tool
SS = Split Spoon

Diagram

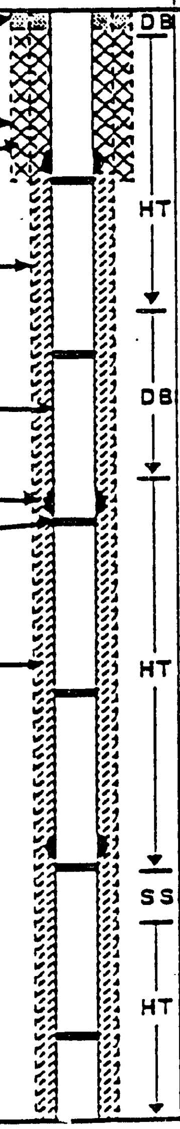

Geologic/Hydrologic Data

Sample Type: ○ Drive Barrel; ● Hard Tool; ▲ Split Spoon

Depth in Feet	Sample Type	Lithologic Description
5	●	Sandy Gravel
10	●	• •
15	●	Muddy Sandy Gravel
20	●	• • •
25	●	Sandy Gravel
30	●	• •
35	●	Slightly Muddy Gravelly Sand
40	○	Sandy Gravel
45	○	Gravelly Sand
50	○	Muddy Sandy Gravel
55	○	• • •
60	●	Sandy Gravel
65	●	Slightly Muddy Gravelly Sand
70	●	Sandy Gravel
75	●	Slightly Muddy Gravelly Sand
80	●	Sandy Gravel
85	●	• •
90	●	Gravelly Sand
95	●	• •
100	●	Sandy Gravel
105	▲	Muddy Sandy Gravel
110	●	• • •
115	●	• • •
120	●	• • •
125	●	Boulder @~125'-126' (No Sample)
130	●	Muddy Sandy Gravel

A-1800-186 (3/87)

Battelle
Pacific Northwest Laboratories

AS-BUILT DIAGRAM

Well Number 299-E35-1

Geologist S. Brandenberger, T. Gilmore, E. Jensen, B. Bjornstad, M. Chamness, L Kennedy, R. Biegan, R. Miller

Page 2 of 2

Reviewed by V. L. McGhan 10-10-89 Date

Well Started: 08/07/89
Well Completed: 12/14/89

Construction Data

Description

8" dia. carbon steel casing (0' - 191.55') - removed

4" dia. stainless steel final casing (+2.03' - 181.45')

8 - 20 mesh bentonite crumbles (20.0' - 173.4')

HT = Hard Tool

3/8" Volclay pellets (173.4 - 178.4')

20 - 40 mesh Colorado silica sand (178.4 - 191.8')

Static Water Table (189.02') - 08/31/89 -

4" dia. stainless steel Johnson continuous wrap, 20 slot screen (181.45 - 192.1')

Bottom of well = 192.1'
Backfill (192.1' - 193.8')

Well Completion Symbols (as per PNL-6392)

- Cement Grout
- Granular Bentonite
- Bentonite Pellets
- Sand Pack
- Backfill

Diagram

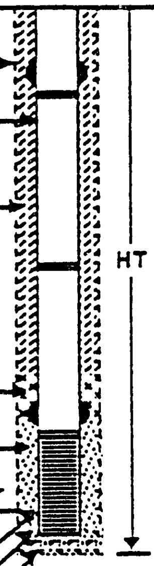

Geologic/Hydrologic Data

Sample Type: ○ Drive Barrel ● Hard Tool ▲ Split Spoon

Depth in Feet	Sample Type	Lithologic Description
135	●	Muddy Sandy Gravel
140	●	" " "
145	●	" " "
150	●	Sandy Gravel
155	●	" "
160	●	Muddy Sandy Gravel
165	●	" " "
170	●	" " "
175	●	" " "
180	●	" " "
185	●	" " "
190	●	" " "
195	●	" " "

A-1800-186 (3/87)

WELL COMPLETION/INSPECTION REPORT (governing procedure DO-1, RO)

cification No. WHC-S-014	Rev. No. 3	Well No. 299-E35-1	Temp. Well No. E12-MW10
ject		Coordinates	
ation 200 East Area		Casing Elev.	Ground Elev.
lling Co.			
iler Robert Perry			
er (companies)			
logist(s) S. Brannenberger, T. Gilmore, E. Jensen, B. Eisenlohr, M. Chamness, ... Kennedy, R. Bleeker, R. Miller			

DRILLING METHOD

Rotary Air N/A Mud N/A

Cable Tool 0-35'-55 ... 35'-55-101,107-194'

Drilling Fluid 200 East ...

Other Split spoon (101-107')

GEOPHYSICAL LOGGING

ondes	Interval	Date
...ss gamma	0'-193'	8/29/89

COMPLETION DATA

Drilled Depth 193.8' 8-25-89

Completed Depth 192.1'

Date Started 8/7/89

Date Completed 12/14/89

Static Water Level/Date 189.02 / 8/31/89

AQUIFER TESTING

Type N/A

Length of Test

Volume Pumped

Drawdown

Date of Test

INSPECTION RESULTS

CLEANING

spection Method Visual

ceptance Criteria As per section 7.6

	Accept	Reject	Date
illing Tools/Rig	[illegible]		8/4/89
mporary Materials	[illegible]		8/7/89
rmanent Materials	BNB		8/31/89

MATERIAL STORAGE/PACKING

Inspection Method Visual

Acceptance Criteria As per section 7.3

	Accept	Reject	Date
Mtl. Handling/Storage	BNB		8/31/89
Material Packing	BNB		8/31/89

SCREEN

Type	Length	Slot Size
Johnson Div. type 304 Continuous wrap stainless steel	10.65'	20

epth(s) 192.10 - 181.45

spection Method Visual

ceptance Criteria As per section 4.2.3

Accept BNB Reject Date 8/29/89

LUBRICANTS/ADDITIVES

Inspection Method Visual

Acceptance Criteria As per section 7.2

	Identity	Accept	Reject	Date
Additives	None	BNB		8/31/89
Lubricants	[illegible] oil	BNB		8/31/89

STRAIGHTNESS TEST

Inspection Method 20' long 3" diameter bailer

Acceptance Criteria As per section 8.3

Accept BNB Reject Date 8/29/89

CASING (permanent)

Type	Size	Placement
Johnson Div. type 304 stainless steel	4"	+2.03'-181.45'

spection Method Visual

ceptance Criteria As per section 4.2.4

Accept BNB Reject Date 8/29/89

WELL PROTECTION

Inspection Method Visual

Acceptance Criteria As per section 4.2.5-4.2.10

	Accept	Reject	Date
Protective Posts	MAC		11/1/89
Locks	BNB		[illegible]

ANNULAR SEAL

Inspection Method Measured with steel tape

Acceptance Criteria As per section 4.2.6-4.2.9

Type	Interval	Volume	Accept	Reject	Date
20-40 Colorado Silica sand	191.5' - 173.4	5.04 ft³	BNB		8/30/89
1/4" Volclay pellets	173.4 - 173.4	1.24 ft³	BNB		8/31/89
8-20 bentonite crumbles	173.4 - 20.0	32.1 ft³	BNB		8/31/89
Cement grout	20 - 2	13.2 ft³	BNB		8/31/89
Cement ...	2.0 - 0.5				[illegible]

OTHER (initial if performed)

N/A Well Abandonment

[illegible] Downhole TV Inspection

____ Complete As-Built Diagram, Driller's/Geologist's Logs

JK Well Development

For all blanks mark N/A if not applicable.

Reviewed by [signature] 10-10-89

APPENDIX B
Part 7

BATCH ADSORPTION DATA FOR 7- TO 10-DAY AND 26-DAY EXPERIMENTS

Table B.7.1. Data from 7- to 10-day Batch Adsorption Experiments

	A	B	C	D	E	F	G	H	I	J	K	L	M
1	Sample Id	Wt. Sed	Solution Left	Solution Weight	Init. conc Pb	Init conc. Pb	7D Pb conc. C	10day conc. Pb	uCi/Gm Soil	Kd C Pb 7D	Kd Rad 10 Day	Kd Rad soil	
2		grams	after wash	grams	cold ppb	uCi/ml	ppb	uCi/ml	Pb		Pb (Init)	10 day	
3	E1A-7	1.004	0.597	39.693		2.09E-02		2.14E-05	6.25E-01		3.86E04	2.92E04	
4	E1B-7	1.101	0.642	38.847		2.09E-02		2.30E-05	5.71E-01		3.21E04	2.48E04	
5	E2A-7	1.003	1.062	36.696		1.68E-02		2.04E-05	4.55E-01		2.16E04	1.60E04	
6	E2B-7	1.012	0.988	38.302		1.68E-02		1.39E-05	4.51E-01		4.60E04	3.25E04	
7	E3A-7	1.035	0.65	39.98		7.51E-03		2.62E-06	2.06E-01		1.11E05	7.87E04	
8	E3B-7	0.999	0.583	38.232		7.51E-03		3.69E-06	1.88E-01		7.79E04	5.10E04	
9	E4A-7	1.005	1.045	38.553		2.50E-03		1.86E-06	5.97E-02		4.87E04	3.04E04	
10	E4B-7	0.999	0.944	38.303		2.50E-03		1.53E-06	6.33E-02		6.26E04	4.14E04	
11	E5A-7	1	0.718	28.995	1.51E02		5.30E-01			8.23E03			
12	E5B-7	0.997	0.65	28.217	1.45E02		3.00E-01			1.37E04			
13	E6A-7	1.01	0.615	38.183	3.03E01		2.80E-01			4.05E03			
14	E6B-7	0.996	1.264	37.577	2.80E01		2.60E-01			4.14E03			
15	E13A-7	1.006	0.534	39.155		2.34E-02		3.18E-05	8.12E-01		2.86E04	1.92E04	
16	E13B-7	1.041	0.514	38.345		2.34E-02		3.29E-05	5.92E-01		2.62E04	1.80E04	
17	E13C-7	1.041	0.458	39.577		2.34E-02		4.73E-05	5.91E-01		1.86E04	1.25E04	
18	E14A-7	1.049	0.488	40.642		2.12E-02		2.58E-05	5.79E-01		3.18E04	2.24E04	
19	E14B-7	1.003	0.599	40.36		2.12E-02		1.93E-05	5.88E-01		4.40E04	3.04E04	
20	E14C-7	0.999	0.662	39.864		2.12E-02		3.03E-05	6.07E-01		2.79E04	2.01E04	
21	E15A-7	1.002	0.434	40.108		1.50E-02		1.16E-05	4.77E-01		5.43E04	4.10E04	
22	E15B-7	0.995	0.892	39.871		1.58E-02		1.25E-05	4.57E-01		5.05E04	3.65E04	
23	E15C-7	1.005	0.905	39.909		1.58E-02		1.59E-05	4.55E-01		3.94E04	2.87E04	
24	E16A-7	1.011	0.628	39.252		1.36E-02		9.34E-06	4.47E-01		5.64E04	4.79E04	
25	E16B-7	1.015	0.57	39.478		1.36E-02		5.99E-06	4.24E-01		8.81E04	7.08E04	
26	E16C-7	1.009	0.547	39.276		1.36E-02		1.61E-05	4.54E-01		3.27E04	2.81E04	
27	E21A-7	1.005	0.81	37.799	1.50E02	2.30E03	6.60E-01			8.51E03			
28	E21B-7	0.994	0.595	38.227	1.55E02	2.52E03	1.17E00			5.06E03			
29	E22A-7	0.997	1.016	37.873	6.02E01	2.57E03	3.70E-01			6.16E03			
30	E22B-7	1.017	0.907	38.243	6.09E01	2.50E03	2.80E-01			8.14E03			
31	E23A-7	1.018	0.407	39.305	1.85E01	2.33E03	1.50E-01			4.72E03			
32	E23B-7	0.978	0.551	39.346	2.06E01	2.55E03	1.60E-01			5.14E03			
33	E24A-7	1	0.435	38.399	8.58E00	2.54E03	2.40E-01			1.33E03			
34	E24B-7	0.993	0.49	36.732	8.75E00	2.53E03	1.90E-01			1.67E03			
35													
36													
37													
38													
39													
40													

Column definitions for Table B.7.1

A - Sample identification.

B - Initial weight of sediment in grams.

C - Weight of solution left in contact with sediment after equilibration steps.

D - Weight of added solution.

E - Initial solution concentration of lead in non-radioactive experiments (μg/L or ppb).

F - Initial solution concentration of ^{210}Pb in tracer experiments (μCi/mL).

G - Seven-day equilibrium solution concentration of lead in non-radioactive experiments (μg/L or ppb).

H - Ten-day equilibrium solution concentration of ^{210}Pb in tracer experiments (μCi/mL).

I - Ten-day equilibrium soil concentration of ^{210}Pb in tracer experiments (μCi/g).

J - Lead R_d values determined for non-radioactive experiments using equation (A.3.4), (mL/g).

K - Lead R_d values determined for tracer experiments using equation (A.3.4), (mL/g).

L - Lead R_d values determined for tracer experiments using equation (A.3.3), (mL/g).

DISTRIBUTION

No. of
Copies

OFFSITE

2 DOE/Office of Scientific
and Technical Information

U.S. Department of Energy -
Headquarters
R. Martinez
EM-322, HQ

EPA Region 10
Hazardous Waste Division
U.S. Environmental Protection
Agency; 1200 Sixth Avenue
Mail Stop HW-111
Seattle, WA 98101

Randall Smith, Acting Director

Golder Associates, Incorporated
S. Eipert, Librarian
4104 148th Avenue N.E.
Redmond, WA 98052

2 U.S. Navy
J. Steele
Naval Sea Systems Command,
Code 08R; James K. Polk Bldg.,
Room 3W 62; 2521 Jefferson Davis
Highway, Bldg. NC2
Arlington, VA 22202

5 Puget Sound Naval Shipyard
R. J. Benze, Code 2300
M. French, NRRO
G. D. Kirk, Code 2300
B. S. Koch, Code 100E
M. G. Wentink, Code 2300.1
Puget Sound Naval Shipyard
Bremerton, WA 98314

No. of
Copies

4 R. Dayal
Ontario Hydro
800 Kipling Ave.
Toronto, Ontario M8Z 5S4
CANADA

M. Fuhrmann
Brookhaven National Lab
Upton, NY 11973

Mr. Elmer Wilhite
Westinghouse Savannah River Co.
Savannah River Site
Aiken, SC 29808-0001

Mr. Frank E. Goodwin
International Lead Zinc
Research Organization, Inc.
2525 Meridian Parkway
P.O. Box 12036
Research Triangle Park,
NC 27709-2036

DISTRIBUTION

No. of Copies		
ONSITE		
8	U.S. Department of Energy Richland Field Office	
	J. M. Hennig	A5-22
	R. M. Carosino	A4-52
	C. E. Clark	A5-19
	R. M. Gordon (3)	A6-55
	R. D. Izatt	A5-19
	R. F. Guercia	A5-21
31	Westinghouse Hanford Company	
	B. J. Broomfield	N3-13
	C. K. Disibio	B3-03
	G. C. Evans (5)	H4-57
	K. R. Fecht	H4-56
	C. J. Geier	B2-19
	R. J. Giroir	R2-97
	W. H. Hamilton	N3-13
	D. G. Hay	T3-21
	K. M. Hoffman	H5-29
	D. G. Horton	H4-56
	G. W. Jackson	B2-35
	G. L. Kasza	H5-29
	R. E. Lerch	B2-35
	K. A. Lindsey	H5-29
	P. J. Mackey	B3-15
	B. K. Olson	T3-02
	R. D. Pierce	N3-13
	S. M. Price	H4-57
	R. J. Roberts	N3-13
	G. S. Robinson	B2-19
	J. W. Shade	R4-03
	J. A. Voogd	R4-03
	M. I. Wood	N3-13
	EDMC (2)	H4-22
	Central Files	L8-15
	Environmental Technical Library	H4-56

No. of Copies		
64	Pacific Northwest Laboratory	
	J. E. Amonette	K6-81
	M. P. Bergeron	K6-77
	B. N. Bjornstad (5)	K6-96
	R. W. Bryce	K6-96
	K. J. Cantrell (5)	K6-81
	M. A. Chamness	K6-96
	L. J. Criscenti	K6-81
	P. G. Doctor	K6-96
	R. L. Erikson	K6-81
	J. W. Falco	K6-78
	A. R. Felmy	K6-81
	M. D. Freshley	K6-77
	W. E. Kennedy, Jr.	K3-54
	C. T. Kincaid	K6-77
	G. V. Last	K6-96
	R. E. Lewis (3)	K6-96
	S. P. Luttrell	K6-96
	E. M. Murphy	K3-61
	B. A. Napier	K3-54
	W. E. Nichols	K6-77
	K. Rhoads (5)	K3-54
	L. H. Sawyer	K3-54
	R. J. Serne (10)	K6-81
	R. L. Skaggs	K6-77
	J. L. Smoot (5)	K6-77
	P. S. Stansbury	K3-53
	S. S. Teel (3)	K6-96
	R. E. Westerman	P8-44
	S. K. Wurstner	K6-77
	Publishing Coordination	K1-02
	Technical Report Files (5)	P8-55

Plate 1. Geologic Map of the 218-E-12B Burial Ground Showing Mapped Units and location of Samples Obtained for Laboratory Analysis

GEOLOGIC MAP OF THE 218-E-12B BURIAL GROUND HANFORD SITE, WASHINGTON

R.E. Lewis, B.N. Bjornstad, and S.S. Teel
1/92

MAPPED UNITS

Qc — Covered—mapped where Hanford Formation is obscured by fill from recent construction

Hanford Formation (Pleistocene)—Mapped units are depicted on stratigraphic sections

Qha — A unit

Qhb — B unit

Qhc — C unit

Contact, dashed where inferred

Trace of measured stratigraphic section

Strike and dip of sedimentary structure

Sample Location, locations of samples from stratigraphic sections are in Figures 6 and 7 of the report

Groundwater Monitoring Wells

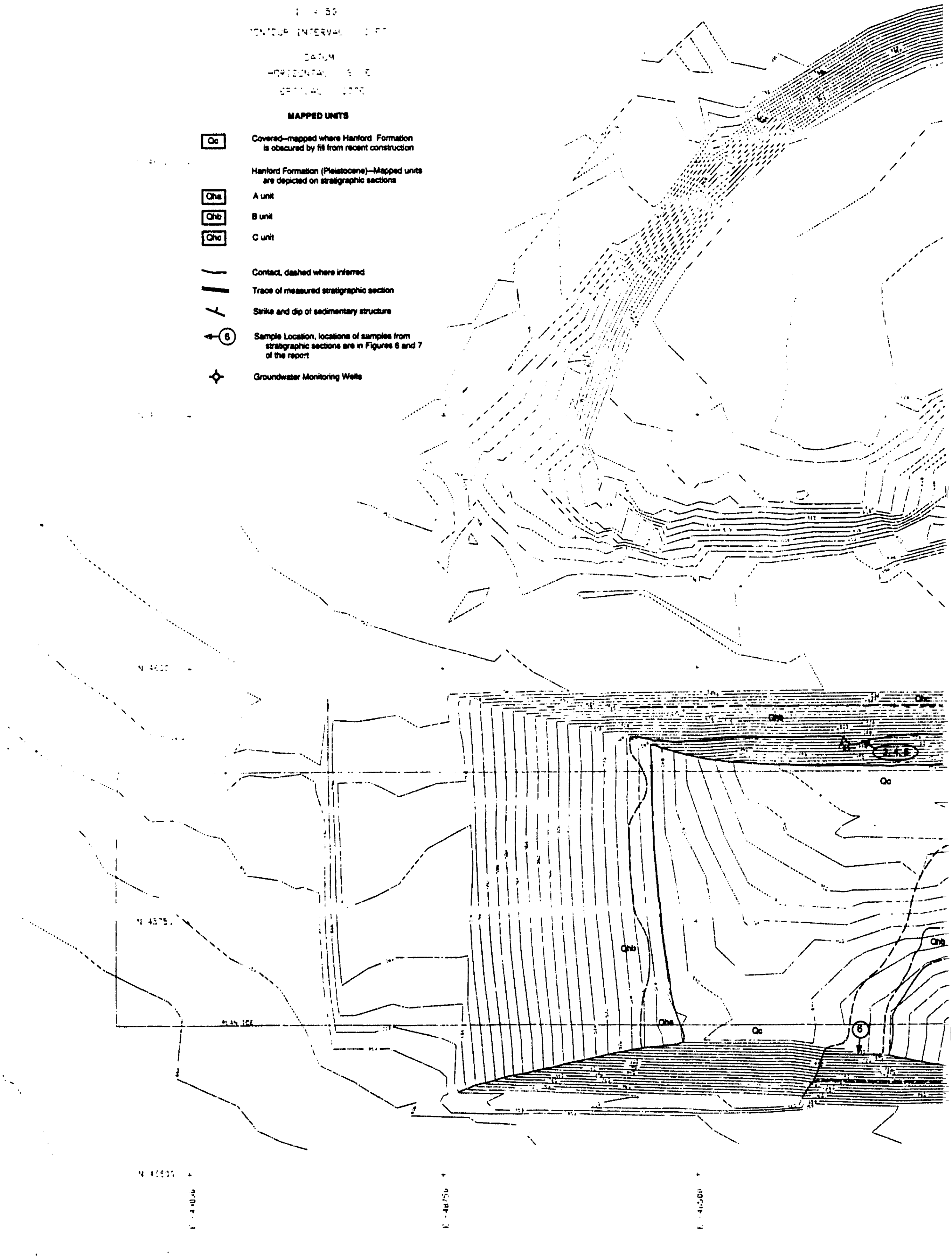

PLATE 1

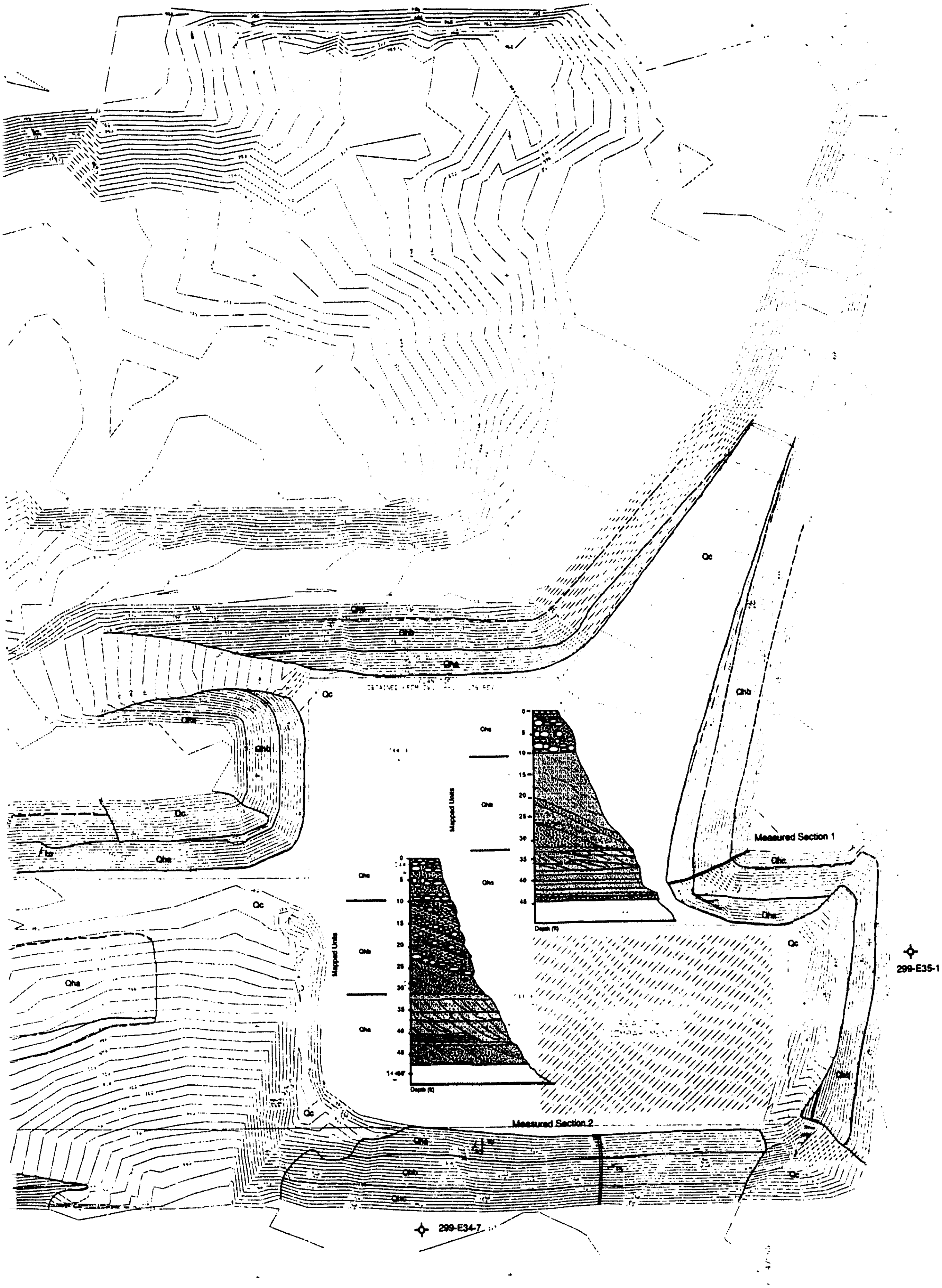

Measured Section 1
Measured Section 2
299-E35-1
299-E34-7
Qc
Qhb
Qha
Qhc
Mapped Units
Depth (ft)

END

DATE
FILMED
4 / 1 / 93